Interconnectedness of Electricity Spot Prices - A Dynamic Network Analysis

Guan Yan

Supervised by

Prof. Stefan Trück

Department of Applied Finance and Actuarial Studies

Faculty of Business and Economics

Macquarie University

A thesis submitted for the degree of

Master of Research

9 October 2017

Contents

Summary

This present study constructs dynamic Granger causality networks based on the spot prices of five regional markets in the Australian National Electricity Market (NEM). Although transmission lines between adjacent states result in physical interconnection in the geographical sense, the degree of integration of wholesale electricity prices is still equivocal. Based on a data set comprising electricity spot prices from 1 July 2010 to 30 June 2017, this study employs principal component analysis and generates Granger causality networks to examine the degree of interconnectedness of the NEM in a time-varying setting. We find that the derived measures of interdependence can be related to actual market events such as price spikes; unexpected high demand for electricity; sudden increase in price volatility; rebidding of dominant generators; the temporary or permanent outage of major power stations; and upgrades and limitations in transmission capacity. The first measure is the cumulative risk fraction of the first few principal components, which conveys information on risk concentration. Another measure is the dynamic causality index generated from the estimated Granger causality network. In the analysed network, we find that stronger dependence is exhibited by regional markets that are linked by interconnectors, while the direction of the relationship can be related to inter-regional trade. Furthermore, this study examines the usefulness of the derived measures as early-warning indicators for upcoming periods of extreme prices and volatility. Our results suggest limited predictive power of the interconnectedness measures for spot price behaviour in the NEM.

Statement of Originality

The work contained in this thesis has not been submitted for a higher degree to any university or institution other than Macquarie University.

To the best of my knowledge and belief, the thesis contains no material previously published or written by another person except where due reference is made in the thesis itself.

Also, the thesis is an original piece of research and any help and assistance received in this process have been acknowledged.

Guan Yan

Student Number: 44692331

9 October 2017

Acknowledgements

Firstly, I would like to express my sincere gratitude to my supervisor Prof. Stefan Trück for his continuous support, inspiring speeches and immense knowledge. His guidance has helped me all through the Master of Research Year 2. I could not have imagined having a better supervisor during this year at Macquarie University. Thanks also go to my supervisor Prof. Zhi Dong Liu who always supports me during my postgraduate study.

I would like to thank Dr. Marc Gronwald, who makes comments on my thesis as the examiner. My grateful thanks also go to other staff in the Department of Applied Finance and Actuarial Studies as well as the Faculty of Business and Economics for their patience and efficient assistance.

Last but not least, I thank my family members and friends for supporting me spiritually and emotionally throughout the writing of this thesis and my overseas life in general.

Chapter 1

Introduction

The Australian National Electricity Market (NEM) was established as a wholesale spot market in December 1998 and currently comprises five state-based regional markets: New South Wales (NSW), Queensland (QLD), South Australia (SA), Tasmania (TAS) and Victoria (VIC). The markets are linked through cross-border electricity transmission lines, which are called "interconnectors", and managed by the Australian Energy Market Operator (AEMO). The most influential price in this market is the half-hourly spot price which is the basis for settling all financial transactions of electricity traded in the NEM. For each regional market, registered generators offer supplied quantities of electricity at different prices for a specific time period. The AEMO then dispatches the demand quota to the cheapest bids and further to the more expensive bids until the production matches the demand for every five-minute interval. The price corresponding to the marginal amount of electricity required to meet consumption becomes the five-minute dispatch price. The average of the dispatch prices over 30 minutes is regarded as the settlement price, or half-hourly spot price. This trading mechanism guarantees that supply is matched with demand in real time (Australian Energy Regulator, 2017).

One of the fundamental objectives in developing the NEM was to ensure reasonable investment in its infrastructure and to guarantee its efficient operation, which would satisfy the long-term interests of customers (Australian Government Productivity Commission, 2013). However, as pointed out by Higgs (2009), Ignatieva and Trück (2016), Nepal et al. (2016) and Apergis et al. (2016), an

integrated and efficient national market has not yet been achieved. One of the most significant characteristics of an integrated market is that price patterns are supposed to reflect long-run convergence. However, in reality, sizable price differences are evident between these jurisdictions as shown in Figure 1.1. The figure provides a plot of daily average spot prices for the five states in the NEM and illustrates the specific price behaviour for each state.

The literature mentions various reasons why integration of the five markets has not yet occurred (Garnaut, 2011; Australian Government Productivity Commission, 2013; Nepal et al., 2016). In particular, these reasons include limited interconnector capacity, significant transmission constraints and a relatively small number of generators in the regional markets, as well as a very different generation mix for electricity in the individual states. It has also been put forward that the market structure of the electricity sector in Australia has the potential to impede effective competition. This concern has prompted the addition of another role within the Australian Energy Regulator (AER), with this role being to monitor and report on the degree of competitive effectiveness in the NEM (Australian Energy Regulator, 2017).

As revealed during recent periods of power outage, electricity supply in the NEM may not be sufficiently reliable. For example, on 28 September 2016, severe storms occurred in South Australia, cutting off three transmission lines and creating voltage instability that also shut down a 400 MW wind generation system and the Heywood interconnector, thus causing a statewide blackout. Furthermore, several aging coal plants have recently been retired, leading to the significant removal of generation capacity from the market. Due to investor uncertainty around new plants, these plants are not even being replaced. The negative outcomes that this may cause are of great concern. One example is the contribution of the shutdown of the Northern power station in SA to the tight supply-demand conditions of the market in July 2016 (Australian Energy Regulator, 2017).

The consequent shortage of power, combined with emerging technologies, is leading to increased reliance on renewable resources. Other contributors are a

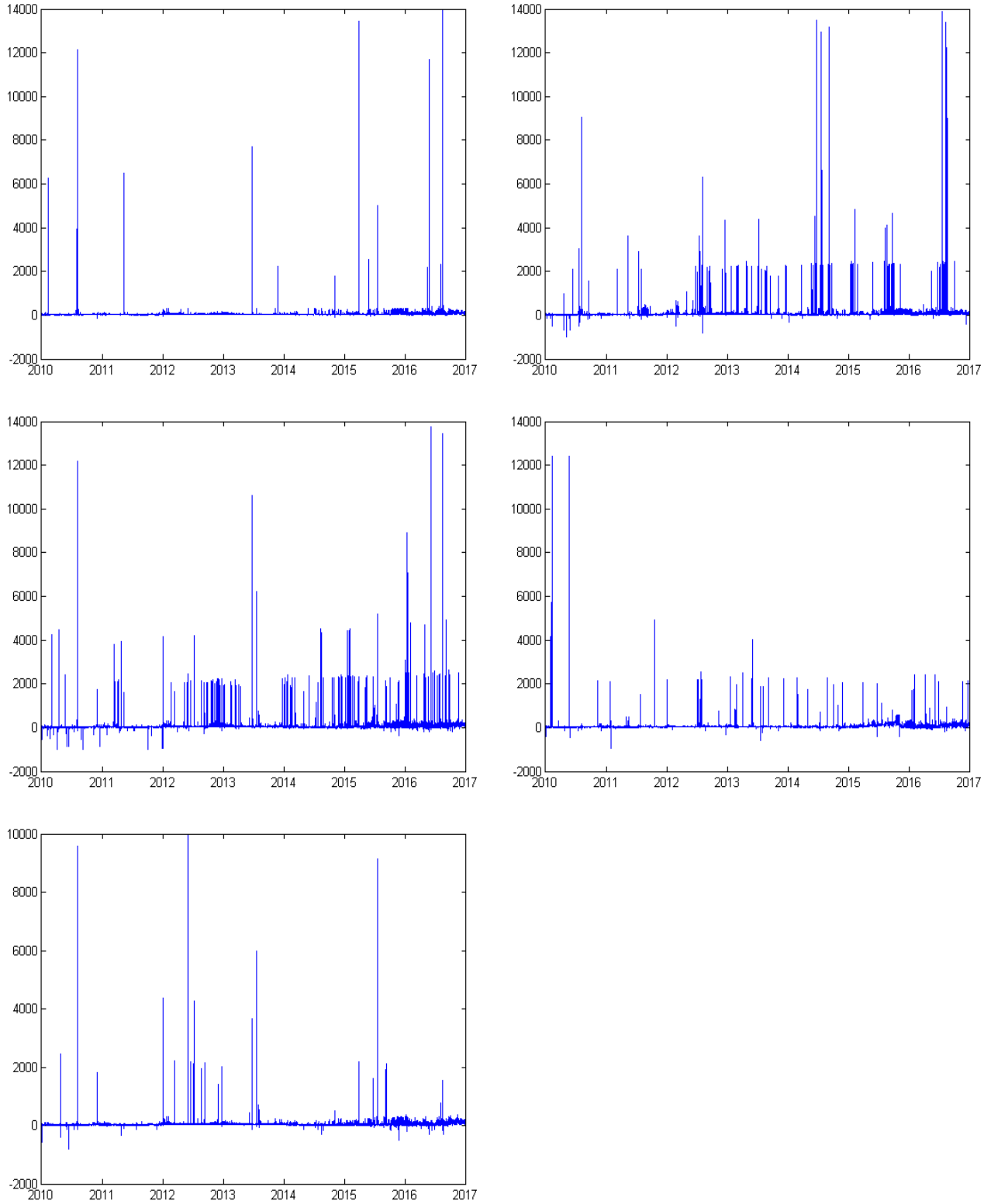

Figure 1.1: Half-hourly spot prices of five regional markets. Data of NSW (upper left panel), QLD (upper right panel), SA (middle left panel), TAS (middle right panel) and VIC (lower left panel) are from 1 July 2010 to 30 June 2017.

series of public policies, including the 2012 - 2014 carbon pricing mechanism, the Direct Action plan and the Australian Government's Renewable Energy Target (RET) scheme as well as feed-in tariff schemes. These initiatives all encourage the abatement of carbon emissions and the adoption of renewable resources. For instance, rooftop solar photovoltaic (PV) and battery storage systems have become increasingly popular among customers who are interested in controlling their energy consumption. The amount of power generated in this way was almost zero until 2000, but by the financial year 2015 - 2016, 1.6 million households had installed PV systems, contributing an amount approximately equal to 3% of the total energy consumption in the NEM (Australian Energy Regulator, 2017). However, some renewables, such as wind, are intermittent and unpredictable. As they depend on favourable weather conditions, they are not qualified to be reliable power sources.

These significant developments over the last decade have caused structural changes to the NEM that are also reflected in the interdependence between spot prices, and the transmission of price volatility or spikes across regional markets. Interestingly, most of the previous literature has typically focused on the long-term trends of market integration from a rather static point of view (Apergis et al., 2016), while the dynamics of price convergence and interconnectedness have often been neglected. Hence, this present study is motivated to capture the time-varying behaviour of dependence measures based on regional electricity prices in the NEM.

As for spot prices in the NEM, a tight supply-demand balance often leads to extreme observations, that is, so-called price spikes that force the market participants to face higher risks. Not only power availability but also power generation costs have an impact on electricity prices. For example, during periods of extreme demand, dispatch prices are typically set based on the bids of gas-powered generation with its significantly higher fuel costs. This was the case during winter 2016 and over summer 2016-2017 when wholesale prices repeatedly spiked.

In fact, coal-fired generators have high costs in start-up and shut-down, but low operating costs. This characteristic typically leads them to offer electricity at rather low prices to ensure it is dispatched. However, other generation technologies, such as gas-powered generation and hydro-generation, are more likely to bid in peak demand periods to make more profits due to their high operating costs (Australian Energy Regulator, 2017).

Both intermittent blackouts and highly volatile prices in the NEM might justify the comprehensive regulation of this industry to ensure customers do not have to accept unreasonably high prices and an unreliable power supply due to the market power of a small number of generators. Especially given the situation described above, policy makers and regulators might be interested in a tool to monitor the overall interdependence structure of the market and to take timely actions accordingly. For example, as mentioned by Australian Energy Regulator (2017), some of the present coal generators are being retired which is causing a significant decrease in supply. If it is possible to inspect the effects of these retirements on the dependence structure of regional spot prices, precautionary measures could be taken to prevent potential breaches of the supply reliability standard. In addition to these concerns, a better understanding of the interdependence of spot prices across regional markets is of great importance in developing risk management and hedging strategies implemented by traders and retailers. Therefore, quantifying the overall connectedness of the NEM is crucial to all the parties involved.

In the global context, the shared goal of many electricity sectors that have experienced liberalization and restructuring is to have one integrated market that can provide a reliable power supply to consumers. Researchers have explored whether and to which level these deregulated and competitive markets have achieved integration, thus exhibiting a long-run common price pattern (e.g. De Vany and Walls, 1999; Dempster et al., 2008; Zachmann, 2008; Smith et al., 2012; Nepal et al., 2016; Apergis et al., 2016). However, even within the same market, the conclusions are different, for reasons such as the differences in the

methodology adopted (e.g. Smith et al., 2012; Nepal et al., 2016; Apergis et al., 2016), the time span of the data sets involved (e.g. De Vany and Walls, 1999; Dempster et al., 2008), and the selected scope.[1]

In addition to long-run price convergence, short-run interdependence[2], such as price contagion and volatility spillovers, is also examined in various markets.[3] Most studies to date only investigate the pairwise relationships between prices in different markets and ignore a systemic view (e.g. Nepal et al., 2016). However, this present study provides a dynamic network perspective to gauge the degree of connectedness within the five-state system.

Network analysis has been employed in different areas of science, such as the technological, social and biological sciences for the last few decades. In addition, it has been widely used to capture the linkages in financial markets, as seen in the rich set of literature concerning financial networks, among which is the growing literature on interbank networks (see, e.g., Hüser (2015) for a review). The current popularity of network analysis is due to the renewed interest in systemic risk (Billio et al., 2012). This is despite no clear consensus having been reached on how to define systemic risk (Bisias et al., 2012), which is generally recognised as the externality that the risk associated with a single institution may create for the entire system (Hüser, 2015). Prior to the Global Financial Crisis (GFC), systemic risks did not attract much attention, as risks in a financial system were typically regarded as the summation of individual risks (Allen and Carletti, 2013). However, the GFC saw the chain reaction after the demise of Bear Stearns and

[1]In the European context, Haldrup and Nielsen (2006) assess the dynamics of electricity prices in the NordPool market and differentiate two regimes: price convergence and price divergence. Zachmann (2008) examines the extent to which a single electricity market for 11 continental European countries had been achieved by mid-2006. Even though the assumption of full market integration is rejected, typically pairwise price convergence is detected. Ciarreta and Zarraga (2012) compare the integrated Iberian Electricity Market (Spain and Portugal) and the interconnected electricity market of Spain and France, and suggest the disparity of integration levels.

[2]The short-term multivariate analysis is of great significance for forecasting prices or managing risks through hedging decisions; thus, it is particularly helpful to market participants who operate in more than one electricity market at the same time (Ignatieva and Trück, 2016). See Weron (2014) for a review of electricity price forecasting approaches.

[3]See Bollino and Polinori (2008), Le Pen and Sévi (2010) and Füss et al. (2015) in Europe and Worthington et al. (2005), Higgs (2009), Aderounmu and Wolff (2014a), Aderounmu and Wolff (2014b), Smith (2015) and Ignatieva and Trück (2016) in Australia. Electricity prices with higher frequency in the NEM have recently been modelled in a number of studies, such as the work of Clements et al. (2013), Clements et al. (2015) and Manner et al. (2016).

the bankruptcy of Lehman Brothers, raising concerns of interconnections between financial entities and, furthermore, the full view of the entire system. This is exactly the focus of the network approach which addresses the role of the network structure formed by a variety of relationships, such as asset co-holdings, repurchase agreements and over-the-counter (OTC) derivative contracts. However, the network methodology has not yet been used in electricity markets except for the work of Castagneto-Gissey et al. (2014). To the best of the author's knowledge, to date, no study with a focus on the NEM has adopted a network perspective to conduct a multivariate analysis on the half-hourly electricity prices. Therefore, this study is the first to construct networks of causal relationships between regional spot prices in the NEM.

Some of the literature suggests reasons for changes to price interdependence, such as institutional design (Boisseleau, 2004; Ciarreta and Zarraga, 2015); physical interconnections (Kalantzis and Milonas, 2010; Ciarreta and Zarraga, 2015); common fundamentals (Bunn and Gianfreda, 2010; Apergis et al., 2016) and closure of major plants (De Menezes and Houllier, 2016). As for the NEM, whether the derived interconnectedness measures contain the information that can help to predict future price patterns is of great interest. The present study fills this gap and examines the potential of these measures to forecast some daily spot price statistics across the five regions, including the average price, the daily volatility and the number of spikes.

Our study is based on half-hourly spot prices from 1 July 2010 to 30 June 2017 in five regional markets, namely NSW, QLD, SA, TAS and VIC. To quantify the interdependence among these jurisdictions and have a better understanding of the integration process in the NEM, the framework in Billio et al. (2012) is employed as it provides two different perspectives on systemic risk. With adaptation to the uniqueness of electricity prices, principal component analysis (PCA) and Granger causality network analysis are applied to the sample data. The generated results

are composed of two interconnectedness measures calculated based on rolling windows, exhibiting the dynamic evolution through time.

We find that these dynamics are highly related to significant events, such as price spikes; opportunistic rebidding of generators; upgrades and limitations in transmission capacity; closure of major power stations; unexpected high demand for electricity and uncertainty in energy-related public policies. Additionally, in the derived network, the Granger causality relationship is more robust between markets that are physically connected through transmission lines, with the direction partly dependent on the interregional trade. In several models of daily statistics, we suggest the limited predictive power of the derived interconnectedness measures. With these measures demonstrating the role played by the specific state and the overall condition of the whole market, they capture unique information different to that from other statistics. The coefficients estimated in the quantile regression show the pattern of elasticity changes for the range of quantiles from 0.1 to 0.9.

In summary, the contribution of this study is threefold. First, it is a pioneer to capture the intricate web of the pairwise Granger causality relationships between five states in the NEM. More broadly, by adapting the risk metrics proposed for financial markets to the unique characteristics of electricity prices, the study also introduces an innovative framework for gauging the risk concentration and systemic risk to the electricity sector. Thus it becomes one of the first studies to apply network theory to the electricity market, following Castagneto-Gissey et al. (2014). Moreover, this study undertakes a trial which examines the validity of these measures in anticipating daily statistics of the half-hourly spot prices one day later for the individual markets.

The remainder of the thesis is organised as follows. Chapter 2 briefly describes the Australian National Electricity Market (NEM), providing the background for our study. Chapter 3 reviews the related literature from two streams, the multivariate analysis of electricity prices and the financial application of complex network theory. Chapter 4 introduces the methodology and the involved research

framework. Chapter 5 provides the empirical analysis, in particular the results for the conducted PCA and the applied Granger causality networks. The chapter also relates findings on the constructed measures to specific periods of demand and price behaviour. Chapter 6 summarises results for the conducted predictive regressions, using two estimation methods: ordinary least squares and quantile regression. Finally, Chapter 7 concludes the thesis and proposes possible directions for further research.

Chapter 2

Literature Review

This chapter provides an overview of the relevant literature and is divided into two sections. The first section is related to the multivariate analysis of electricity prices, covering different markets and a variety of empirical methods. The second section is concerned with the financial application of complex network theory. This forms the basis of our research framework in which we address the dynamic interactions between spot prices in the NEM.

2.1 Literature on Electricity Price Interdependence

Electricity is regarded as a peculiar commodity that is non-storable, even though recent technology developments have occurred regarding its storage. When combined with transmission constraints, this characteristic is revealed in sizable differences between regional prices; at times, sharp spikes occur because demand and supply must be instantly matched. These features have motivated a number of studies on the pattern of electricity prices. Due to the similarity between the price series of electricity and that of financial assets, these studies have applied finance methodology to model the behaviour of electricity prices (Ciarreta and Zarraga, 2012). In fact, the overwhelming majority of electricity-pricing models are adapted from the financial econometrics literature (Christensen et al., 2012).

On the one hand, diminishing differentials among prices could be seen as

evidence of market integration in the long run. They are influenced by a variety of factors, such as the power supply structure; generator competitiveness; costs and availability of the primary energy sources; technological changes and market regulation. However, in the short run, price convergence is driven by opportunities of arbitrage but is also restricted by transmission capacity as pointed out by Apergis et al. (2016). On the other hand, volatility spillovers and price contagion usually refer to negative results such as price spike interdependence.

2.1.1 Market Integration and Price Convergence

As mentioned previously, the liberalisation and restructuring of the electricity sector have occurred worldwide in recent decades, with the shared goal being to have one integrated electricity market. The aim is to provide a reliable power supply to retailers and consumers. The question that naturally occurs is whether and to what extent these deregulated and competitive markets have achieved integration, thus exhibiting a common long-run price pattern. The contrasts evident in the study results presented next are mostly due to differences in the methodology used and the data sets studied in terms of the selected time span and scope.

De Vany and Walls (1999) present the first evidence on price transmission in decentralised power markets. They test the market integration of 11 regions in the western United States (US). Based on cointegraion analysis of spot electricity prices, they suggest the pricing efficiency of power and transmission. Using an identical data set but with the time period extended to September 1999, Dempster et al. (2008) demonstrate a moderate degree of integration among these markets by employing Granger causality tests, with their conclusion being contrary to that of De Vany and Walls (1999). In particular, through using common features analysis, they find an obvious decrease in the level of price integration after the creation of California's independent system operator (ISO)'s power exchange. Park et al. (2006) examine the relationship between spot prices in 11 US electricity markets. They argue that the separation of prices disappears over longer time

frames and attribute this not only to physical assets but also to institutional arrangements.

In the European context, Haldrup and Nielsen (2006) assess the dynamics of electricity prices in the NordPool market with a Markov regime model with a long memory (fractional integration). They differentiate the two regimes of price convergence and price divergence. Zachmann (2008) examines the extent to which a single electricity market for 11 continental European countries had been achieved by mid-2006. Even though the assumption of full market integration is rejected by principal component analysis (PCA), pairwise price convergence is detected by stationary tests and the Kalman filter after considering congestion charges. Nonetheless, Houllier and de Menezes (2012) argue the deficiency of the commonly used stationary test framework, proposing the parametric fractional Autoregressive Integrated Moving Average (ARIMA) model to find cointegration relationships between electricity spot prices in four markets. Furthermore, De Menezes and Houllier (2016) employ a time-varying fractional cointegration analysis among nine European electricity markets. They conclude that the closure of German nuclear plant exerted a negative effect on most European electricity markets.

Boisseleau (2004) conducts an empirical estimation of the level of integration of the European electricity market with respect to the role played by power exchanges. He demonstrates that the low degree of market integration observed at the European level was as a result of the lack of an efficient transmission pricing in the wholesale market design. With regard to the same question, Kalantzis and Milonas (2010) explore the determinants of pairwise spot price differentials among eight major power exchanges to address the integration of the European electricity market. Based on the regression results in the model estimation, they suggest a convergence over time as well as the significance of physical interconnections. However, Bunn and Gianfreda (2010) point out that market integration is not simply related to geographical distance, but also to common fundamentals. Using causality tests, cointegration and impulse-response techniques, they

conclude that market integration increased over time with regard to the French, German, British, Dutch and Spanish power markets.

From a comparative perspective, Ciarreta and Zarraga (2012) address the differences between the integrated Iberian Electricity Market (Spain and Portugal)and the interconnected electricity market of Spain and France based on Dynamical Conditional Correlation (DCC) and Constant Conditional Correlation (CCC) models with different univariate variance specifications. The results suggest the disparity of both the integration level and the respective best-fitting models. Using the Granger causality concept, Castagneto-Gissey et al. (2014) investigate whether the goal of having one single European electricity market had been reached by the integration of the individual national electricity markets. They construct dynamic multivariate networks with 13 European wholesale electricity prices and argue that this time-varying network can be used to monitor development in the market integration process. Recently, Ciarreta and Zarraga (2015) apply the Multivariate Generalized Autoregressive Conditional Heteroskedasticity (MGARCH) model to examine the market integration level across Spain, Portugal, Austria, Germany, Switzerland and France. They identify the important roles of transmission lines and efficient rules for market operation.

To date, in the Australian context, only a few studies have focused on market integration . Based on a copula with skew t distribution as constructed by Sahu et al. (2003), Smith et al. (2012) observe the complex non-Gaussian margins and non-linear interregional dependence among spot prices with regard to market integration. Nepal et al. (2016) suggest that the Australian NEM has not yet achieved full integration. They apply different econometric techniques including pairwise unit root tests, cointegration analysis and Kalman filter methodology based on a state-space model that allows time varying coefficients. However, Apergis et al. (2016) suggest that different convergence groups called "clubs" are detected among six regional electricity markets in Australia. Employing a non-linear time varying factor model originally proposed by Phillips and Sul (2007), they cluster panels into clubs. They find that the first club is composed of three

states in the NEM and that the second club comprises West Australia (WA) and Tasmania (TAS). The latter group shares a convergence pattern despite the absence of physical connection and the major differences in market design and power supply structure.

2.1.2 Volatility Spillovers and Price Contagion

In addition to the long-run price convergence that indicates market integration, many studies have analysed short-run phenomena, especially volatility spillovers and price contagion. These studies aim to forecast prices or manage risks through hedging decisions. These multivariate results are of significance for market participants, especially those who operate in more than one electricity market at the same time (Ignatieva and Trück, 2016).

In the European context, Bollino and Polinori (2008) identify the contagion effect from mere interdependence among the electricity prices of seven regions in Italy. This is based on an econometric model which considers the market-specific variables and uses instrumental variables to correct the estimation. Applying a VAR-BEKK model, Le Pen and Sévi (2010) suggest the existence of return and volatility spillovers among the German, Dutch and British forward electricity markets. They employ the Volatility Impulse Response Function (VIRF) proposed by Hafner and Herwartz (2006) to quantify the shock's impact on the expected conditional volatility. They find the asymmetric distribution of VIRF density at different forecast horizons. Promoting the market coupling mechanism, Füss et al. (2015) use a fundamental multi-market model to manifest the impact of different allocation schemes for cross-border transmission capacity on the dynamics of both electricity spot and derivative prices. De Menezes and Houllier (2015) combine the long-term analysis mentioned above with short-term interdependence analysis. To examine the national policy implications, they conduct the latter analysis based on two MGARCH models with dynamic correlations.

Several studies focusing on price spikes and volatility spillovers have been conducted in Australian electricity markets. Worthington et al. (2005) apply the

MGARCH model to identify the source and scale of the spillovers concerning price and price volatility among the five regional electricity markets in the NEM. They find no mean spillovers between any pair of markets but a large number of salient own-volatility and cross-volatility spillovers in all markets. In addition, they argue that these spot prices are stationary, and that this property is contrary to that of North America. Among three MGARCH models with constant and dynamic conditional correlations, Higgs (2009) suggests that the MGARCH model proposed by Tse and Tsui (2002) provides the best fit for the wholesale price series of four regions in the NEM. In addition, she finds significant interdependence between well-connected markets. However, Aderounmu and Wolff (2014a), in pointing out the inadequacy of linear correlation, as in the CCC and DCC models, apply a copula approach to analyse the tail dependence across regional electricity markets. They suggest the likelihood of joint jumps in the prices. Using the same sample data, Aderounmu and Wolff (2014b) then present a non-parametric estimator of the simultaneous price spikes called 'tail dependence' and complement point estimation with a hypotheses test. They find evidence of tail dependence in five Australian regional electricity markets. Based on a copula model that defines a multivariate time series on the unit cube, Smith (2015) identifies substantial asymmetric and heavy-tailed cross-sectional and time-serial dependence among daily electricity spot prices. Ignatieva and Trück (2016) apply various copula models within the framework of the Generalized Autoregressive Conditional Heteroskedasticity (GARCH) approach. They demonstrate that the overall best fit is achieved by using copula mixture models as these models capture the asymmetric dependence in the tails of the distribution. In their study, as is also found in the study by Higgs (2009), the strongest dependence is found between well-connected markets.

Electricity prices with high frequency in the NEM have recently been modelled in several studies, most of which have been aimed at predicting electricity prices.[1] For example, with half-hourly electricity prices in four Australian markets, Clements et al. (2013) construct a semi-parametric method with state-

[1]See Weron (2014) for a comprehensive literature review of electricity price forcasting.

dependent weights derived from a kernel function in order to forecast price spikes. Clements et al. (2015) further propose a multivariate self-exciting point process model for the sake of predicting prices more accurately. They also find evidence of the price spike transmission. Also, Manner et al. (2016) propose a novel dynamic multivariate binary choice model as a better method for fitting and forecasting abnormally high prices. In this method, the latent variables are allowed to follow a vector autoregressive (VAR) process, with the method including a copula to represent the joint distribution.

2.2 Literature on Financial Networks

The network analysis framework has been employed in different areas of science, such as the technological, social and biological sciences for the last few decades. In addition, the framework has been widely used to capture the linkages in financial markets, as seen in the rich set of analytics of financial networks[2] that contain financial institutions and financial products. The current popularity is due to renewed interests in systemic risk (Billio et al., 2012). Even though consensus has not yet been reached on how to define systemic risk (Bisias et al., 2012), it is generally recognized as the externality that the risk associated with a single institution may create for the entire system (Hüser, 2015). Systemic risk has not attracted much attention before as, in past decades, risks in a financial system were regarded as the summation of individual risks (Allen and Carletti, 2013). However, the chain reaction in the Globe Financial Crisis (GFC) after the demise of Bear Stearns and the bankruptcy of Lehman Brothers, raised concerns of interactions between financial entities and, furthermore, the overall view of the entire system. This is exactly the focus of the network approach which addresses the role of the network structure formed by a variety of relationships, such as asset co-holdings, repurchase agreements and over-the-counter (OTC) derivative contracts.

[2]Among them is the growing amount of literature on interbank networks: see Hüser (2015) for a review.

2.2.1 Simulation Studies

Simulation studies focus on building various networks to investigate the impacts of the interaction structure on the contagion mechanism and loss propagation. The three categories of network formation are: firstly, the Poisson random network where each link is built independently with some fixed probability (p); and, secondly, the scale-free network which can be generated by various models, including the preferential attachment model and the fitness model. The third is the endogenous network that evolves with specified rules, such as profit maximisation and the liquidity needed in banks' transactions.

In the first category, Gai and Kapadia (2010) model an interbank network where the linking probability is p independently. In this network, by changing p, different scenarios of the average degree are examined. The network is composed of 1000 identical banks: each bank initially has 80% external (non-bank) assets and 20% interbank assets which are evenly distributed among its partners. The capital buffer is 4% of the total assets. The shock in this model is achieved by wiping out the external asset of one randomly-chosen bank. If the capital buffer is insufficient to cover the loss, default and liquidation occur at the same time, and the failure bank is set to default on all its interbank liabilities. When the number of the failure banks accounts for 5% or more of all the banks, this is called a systemic crisis. Caccioli et al. (2014) also build a network model based on Poisson degree distribution. As the focus of their study is overlapping portfolios rather than interbank connectedness, links only exist between banks and assets. The probability for each possible bank-asset pair is drawn with μ_b/M where μ_b represents the average degree of banks in the network and M represents the number of assets. In the simulation, the authors assume 10000 identical banks that each has 20% cash and 80% other assets. The initial equity buffer accounts for 4% of the total asset. When a shock occurs, which is either the devaluation of a asset or the bankruptcy of a randomly chosen bank, the liquidation of insolvent banks causes a fire-sale. Furthermore, the consequent devaluation then causes the failure of other banks, with this turning out to be a vicious loop. Once the

fraction of bankrupt banks exceeds 5%, this is called a systemic financial crisis.

As random linkages cannot model the hierarchy structure and the fat-tail distribution that are commonly detected in the real world, the scale-free network (Barabási and Albert, 1999) has been used by some simulation studies to capture these properties. Amini et al. (2013) assume a Pareto distribution for connections, generating a scale-free network. They set the shock as one or a randomly picked group of initially insolvent institutions. The defaults also cause their respective counterparties to become insolvent as long as the consequent losses exceed their capitals. The number of defaulted nodes is used as the severity measure of a financial crisis. Lenzu and Tedeschi (2012) start with d random outgoing links, and then rewire the ending point towards other nodes with a probability of $1/(1+e^{-\gamma(\phi_j^t-\phi_k^t)})$ where γ signals credibility. γ measures how much banks trust the information about other agents' performances, while ϕ represents bank fitness which depends on the threshold of each bank's probability of default. This is a dynamic process in which each bank's balance sheet changes in every time period. During each time period, two randomly selected banks receive a liquidity shock of equal magnitude but opposite signs. Thus, banks connected to the illiquid banks may be unable to absorb the credit loss from their defaulting borrowers. This study measures systemic risk as the failures of indirect lenders.

Several previous papers compare two or more methods of network formation to assess the effect of different structures on systemic risk. Gai et al. (2011) consider two situations: uniform distribution and geometric distribution. In the numerical simulation, banks are identical in the sense that 4% of the total asset is capital buffer and 15% of the balance sheet is the interbank liability which is evenly distributed among their counterparties. They simulate three types of shocks: random idiosyncratic haircut shock, aggregate haircut shock and targeted shock. The main contagion channel is liquidity hoarding. If 10% of institutions hoard liquidity, this is regarded as a systemic crisis. Furthermore, Arinaminpathy et al. (2012) analyse two structures: the random network and the network with preferential lending. The banks are classified into two categories: big banks

have a larger amount of assets, while small banks have less in assets and capitals. Big banks have a comparatively larger average degree that follows Poisson distribution with the same mean. However, both big banks and small banks share the same capital liquidity ratio and capital-to-asset ratio. Again, two types of shocks are considered: the capital buffer deduction of a randomly chosen bank and the devaluation of a randomly chosen external asset. In summary, three channels contribute to systemic risk: asset price contagion, counterparty defaults and liquidity hoarding due to worsening conditions of market confidence and/or individual health.

In addition to the above studies in which the link formation follows exogenous rules, a number of researchers generate financial networks in a different endogenous way. Iori et al. (2006) establish a network model where edges between two banks exist when a bank exchanges credit with $c\%$ of other banks in the system. The credit exchange happens when the liquid holding becomes negative. In a variety of experiments, they consider different values of c, as well as homogeneous or heterogeneous banks . The capital buffer is set to be 30% of the initial deposit. In this setting, the shock comes from the fluctuation of deposits and investment opportunities. A bank may fail due to its debtors' failures, starting a contagion process. Bluhm et al. (2014) build a network by a constrained minimisation problem without specifying the average degree. In this network, the banks differ in their balance sheets and interbank assets because each interbank asset is generated by the bank's own function. However, the banks have the same amount of deposits (i.e. 600 billion) and the distribution of capital buffer is normal with a mean of 65 and a variance of 10. Shocks are drawn from multivariate normal distribution with a mean of 5, a variance of 25 and a covariance of 0. Given these conditions, contagion takes place when a further loss is caused by exposure to defaulting banks or a devaluation occurs due to the fire-sale of illiquid assets. These authors define systemic risk as the ratio of the assets from defaulting banks over the total assets.

2.2.2 Results from Empirical Studies

Empirical studies provide a number of stylised facts on the financial network topology that may be strongly related to what happens at an aggregate level, that is, systemic risk. Most of these studies adopt either exposure data or transaction data.

Using exposure data, several studies have been undertaken in the European context. Boss et al. (2004) collect Austrian interbank network data from the Central Bank and estimate the liability adjacency matrix using the local entropy maximisation method. They calculate the degree distribution, clustering coefficients and the average shortest path length. The results indicate similar structural features to those in the real-world complex network: a low clustering coefficient and a comparatively short average shortest path length. Degryse et al. (2007) address monthly detailed information on aggregate interbank exposures of 65 individual banks, large bilateral interbank exposures and cross-border interbank exposures in the Belgian banking system from 1993 to 2002. With the RAS algorithm, the authors infer the matrix of bilateral exposures by maximising the dispersion of interbank activities. Two kinds of shocks are simulated in the study, domestic shocks and foreign shocks. They implement regression analysis to examine the impact of interbank market structure and internationalisation on contagion risks. Mistrulli (2011) uses the actual bilateral exposures of all Italian banks to reveal the disadvantages of the maximum entropy method, which is a commonly used estimation method for bilateral liabilities. At first, following Degryse et al. (2007), Mistrulli (2011) mimics the simulation of domestic defaults and foreign defaults, and then examines how the bail-out within conglomerates affects contagion. From the analysis above, the GFC is explained from the perspective of network theory. Craig and Von Peter (2014) calculate statistics on large loans and concentrated exposures of financial institutions in Germany from 1999Q1 to 2007Q4. They employ the core-periphery model to fit data and check the robustness and significance of the results. With the core bank identification, they implement *probit* regression to demonstrate the typical characteristics of

core banks.

In the Brazilian context, Cont et al. (2011) build a network of conglomerates after consolidating 2400 financial institutions. Based on the mutual exposure and capital level of each institution in 2007 and 2008, they conduct a descriptive analysis on, among others, connectivity distribution, heterogeneity of exposure sizes and clustering. In addition, they develop a contagion index based on stress scenarios to measure systemic risk and define counterparty susceptibility to locate systemically important institutions.

Due to its relatively high availability, transaction data with different frequencies are examined by several studies to demonstrate the short-term funding networks of financial intermediaries. Using intraday data, Imakubo et al. (2010) build a payment network of participants in the BOJ-NET real-time gross settlement system that records intraday fund flows. They show the network characteristics with regard to the settlement value, degree, payment volume and the amount of interbank fund transfers. In addition, they simulate a liquidity shock to analyse the contagion in six different scenarios.

Using overnight transaction data between financial institutions in the federal fund market of the United States from 1997 to 2006, Bech and Atalay (2010) illustrate topological characteristics such as size; degree of completeness and reciprocity; degree distribution; node strength; assortativity; clustering coefficient; distance; diameter; and node centrality of the constructed network. They suggest centrality measures as useful predictors of the interest rate of loans. Fricke and Lux (2015) assess overnight loans recorded on the e-MID trading platform from January 1999 to December 2010. This platform registers all the trades in Euro among all Italian banks. The authors show the distribution of degree and that of the number of transactions, and then fit the data to a variety of models: exponential; gamma; geometric; log-normal; negative binomial; poisson; discrete power-law (or Pareto and Weibull); and stretched exponential models. Due to the lack of evidence of power-law properties, they cast doubts on the conclusion made by previous studies that the transaction network is a scale-free network.

Applying monthly returns of banks, broker/dealers and insurers from January 1994 to December 2008, Billio et al. (2012) employ principal component analysis (PCA) to examine the evolution of risk concentration. They also establish networks based on Granger causality relationships (at 5% level of statistical significance) from which they obtain the number of connections as well as the measures of centrality. Moreover, they propose the original connectedness measures, with these measures proved to be superior predictors in out-of-sample forecasts.

Chapter 3

Background

This chapter provides relevant background information and underpins the subsequent chapters of the thesis. Section 3.1 generalises the operation of the Australian National Electricity Market (NEM) in which power generation exerts a considerable influence. Section 3.2 then summarises the supply side of this market from two perspectives: the power source structure and the generators' market power. Moreover, information on interconnectors in the NEM is provided in Section 3.3. Last but not least, Section 3.4 introduces three price characteristics in the NEM.

3.1 Overview of the National Electricity Market (NEM)

The Australian National Electricity Market (NEM) was established by the Australian government as a wholesale spot market in December 1998 and currently comprises five state-based regional markets, namely New South Wales (NSW), Queensland (QLD), South Australia (SA), Tasmania (TAS) and Victoria (VIC). The most influential price in this market is the half-hourly spot price which is the basis for settling all financial transactions of electricity traded in the NEM. For each regional market, registered generators offer supplied quantities of electricity at different prices for a specific time period. The Australian Energy Market Operator (AEMO) then dispatches the demand quota to the lowest priced and

higher priced electricity further until production matches demand for every five-minute interval. The price that corresponds to the marginal amount of electricity required to meet the consumption becomes the five-minute dispatch price. The average of the dispatch prices over 30 minutes is regarded as the settlement price, or half-hourly spot price. Furthermore, a price cap of $14000 per megawatt hour (MWh) and a price floor of -$1000 per MWh apply. This trading mechanism guarantees the lowest generation cost and that supply is matched with demand in real time (Australian Energy Regulator, 2017).

One of the fundamental objectives in developing the NEM is to ensure reasonable investment in its infrastructure and to guarantee its efficient operation in order to satisfy the long-term interests of customers (Australian Government Productivity Commission, 2013). In a national efficient market, any significant price difference across jurisdictions could direct the future investment in power infrastructure. The primary characteristic of an integrated market is the long-run convergence of price patterns so that the differences between regional prices diminish. However, as identified by Higgs (2009), Ignatieva and Trück (2016), Nepal et al. (2016) and Apergis et al. (2016), an integrated and efficient national market has not yet been achieved. This is demonstrated by sizable price differences between the markets as shown in Figure 3.1. The figure provides a plot of daily average spot prices for the five states in the NEM and illustrates the specific price behaviour for each of them.

The literature mentions various reasons why integration of the five markets has not yet occurred (Garnaut, 2011; Australian Government Productivity Commission, 2013; Nepal et al., 2016). These include limited interconnector capacity, significant transmission constraints, a relatively small number of generators in the regional markets, as well as a very different mix for electricity generation in individual states. It has also been put forward that the market structure of the electricity sector in Australia might impede effective competition.

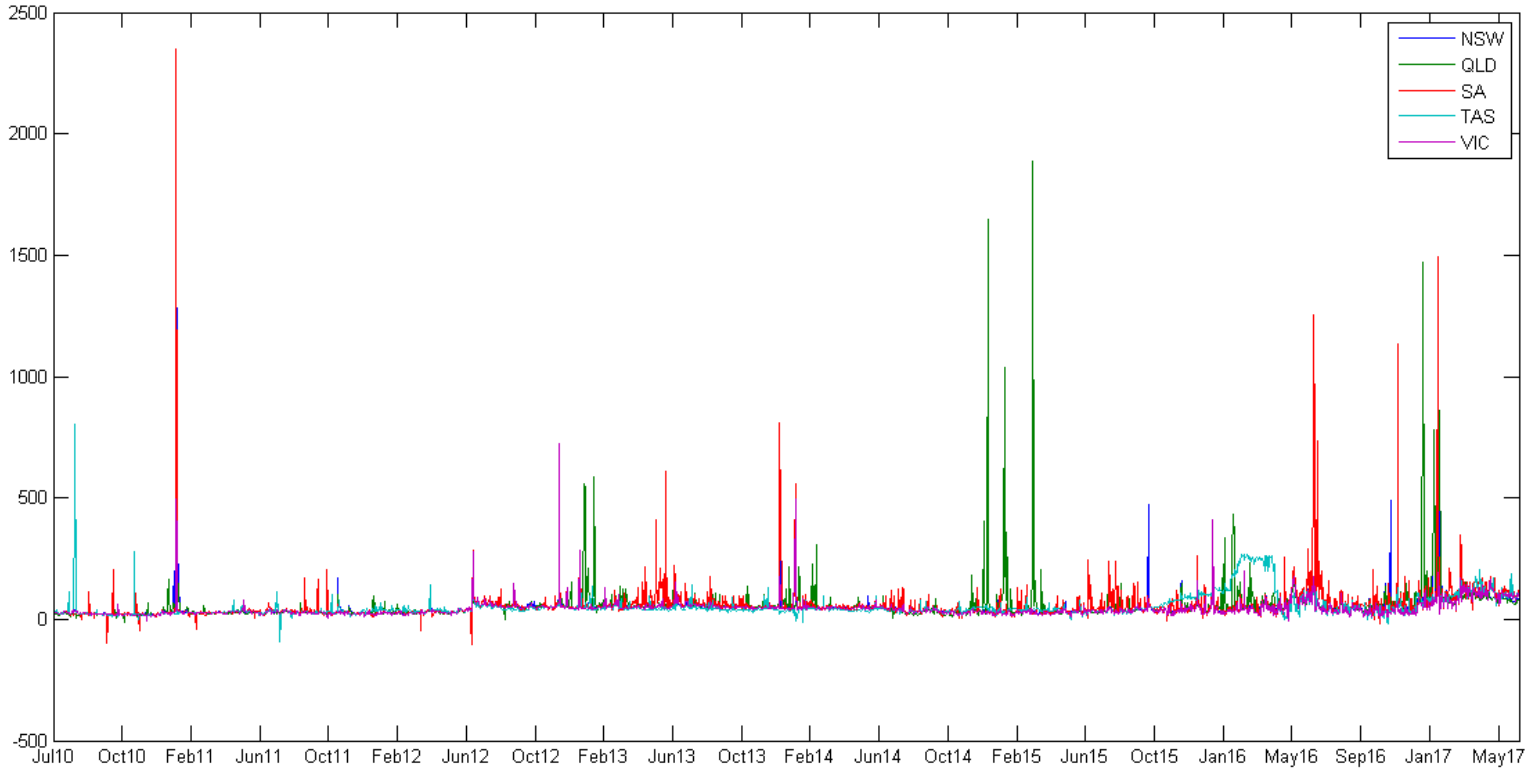

Figure 3.1: Daily electricity spot prices [AUD/MWh] from 1 July 2010 to 30 June 2017

Source: `https://www.aemo.com.au/Electricity/National-Electricity-Market-NEM/`.

3.2 Power Supply in the NEM

Given that electricity is a necessity, and demand is inelastic and not sensitive to prices, spot prices are closely related to power supply. Generators rely on a variety of natural resources, including fossil fuels (coal and gas) and renewable resources (hydro, wind, biomass and solar). Among them, coal-fired generation is the dominant supply technology in the NEM. However, several aging coal plants have retired recently, including the South Australia's Northern power station in 2016 and the Victoria's Hazelwood plant in 2017, which significantly subtracts generation capacity from the market. These plants are unfortunately not being replaced owing to investor uncertainty around new generators. These shutdowns are of great concern due to the negative outcome that they could possibly cause. One example is that the shutdown of the Northern power station contributed to the tight supply-demand condition of the whole market in July 2016 (Australian Energy Regulator, 2017).

Gas is considered to be a transition fuel towards a more environmentally friendly economy. It has lower carbon emissions compared to coal, and gas-fueled generation has a short response time, which could complement the generation that is adopting intermittent energy, such as wind and solar. However, the growth in gas-powered generation has stalled as several generators have postponed the operation of new gas plants. The main reason is the repeal of the carbon pricing as well as increasing gas fuel costs due to the Queensland's liquefied natural gas (LNG) projects. For instance, the Queensland generator Stanwell has twice put off commencing operation at its new gas plant. The first time followed the abolition of the carbon pricing, while the second time was due to recent rises in gas fuel costs.

The consequent power shortage, combined with emerging technologies, is leading to an increased reliance on renewable resources, such as wind and solar energy. For instance, rooftop solar photovoltaic (PV) and battery storage systems have become increasingly popular among customers who are interested in controlling their electricity bills. The amount of power generated in this way was almost zero

until 2000 but, by the financial year 2015 - 2016, 1.6 million households had installed PV systems, contributing approximately 3% of the total energy supply in the NEM (Australian Energy Regulator, 2017). However, some renewables, like wind, are intermittent and unpredictable. They depend on favourable weather conditions, thus they are not qualified to be reliable power sources (Australian Energy Regulator, 2017).

The structure of the power supply is also dramatically impacted by government policies. These include measures that encourage the abatement of carbon emissions and the adoption of renewables, for example, the carbon pricing mechanism, the Direct Action Plan, the Australian Government's Renewable Energy Target (RET) scheme as well as feed-in tariff schemes. The carbon pricing scheme refers to the fixed price charged on carbon dioxide emitted from July 2012 to June 2014. The Direct Action Plan was a replacement for carbon pricing in 2014, under which the government pays for carbon emission abatement by auctions. The RET, introduced in 1997, requires electricity retailers to obtain a fraction of their power from renewable resources. The feed-in tariff schemes were schemes for premium payments by most state governments for small-scale solar PV generation between 2008 and 2012.

Figure 3.2 illustrates the significant difference in the fuel source structure of the five regional markets in the NEM. Fossil fuel, especially coal, is notably the predominant power source in Queensland and New South Wales, accounting for 67.5% and 63%, respectively, while Victoria has a more balanced structure in the power supply. South Australia mainly relies on gas generation, which has recently exposed the state to high prices. Tasmania generates power mostly from hydropower, which is intermittent and susceptible to unfavourable weather. For example, the unprecedented dry conditions, combined with the outage on the Basslink interconnector raised the electricity price above $160 for more than two months in autumn 2016.

The market concentration of the power supply is another issue of concern. As demonstrated by evidence, some large generators have abilities and incentives to

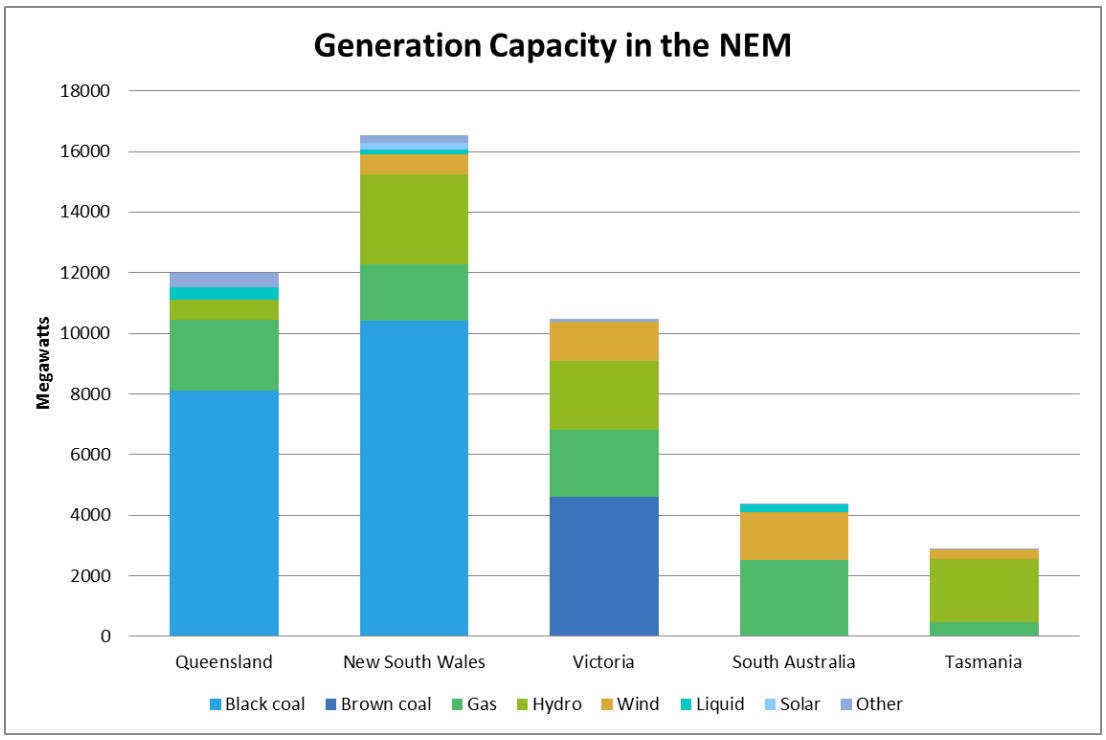

Figure 3.2: Generation capacity in the NEM. This is the registered capacity in each region (in megawatts) by fuel source at 30 June 2017.

Source: `https://www.aer.gov.au/industry-information`.

exercise their market power. One indicator that measures the importance of the largest generators is the *residual supply index* (RSI). The RSI calculates the ratio of demand that can be met by all but the largest generator over total demand in a market. Therefore, if RSI is greater than 1, it is possible to meet all demand without the largest generator. Conversely, the largest generator is the key to satisfying demand. From records that track the RSI for the regional markets in the NEM, the largest generator is shown to be indispensable to meet the peak demand in all of these jurisdictions. For example, the corporations, Stanwell and CS Energy, account for 65% of the power generation capacity in QLD, while the dominant generator in SA, AGL Energy, controls 42% of the capacity (Australian Energy Regulator, 2017). Additionally, Australian Energy Regulator (2017) has suggested that a sample of large power plants tends to take advantage of high prices and to rebid large volumes of capacity from low to higher prices. These power plants might even intentionally withhold capacity to tighten supply and raise wholesale prices.

Recent power outages have revealed that the electricity supply in the NEM

might not be sufficiently reliable. For example, on 28 September 2016, severe storms occurred in South Australia, cutting off three transmission lines and creating voltage instability. These accidents also shut down a 400 MW wind generation system and the Heywood interconnector, thus causing a statewide blackout (Australian Energy Regulator, 2017).

In summary, these significant developments over the last decade have caused structural changes to the NEM, and they are reflected in the interdependence of spot prices and the transmission of price volatility or spikes across regional markets.

3.3 Interconnectors in the NEM

Transmission lines, so-called interconnectors, between the adjacent states make an integrated market possible in the NEM. According to an economics analysis by Apergis et al. (2016), the two types of price convergence are short run and long run. In the short run, arbitrage can be exerted if price differentials exist and the different regions are physically connected. In this case, the quantity of transmission capacity decides the speed of short-run price convergence. The convergence direction depends on the adequacy of cheaper power supply in the exporter region. If interconnection capacity is limited, long-run price convergence can still be achieved through new investment in power plants. However, this process relies on the homogeneousness of the involved markets in terms of power supply; the extent of market competitiveness; load profiles; the costs and availability of energy sources; financial costs and risk preferences; market design and technological innovation (Apergis et al., 2016).

Currently, six interconnectors operate in the NEM, namely: Terranora interconnector and QNI between Queensland and New South Wales; the Victoria to New South Wales interconnector; Basslink between Victoria and Tasmania; and Heywood and Murraylink between Victoria and South Australia, with these represented separately by the red lines in Figure 3.3. Both Australian Government Productivity Commission (2013) and Nepal et al. (2016) reveal the concerns

about the lack of investment in interconnectors in the NEM. Nepal et al. (2016) address the violation of *law of one price* in the Australian NEM, attributing this to the presence of significant transmission bottlenecks.

Figure 3.4 shows the interregional trade every quarter from July 2009 to June 2017 as a percentage of regional electricity consumption. As mentioned in Section 3.2, Tasmania's volatile behavior in interregional trade is a result of its high level of dependency on favourable weather conditions as hydropower is its dominant power source. Thus it is only Tasmania that has traded more than 30% of its power consumption with other regions in the NEM. In line with Tasmania, South Australia has also relied heavily on the interregional trade compared to the other states and, in most cases, this region was an electricity importer rather than exporter. This was also the case with New South Wales but to a lesser extent. In contrast, Victoria usually acts as a power exporter due to its balanced and reliable power source. Queensland also exports part of its power most of the time.

3.4 Prices in the NEM

In addition to power availability and arbitrage opportunities, generation costs affect electricity prices. For example, during periods of extreme demand, dispatch prices are typically based on the bids of gas-powered generation which has significantly higher fuel costs. This was also the case during winter 2016 and over summer 2016-2017 when wholesale prices repeatedly spiked. In fact, coal-fired generators need up to three days to start up and have high costs in start-up and shutdown, although their operating costs are low. This feature typically leads to their offers of electricity at low prices to ensure that the power is dispatched. However, other generation technologies, such as gas-powered generation and hydro-generation, are more likely to offer in peak demand periods to make more profits due to their high operating costs and the flexibility of changing output levels (Australian Energy Regulator, 2017).

It is widely recognised that in modelling the dynamics of electricity spot prices,

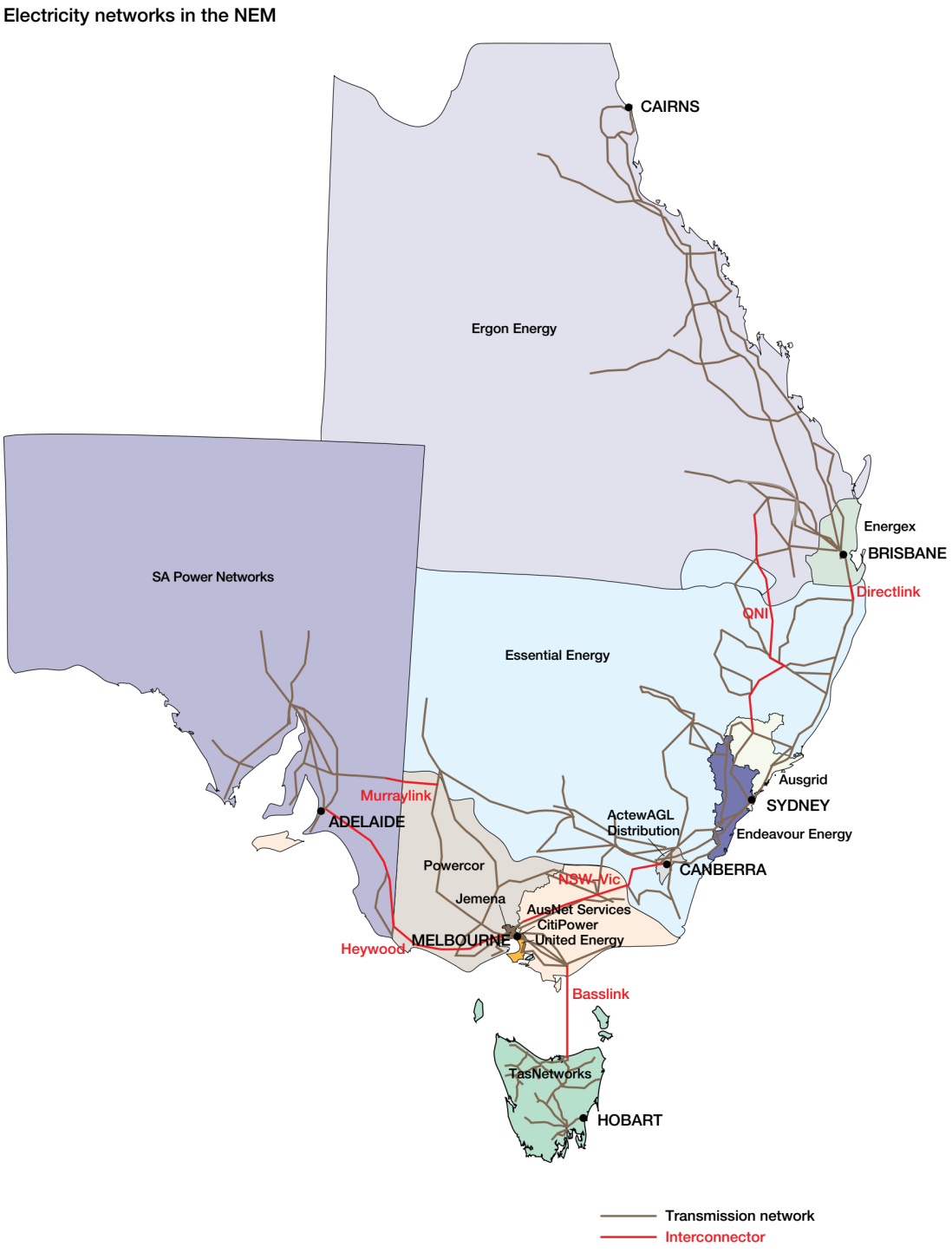

Figure 3.3: Electricity network in the NEM

Source: *State of the Energy Market May 2017.*

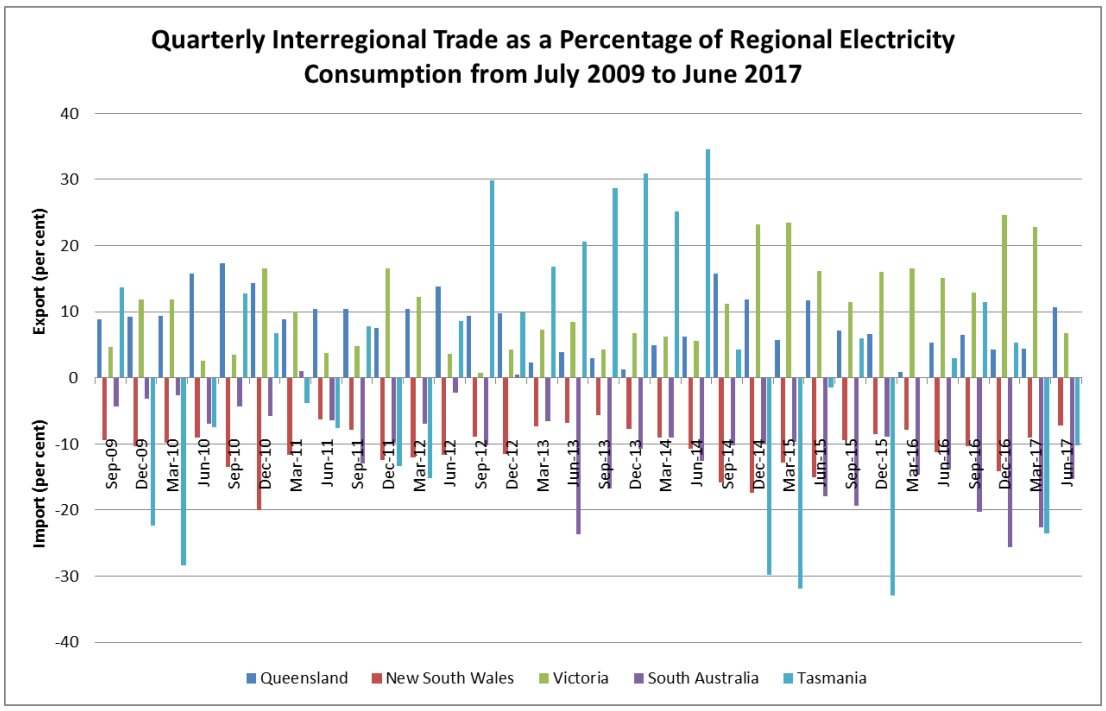

Figure 3.4: Quarterly interregional trade as a percentage of regional electricity consumption from July 2009 to June 2017

Source: `https://www.aer.gov.au/industry-information`.

three characteristics should be considered: seasonality, mean-reversion and spikes (Janczura et al., 2013; Weron, 2006; Benth et al., 2012; Higgs and Worthington, 2008; Eydeland and Wolyniec, 2003). Daily, weekly and yearly seasonality can be observed as electricity demand has cyclical fluctuations that are influenced by weather and everyday activities.

A mean-reversion process describes the inclination of values to go back to the long-term average level. Weron (2006) suggests this effect is much stronger in electricity markets than in other markets. In most cases, the mean-reversion process follows extreme price observations and brings prices back to the previous values (Pilipovic, 2007; Benth et al., 2008). The mechanism behind this effect is as follows. When an increase in electricity demand occurs in the market, expensive generators will enter and be dispatched, pushing up the price. Once the demand falls, these generators will leave the market and the price will return to its normal level.

Unanticipated weather changes or outages of equipment are likely to cause unexpectedly extreme observations or so-called spikes in spot prices (Benth et al.,

2012). Price spikes force market participants, especially generators and retailers to face higher risks. For instance, retailers sign contracts with customers to sell electricity at an agreed price while, at the same time, being vulnerable to dramatic fluctuations in the wholesale prices. Two energy retailers - GoEnergy in April 2016 and Urth Energy in February 2017 - become insolvent partly due to financial distress related to their exposure to high wholesale prices. One way to hedge this risk is to participate in the derivative markets to reduce the uncertainty in prices. Over-the-counter (OTC) markets and the Australian Securities Exchange (ASX) provide a variety of traded products, including exchange-traded swap futures (also known as AU$300 cap futures).

Chapter 4

Methodology

This chapter illustrates the methodology adopted in this thesis. In order to analyse the multivariate interdependence among regional electricity prices, a method that could provide a systemic view was considered preferable. Therefore, this thesis adopts a framework that has originally been suggested to study systemic risks in finance and insurance sector (Billio et al., 2012). Furthermore, regression analysis is also included to examine the predictive power of the constructed measures of connectedness.

The price pattern of electricity resembles that of financial assets and this feature justifies applying a methodology from finance to model the behaviour of electricity prices (Ciarreta and Zarraga, 2012). In fact, the overwhelming majority of electricity-pricing models are adapted from the financial econometrics literature (Christensen et al., 2012).

4.1 Deseasonalisation

Even though evidence shows that the price series in electricity markets is similar to that in financial markets, the different properties still can not be ignored in the sense that electricity still has to be considered as a basically non-storable commodity. These peculiarities cause inelastic demand, with extreme price observations happening at times as demand and supply must be instantly matched.

Furthermore, electricity prices show a strong seasonal pattern[1] as consumers have regular activities at different times within a day, on different days within a week and in different seasons across a year. This study conducts a preprocessing procedure[2] which removes the long-term seasonal component (LTSC) as well as the short-term seasonal component (STSC). In other words, we assume the observed price (P_t) for each state is composed of a stochastic part (X_t) and a deterministic part which comprises LTSC (l_t) and STSC (s_t):

$$P_t = l_t + s_t + X_t \tag{4.1}$$

With regard to deseasonalisation, three methods are mainly used in the literature to deal with seasonality in energy prices (Janczura et al., 2013; Weron, 2014; Ignatieva and Trück, 2016). The first consists of dummies or piecewise constant functions (e.g. Lucia and Schwartz, 2002; Higgs and Worthington, 2008; Gianfreda and Grossi, 2012; Fanone et al., 2013). This method is straightforward, but the estimated trend has abrupt changes, and thus lacks smoothness, which is not credible. The second consists of sinusoidal functions (e.g. Pilipovic, 1997; Cartea and Figueroa, 2005; Geman and Roncoroni, 2006; Bierbrauer et al., 2007; Benth et al., 2012; Green et al., 2014; Clements et al., 2015). Even though a sinusoidal LTSC captures the cyclical pattern in price series, sinusoidal functions are too regular to reflect the continuing structural changes in the NEM. The third comprises the wavelet transform (e.g. Stevenson et al., 2006; Bierbrauer et al., 2004; Weron, 2006; Janczura and Weron, 2010; Schlueter, 2010; Aderounmu and Wolff, 2014b; Ignatieva and Trück, 2016). As this decomposition is flexible and able to model irregular patterns in the long-term trend, the deseasonalisation in the present study refers to wavelet decomposition.

A wavelet family is composed of a father wavelet ϕ to model the smooth trend, and a mother wavelet ψ to fit the deviation from the trend. The price series P_t

[1] Aderounmu and Wolff (2014a), Aderounmu and Wolff (2014b) and Ignatieva and Trück (2016) remove seasonality to analyse the stochastic component.

[2] Before deseasonalisation, the logarithm transformation is conducted to normalise the data. In consideration of some negative prices, we shift all prices up by AU$1001 to make them consistently positive and calculable, as -1000 AUD/MWh is the floor price in the NEM.

will be projected onto one father and a few mother wavelets with the index of $k = 0, 1, 2, \ldots$ and $s = 2^j, j = 0, 1, 2, \ldots, J$.

$$P_t = F_J + M_J + M_{J-1} + \cdots + M_1 \tag{4.2}$$

where

$$F_J = \sum_k f_{J,k}\phi_{J,k}(t) \; and \; M_j = \sum_k m_{j,k}\psi_{j,k}(t) \tag{4.3}$$

The coefficients $f_{J,k}, m_{J,k}, m_{J-1,k}, \ldots, m_{1,k}$ represent the weight of corresponding wavelet function in the overall approximation. Specifically, the wavelet functions are

$$\phi_{J,k}(t) = 2^{-J/2}\phi(\frac{t - 2^J k}{2^J}) \; and \; \psi_{j,k}(t) = \psi(\frac{t - sk}{s})/s \tag{4.4}$$

The approximation of l_t in Equation 4.1 is realised by the reconstruction based on Equation 4.2. To be specific, F_J gives a rough approximation of P_t. Adding M_j further provides a higher refinement in the approximation, thus yielding a better estimation. More mother wavelets of lower scales ($j = J - 1, J - 2, \ldots$) are added until the desired accuracy is reached. The obtained estimator then becomes the long-term seasonal component (LTSC).

As s changes, $\psi_j(t)$ covers different frequency ranges (large values of the scaling parameter s correspond to small frequencies, or large scale ψ; small values of s correspond to high frequencies or very fine scale ψ). On the other hand, changing the parameter k allows us to move the time localisation centre: each $\psi_{j,k}(t)$ is localised around t=k. The advantage of this time-frequency description of P_t is that $\psi_{j,k}$ have time-widths adapted to their frequencies: high frequency $\psi_{j,k}$ is very narrow, while low frequency $\psi_{j,k}$ is much broader. As a result, the wavelet transform is able to zoom in on very short-lived high-frequency phenomena, such as spikes in series (Daubechies, 1992).

Data in this present study consists of daily and half-hourly spot prices between 1 July 2010 and 30 June 2017 to reflect the recent trend and changes in the interregional relationships in the NEM. Daily spot prices are included only for

estimating the LTSC by the recursive filter approach which is suggested as generally performing better in the comparative studies of Janczura et al. (2013) and Nowotarski et al. (2013). To be specific, observations which are beyond three standard deviations after first-time deseasonalisation are regarded as outliers because these fast-disappearing spikes have significant and always unnecessary effects on the long-term estimation. In the estimation of the LTSC, they are temporarily discarded. The removal of the LTSC is implemented as follows:

1. Remove the long-term seasonal part S from the original series P by wavelet decomposition. Define D as the time series after removal of the LTSC S.

2. Replace observations which are outside three standard deviations with the average value in D . Define D^* as the time series after the replacement.

3. Add back the first-time long-term seasonal part S to D^*. Define the summation as P^*.

4. Estimate the long-term seasonal part S^* for P^* by wavelet decomposition.

5. Subtract S^* from the original series P and get the final series D^{**}.

Not only the LTSC but also the STSC is estimated separately for each state. Therefore, the deseasonalisation reduces the impact of time-differences such as daylight saving across states. In the estimation of the STSC, half-hourly prices are classified according to days in a week as well as the corresponding month, for example, Mondays in January, Tuesdays in January,..., Wednesdays in February,..., Sundays in December. Noticeably, public holidays are regarded as Sundays. This classification considers the weekly as well as yearly patterns in the STSC. Initially, 84 (7×12) groups are classified. Except for the inter-day periodicity, the intra-day periodicity in half-hourly prices is also considered in the same vein. In one day, there are 48 intervals; thus, 4032 (84×48) groups are finalised. The STSC for each group is calculated as the median value in the group. The reason for this selection is that the median value is less impacted upon by extreme observations compared to the mean value; thus, the median value is more representative.

4.2 Analysis Framework in Billio et al. (2012)

The analysis framework developed by Billio et al. (2012) comprises two components. First, principal component analysis (PCA) is originally employed to demonstrate the degree of risk concentration in financial markets before the GFC outbreak in 2008. Second, the Granger causality network is adopted to identify the risk source and the risk sink. In other words, this method aims to reveal the influential and vulnerable financial institutions and sectors. As this present study intends to shed light on the connectedness of the five-region system in the sense of electricity price contagion, the framework in Billio et al. (2012) is preferable in regard to our research question. Furthermore, these two methods have been separately used in the context of electricity prices (Zachmann, 2008; Dempster et al., 2008; Castagneto-Gissey et al., 2014).

4.2.1 Principal Component Analysis

Principal component analysis (PCA) is a technique in which the total variance of a set of time series data is decomposed into orthogonal factors of decreasing explanatory power. Let X^i be the price in each market $i, i = 1, \ldots, N$, and suppose that the vector of observations $X' = (X^1, X^2, \ldots, X^N)$ has a variance-covariance matrix Σ. Let $\lambda_{(1)}$ be the largest eigenvalue of Σ and $\gamma_{(1)}$ be the corresponding eigenvector. Hence the first principal component can be written as $Y_{(1)} = \gamma'_{(1)}X$. Similarly, $\gamma_{(2)}$ is the eigenvector corresponding to the second largest eigenvalue of Σ, namely $\lambda_{(2)}$. Another expression is to orthogonally decompose the matrix Σ as follows:

$$\Sigma = P\Lambda P' \tag{4.5}$$

where Λ is a diagonal matrix whose diagonal elements are $\lambda_{(1)}, \lambda_{(2)}, \ldots, \lambda_{(N)}$; and P is an orthogonal matrix of order N whose k th column is the eigenvector $\gamma_{(k)}$ corresponding to $\lambda_{(k)}$. The vector of principal component variate, $Y' = (Y_{(1)}, Y_{(2)}, \ldots, Y_{(N)})$, can be written as $Y = P'X$. The variance-covariance matrix

of Y is given by $var(Y) = P'\Sigma P$. By substituting Σ

$$var(Y) = P'(P\Lambda P')P = \Lambda \tag{4.6}$$

which shows that the principal component variates in Y are uncorrelated and the variance of $Y_{(k)}$ is given by $\lambda_{(k)}$.

The total risk of the system is defined as

$$\Omega \equiv \sum_{k=1}^{N} \lambda_{(k)} \tag{4.7}$$

and the cumulative risk fraction related to the first n principal components as

$$w_n \equiv \sum_{k=1}^{n} \lambda_{(k)} / \sum_{k=1}^{N} \lambda_{(k)} \tag{4.8}$$

It provides general evidence for how a common price pattern is able to explain most of the national price variation as a whole.

4.2.2 Granger Causality Network

To assess the interdependence structure in the system, it is important to measure the degree of connectedness as well as the directions of these relationships. The directed connectivity network is constructed under a predictive interpretation. Time series X_j Granger-causes time series X_i if past information contained in X_j is helpful for predicting X_i after considering the information in past X_i, and vice versa. Let $X_{i,t}$ and $X_{j,t}$ be two stationary time series. The model representing their linear inter-relationships is as follows:

$$\begin{aligned} X_{i,t+1} &= a^i X_{i,t} + b^{ij} X_{j,t} + e_{i,t+1} \\ X_{j,t+1} &= a^j X_{j,t} + b^{ji} X_{i,t} + e_{j,t+1} \end{aligned} \tag{4.9}$$

where $e_{i,t+1}$ and $e_{j,t+1}$ are two uncorrelated white noise processes and others are coefficients in the model. Among them, b^{ij} and b^{ji} convey the information that matters. If b^{ij} is significantly different from zero, X_j is said to Granger-cause

X_i. Similarly, X_i Granger-causes X_j if b^{ji} is non-zero at some confidence level. The rejection of a linear Granger causality relationship is based on $\tilde{b}^{ij} = \hat{b}^{ij}/\hat{\sigma}^j$, where $\hat{\sigma}^j$ is the heteroskedasticity and autocorrelation consistent estimator which is also called the Newey-West estimator. Therefore, the network is established according to the indicator:

$$(j \to i) = \begin{cases} 1 & \text{if j Granger-causes i,} \\ 0 & \text{otherwise} \end{cases} \tag{4.10}$$

and obviously $(j \to j \equiv 0)$. The degree of Granger causality shown among regional prices can be seen as a proxy for spillover effects in the NEM. The dynamic Granger causality networks of electricity spot prices are then calculated by adopting rolling windows.

Once the network is built, the*Dynamic Causality Index* (also known as *Degree of Granger Causality*) is defined as the ratio of statistically significant Granger-causality relationships to all possible directed relationships in the network:

$$DCI \equiv \frac{1}{N(N-1)} \sum_{i=1}^{N} \sum_{j \neq i} (j \to i) \tag{4.11}$$

For each node that represents each regional market, the degree of node j is defined as

$$\begin{aligned} In - degree : (S \to j) &= \sum_{i \neq j} (i \to j) \\ Out - degree : (j \to S) &= \sum_{i \neq j} (j \to i) \end{aligned} \tag{4.12}$$

where S is the whole system. A higher in-degree means greater susceptibility of electricity prices in the specific region j to price volatilities in other regions, and vice versa. In line with that, a higher out-degree means that electricity prices in specific region j are comparatively influential in shaping prices in other regions.

4.3 Regression Analysis

Based on the generated interconnectedness measures, regression analysis is conducted on the preprocessed price series to examine the predictive power of the estimated multivariate relationships. In the predictive model, dynamic overall connectedness measures and other explanatory variables are calculated every day based on the deseasonalised half-hourly spot prices over the last seven days, equivalent to 336 observations. To be specific, the width of a rolling window is seven days (336 observations) and the distance between two adjacent rolling windows is one day (48 observations). If the rolling window is too narrow, such as only one day, the contained information is not enough to obtain reasonable values for the overall interconnectedness. If it is too wide, such as one month or one quarter, the measures could not capture the most recent conditions of the whole market, thereby having less predictive power.

The five measures derived from the descriptive analysis considered in the model are: (1) cumulative risk fraction of the first principal component; (2) cumulative risk fraction of the first two principal components; (3) dynamic causality index; (4) in-degree of the individual state; (5) out-degree of the individual state. Other explanatory variables of concern are statistics calculated from the deseasonalised half-hourly spot prices over the last seven days. Among these variables, two ways are used to measure the volatility over the sample period, namely, range and standard deviation. The range is defined as:

$$Range_{i,T} = H_{i,T} - L_{i,T} \tag{4.13}$$

where $H_{i,T}$ and $L_{i,T}$ are highest and lowest values, respectively, of ith time series over the period T. And the standard deviation is defined as:

$$SD_{i,T} = \sqrt{\frac{\sum_{t=1}^{T}(p_{i,t} - \bar{p}_{i,T})^2}{T-1}} \tag{4.14}$$

where $p_{i,t}$ is tth half-hourly value of ith time series over the period T and $\bar{p}_{i,T}$ is

the average value in this period. This standard deviation is the square root of an unbiased estimator of the variance. Spikes refer to any value whose original price is over 300 AUD/MWh, which follows the cap price set by the Austrlian electricity swap futures traded in the ASX (Australian Securities Exchange). See Figure 4.1 for a summary of all explanatory variables.

Table 4.1: Explanatory variables in the predictive model. They are calculated based on the deseasonalised half-hourly spot prices over the last seven days. The sample period is from 1 July 2010 to 30 June 2017.

Variable	Factor	Description
Mean	Price	Average spot price
Maximum		Maximum spot price
Minimum		Minimum spot price
Range	Volatility	Range of the sample
Range2		Average daily range
SD.		Standard deviation of the sample
SD.2		Average daily standard deviation
Skewness	Distribution	Skewness of the sample
#Spikes		Number of spikes over the sample
PCA1	PCA	Cumulative risk fraction of PC1
PCA2		Cumulative risk fraction of PC1-2
DCI	GC Network Analysis	Dynamic causality index
In-degree		In-degree of the individual state
Out-degree		Out-degree of the individual state

The primary daily statistics of the deseasonalised half-hourly spot prices are dependent variables of interest in the predictive model. See Table 4.2 for a summary.

Two estimation methods are considered in this present study. The first one is ordinary least squares (OLS) that provides parameters which describe the relationship quantitatively in a linear regression model. The model is assumed to be

$$y_t = V'_{t-1}\beta + z\alpha + \epsilon_{t-1} \tag{4.15}$$

There are K regressors in V_{t-1}, not including a constant term z. The independent

Table 4.2: Summary of dependent variables in the predictive model. They are calculated daily based on the deseasonalised half-hourly spot prices during the day. The sample period is from 1 July 2010 to 30 June 2017.

Variable	Factor	Description
Mean	Price	Average spot price
Maximum		Maximum spot price
Minimum		Minimum spot price
Range	Volatility	Range of the sample
SD.		Standard deviation of the sample
Skewness	Distribution	Skewness of the sample
#Spikes		Number of spikes over the sample

variables V_{t-1} considered in the model are shown in Table 4.1.

Another method is least absolute deviations (LAD). Under the same model specification, the various quantiles of the distribution of dependent variables are examined in quantile regression. The linear quantile regression model can be defined as

$$Q[y|V,q] = V'\beta_q \text{ such that } Prob[y \leq V'\beta_q|V] = q, 0 < q < 1. \tag{4.16}$$

where V has K regressors and y represents the dependent variable. As a nonparametric model, the quantile regression model has a richer specification as the coefficients in Equation 4.16 are indexed by q which can vary continuously between zero and one. Thus there are an infinite number of possible parameter vectors. The estimator, b_q of β_q for a specific quantile is computed by minimising the function

$$F_n(\beta_q|y,V) = \sum_{i:y_i \geq V_i'\beta_q}^{n} q|y_i - V_i'\beta_q| + \sum_{i:y_i \leq V_i'\beta_q}^{n} (1-q)|y_i - V_i'\beta_q| = \sum_{i=1}^{n} g(y_i - V_i'\beta_q|q) \tag{4.17}$$

where

$$g(e_{i,q}|q) = \left\{ \begin{array}{ll} qe_{i,q} & \text{if } e_{i,q} \geq 0 \\ (1-q)e_{i,q} & \text{if } e_{i,q} < 0 \end{array} \right\}, e_{i,q} = y_i - V_i'\beta_q \tag{4.18}$$

It is reasonable to regard the coefficients $\beta(q)$ as features of the distribution of $y|V$ rather than fixed parameters (Greene, 2012). Any qualitative difference or the lack of such differences between estimates in different quantiles is an interesting property of the sample.

Chapter 5

Data and Descriptive Analysis

This chapter presents the deseasonalisation process and the main results from the analysis framework adopted from Billio et al. (2012). Based on principal component analysis (PCA) and Granger causality network analysis, the overall interconnectedness measures are calculated and demonstrated to be related to the price pattern in the NEM.

As the originally recorded spot prices in the NEM, half-hourly prices are analysed because we intend to capture the dynamic price transmission in a more accurate way. Moreover, high-frequency data could provide rather rich information, compared with daily prices.

5.1 Deseasonalisation

This section introduces the data analysed in our study. The first two subsections provide the detailed procedure of preprocessing. The last subsection summarises the descriptive statistics generated through this procedure. As explained in Chapter 4 'Methodology', all prices are shifted by AU$1001 to ensure values are positive before the logarithm transformation, as -1000 AUD/MWh is the floor price in the NEM. The natural logarithm of the shifted prices is then used in the deseasonalisation. Deseasonalisation is employed to remove seasonality from the original data beforehand, and our entire analysis is based on the stochastic part of half-hourly spot prices, following Aderounmu and Wolff (2014a), Aderounmu

and Wolff (2014b) and Ignatieva and Trück (2016). The average daily price is only adopted to estimate the long-term seasonal component in Section 5.1.1.

5.1.1 Long-Term Seasonal Component

The long-term seasonal component (LTSC) is estimated from daily data by the recursive filter approach in which outliers are replaced with normal values to reduce their influence on estimation. As explained in Section 4.1, the estimation is based on the wavelet decomposition with the adoption of Daubechies wavelet family, following Weron (2006), Ignatieva and Trück (2016) and Janczura et al. (2013). $J = 5(2^5 = 32)$ is chosen to roughly correspond with the monthly smoothing.

Figure 5.1 shows the logarithm shifted daily data and their estimated long-term seasonal components (LTSCs). Cross-sectionally, no consistent pattern is found for either the LTSCs or the original prices across five states. With regard to the states, prices in TAS were shaped significantly differently from those in other regions. The pattern in TAS had less number of spikes but frequent fluctuations of limited size. The prices ratcheted up between 2015 and 2016 due to low dam levels combined with an outage of the Basslink interconnector to the mainland. Among the other four states, NSW had relatively less extreme observations. Furthermore, some commonality was found in the LTSC of NSW and that of QLD. Both QLD and SA had spike clusters and prices in these two regions were comparatively more volatile. From a time-series perspective, an upward trend was revealed from the LTSCs of the five jurisdictions in the NEM, especially for the year 2016 - 2017. The carbon pricing in 2012 - 2014 raised prices up to a slightly higher plateau, with this shown in the LTSCs of each individual market, especially in NSW, QLD and VIC.

5.1.2 Short-Term Seasonal Component

After removal of the LTSC, the short-term seasonal component (STSC) refers specifically to yearly, weekly and daily cycles obtained from the remaining component. The STSC is mainly dependent on electricity demand which is inelastic

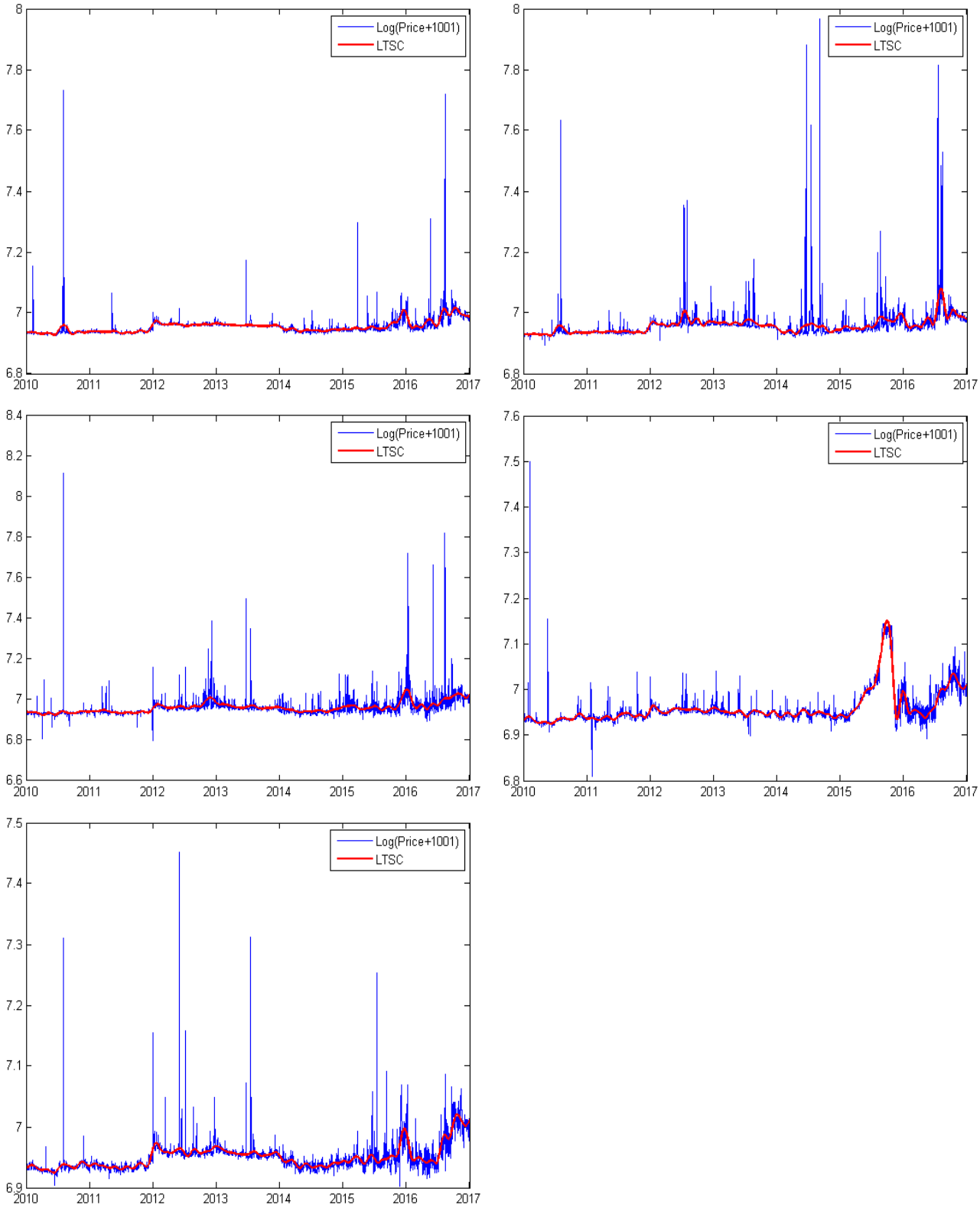

Figure 5.1: Daily spot prices after the logarithm transformation and the corresponding long term seasonal components. Original prices are shifted by AU$1001 and natural logarithms are taken before deseasonalisation. The LTSC is estimated based on the recursive filter approach in which the wavelet transform is adopted. The scale applied is $J = 5$ ($2^5 = 32$), approximately one month. The sample data of NSW (upper left panel), QLD (upper right panel), SA (middle left panel), TAS (middle right panel) and VIC (lower left panel) is from 1 July 2010 to 30 June 2017.

and has its own regularities which include daily, weekly and yearly cyclicalities. Ambient temperature also affects electricity demand at times. For example, when the weather is too cold or too hot, the high demand for electricity is due to the usage of heaters or air-conditioners, respectively, which will cause the tight supply-demand balance and increase the price.

We consider daily, weekly and yearly patterns at the same time in the estimation of the STSCs. As explained in Section 4.1, all values in a time series are grouped according to similarities in their time stamp, weekday and month. The median of this group is treated as the STSC at a specific time. For example, the median of all prices at 12 pm on Mondays in January is regarded as the STSC at this specific time stamp. From the yearly pattern of the STSC, electricity demand for the year peaks in summer due to the wide use of air conditioners. This finding could be drawn from all five states. As shown in Figure 5.2, NSW is taken as an example, with the other states illustrated from Figure A.1 to Figure A.4. According to Table 5.1, even after removal of the yearly STSCs, the majority of the volatility remains unexplained.

As shown in the yearly pattern in Figure 5.2, significant differences are apparent between weekly patterns across the months. This is the reason why it is more appropriate to remove the yearly pattern rather than only the weekly pattern in the STSC. To gain an insight into the weekly pattern, Figure 5.3 shows the STSC on a weekly basis estimated from the preprocessed spot prices of the five states. No obvious difference is observed between the regions and the daily peak occurs at about 6 pm across the five jurisdictions. In addition, weekdays share similar intra-day patterns and have another peak at around 7 am. These patterns and peaks are closely related to regular business and household activities. The distributions of the STSCs at weekends and on public holidays are evidently different from those on weekdays, and even have their respective patterns. For example, the STSC has a morning peak at 9:30 am on Saturdays, which is later than the morning peak at approximately 7 am on weekdays. This morning peak of demand and price becomes indistinct on Sundays and even invisible on public

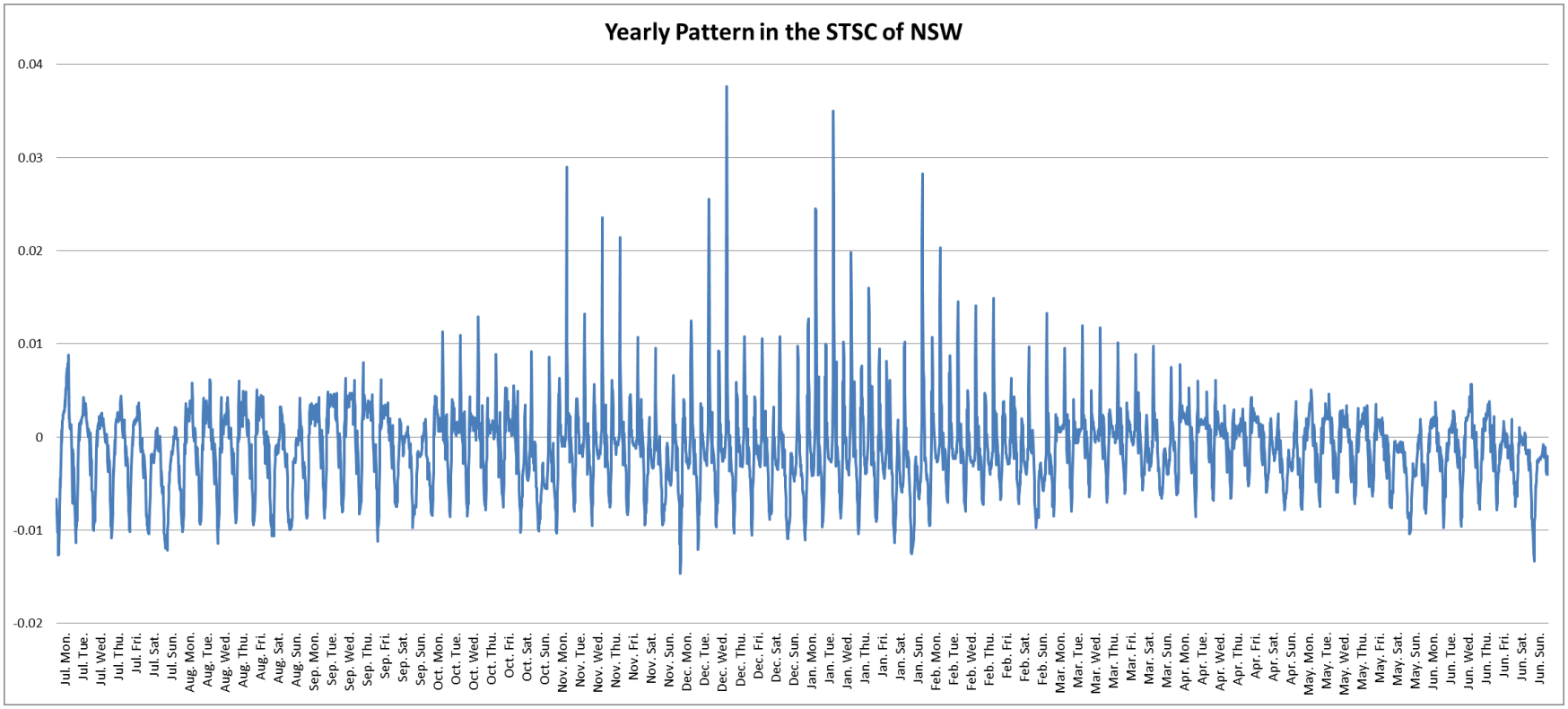

Figure 5.2: Yearly pattern in the STSC estimated from the half-hourly spot prices in NSW. The STSC is estimated after removal of the estimated LTSC. The median of all values at the same time stamp is treated as the STSC of that time.

Table 5.1: Volatility removal in deseasonalisation

Standard Deviation (Half-hourly)				
	Original[a]	Shifted log.[b]	-LTSC[c]	-Yearly STSC[d]
NSW	146.452	0.046	0.042	0.042
QLD	213.601	0.082	0.078	0.078
SA	196.648	0.087	0.083	0.082
TAS	101.207	0.053	0.039	0.039
VIC	86.197	0.039	0.035	0.034

[a] The standard deviation in this column is based on the original time series data of NSW, QLD, SA, TAS and VIC.

[b] The standard deviation in this column is based on natural logarithm of the shifted price series.

[c] The standard deviation in this column is based on natural logarithm of the shifted price series after removal of the estimated LTSCs.

[d] The standard deviation in this column is based on natural logarithm of the shifted price series after removal of the estimated LTSC as well as the STSC on a yearly basis.

holidays.

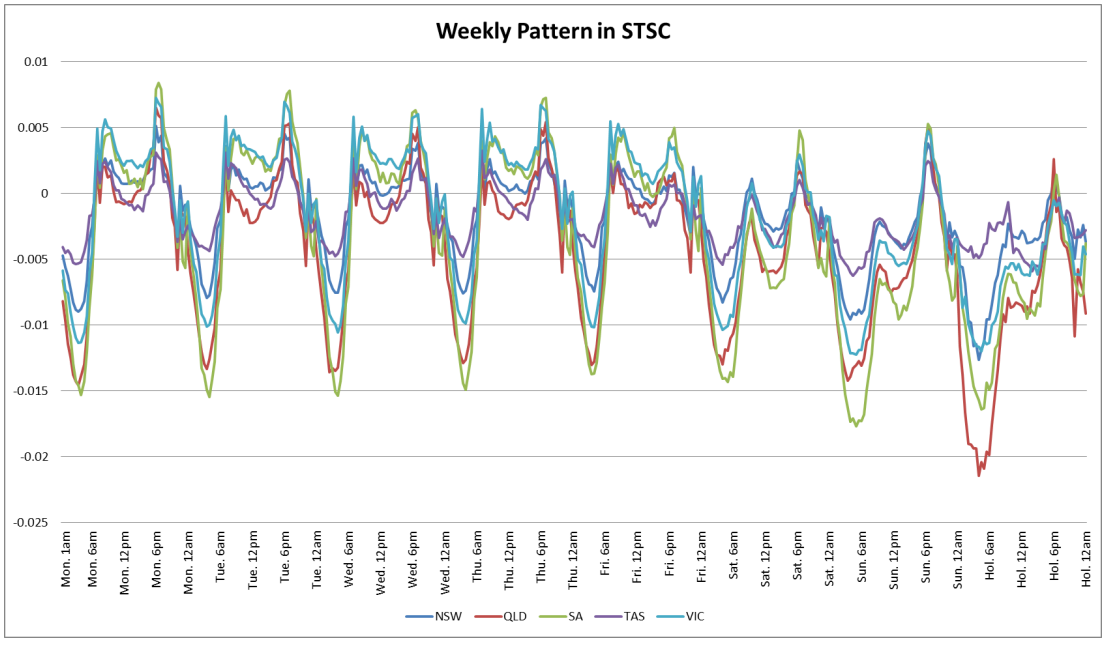

Figure 5.3: Weekly pattern in the STSC estimated from the preprocessed half-hourly spot prices of five states. The STSC is estimated separately after removal of the corresponding LTSC. The median of all values at the same time stamp is treated as the STSC at that time.

5.1.3 Descriptive Statistics

Spot prices used in the descriptive and regression analyses all refer to preprocessed, namely, deseasonalised data. Specifically, the original prices are firstly shifted by AU$1001 and then the natural logarithm is taken. The LTSCs and STSCs are then removed. Table 5.2 shows the descriptive statistics of the sample data which is presented in two different forms, the shifted natural logarithm and the deseasonalised logarithm. As revealed in Table 5.2, SA has the most volatile series in regard to standard deviation. It also has the highest original prices according to the mean and median values. Only SA has negative values in terms of skewness, which means a right-leaning curve and a concentration towards higher values. The time series of all other regions have positive values for skewness, regardless of their forms, indicating a right tail. Several characteristics of SA contribute to this pricing behaviour, such as a relatively high concentration of generator ownership. In SA, AGL Energy has 42% market share in generation capacity according to recent availability, as reported by the Australian Energy Regulator (2017). Other factors include the historical reliance on gas-powered generation; the high proportion of intermittent wind capacity; the frequent rebidding of generators to take advantage of favourable electricity prices; capacity constraints in the interconnectors which limit imports; and recent coal plant closures. In addition, among all regions, SA had the most spikes. QLD also experienced many extreme observations of electricity prices for the seven-year sample period. According to the results of the augmented Dickey-Fuller test, natural logarithms of the original prices for NSW, TAS and VIC follow a non-stationary process. However, after deseasonalisation, each time series becomes stationary, which satisfies the requirement of regression models.

5.2 Descriptive Analysis

This section provides the analytical results of this present study. After preprocessing the original prices, two different approaches are employed to gain an insight

Table 5.2: Summary statistics. The descriptive statistics are calculated based on the half-hourly spot prices of five regional markets from 1 July 2010 to 30 June 2017. Data is in two different forms: the shifted natural logarithm and the deseasonalised logarithm. There are 122736 observations for each series.

	NSW		QLD		SA		TAS		VIC	
	log.	des.	log.	des.	log.	des.	log.	des.	log.	des.
Mean	6.954	0.002	6.958	0.005	6.960	0.003	6.958	0.001	6.950	0.002
Median	6.949	0.000	6.948	0.000	6.950	0.000	6.947	0.000	6.945	0.000
Max.	9.616	2.619	9.608	2.615	9.600	2.629	9.503	2.574	9.303	2.335
Min.	6.750	-0.183	0.000	-6.926	1.459	-5.457	3.799	-3.133	5.215	-1.700
SD[a]	0.046	0.042	0.082	0.078	0.087	0.082	0.053	0.039	0.039	0.034
Skewness	30.110	39.309	9.614	10.128	-1.604	-2.474	6.536	13.308	20.530	31.668
Kurtosis	1362.067	1971.288	733.754	875.907	853.667	1056.094	502.060	1665.841	976.811	1795.287
#Spikes[b]	99	97	656	557	840	541	365	303	103	84
#Days[c]	31	30	225	205	244	204	118	100	41	33
ADF Test[d]	-0.751[e] (p=0.377)	1.984[f] (p<0.001)	-1.970 (p=0.047)	0.390 (p<0.001)	-2.038 (p=0.040)	0.567 (p<0.001)	-1.090 (p=0.253)	1.414 (p<0.001)	-0.741 (p=0.381)	1.645 (p<0.001)

[a] Standard deviation.

[b] The number of spikes in the sample period. Spikes refer to the observations which are above 300[a] AUD/MWh.

[c] The number of days when spikes occur.

[d] Augmented Dickey-Fuller (ADF) test. The null hypothesis is the existence of a unit root in a time series, which means non-stationary. This row lists the test statistics and the corresponding p-value in the bracket.

[e] For logarithmic data, the critical value is -1.942.

[f] For deseasonalised data, the unit of the test statistics is 10^{10} and the critical value is 5.991.

[a]The Austrlian electricity swap futures traded in the ASX (Australian Securities Exchange) have the cap set at 300 AUD/MWh.

into the interdependence in the NEM. The PCA and the Granger causality network provide a systemic perspective to gauge the overall interconnectedness of the NEM. To obtain this in a dynamic way, these measures are calculated every day based on the half-hourly spot prices in seven days, equivalent to 336 observations. To be specific, the width of a rolling window is seven days (336 observations) and the distance between two adjacent rolling windows is one day, 48 observations. If the rolling window is too narrow such as one day, the information contained is not enough to obtain reasonable values for overall interconnectedness. If it is too wide, such as one month or one quarter, the measures could not capture the most recent conditions of the whole market; thus, they would have less accuracy.

5.2.1 Principal Component Analysis

Principal component analysis (PCA) provides a measure of risk concentration which is called 'cumulative risk fraction' in this present study. As explained in Section 4.2, this is the relative importance of the first few principal components in explaining the total variance of a set of time series. Specifically, the percentage of total variance explained by the first few principal components represents the degree of risk concentration in this five-market system. Figure 5.4 demonstrates the dynamics of this measure which is calculated daily in a backward-looking way over the past seven years. The length of the rolling window is seven days, equivalent to 336 observations of half-hourly spot prices.

For PCA, a sudden increase in the measure is always driven by extreme observations or volatile pricing behaviour in the sub-market. For example, the fraction of variance explained by the first principal component rose from approximately 58% to 91% and remained above 95% for more than one week in January, 2011. The reason was a transition to summer when prices always fluctuate significantly and spikes occur frequently due to high electricity demand. In particular, the record electricity demand that occurred in NSW and SA caused a tight supply-demand balance and, consequently, the significant change in the cumulative risk fraction between January and February 2011. The daily price in NSW was nor-

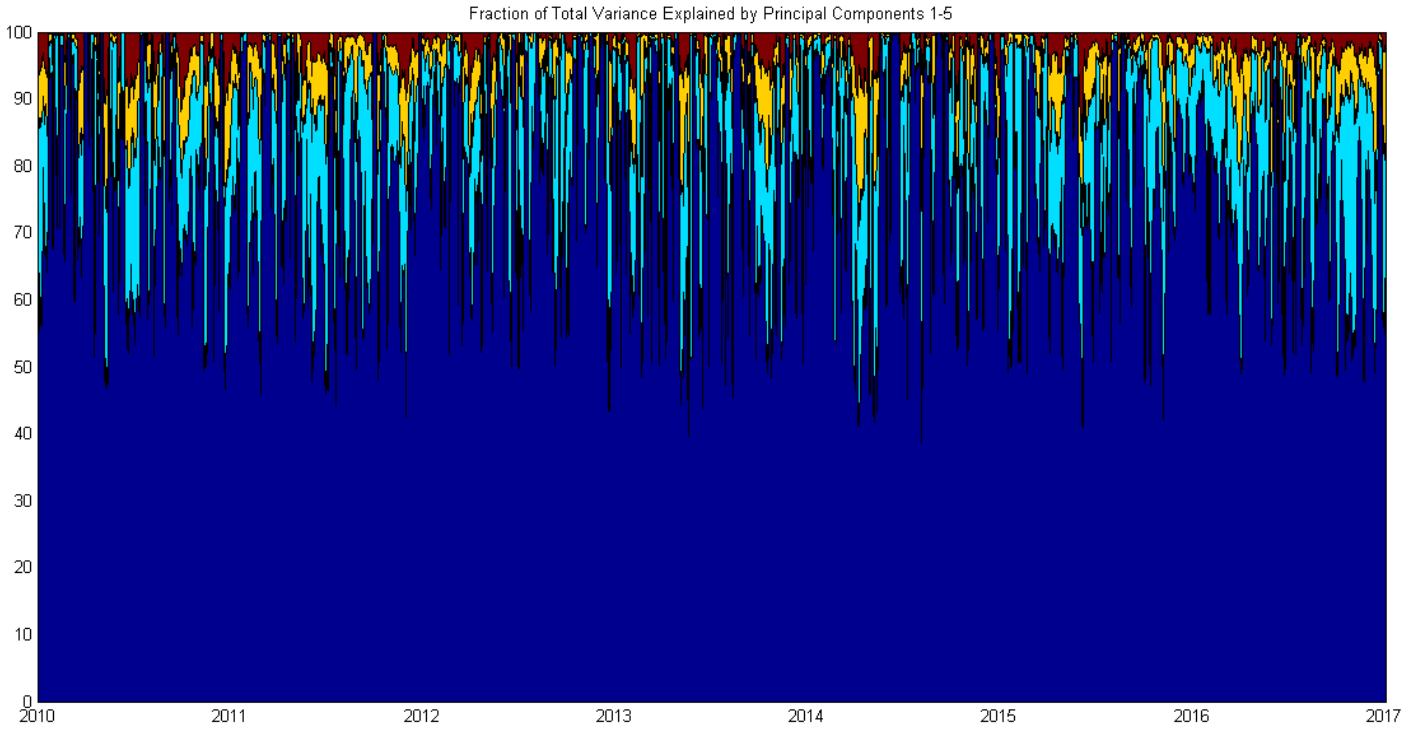

Figure 5.4: Cumulative risk fraction of the 1st-5th principal components. PCA is applied to the deseasonalised half-hourly spot prices of five individual markets from 1 July 2010 to 30 June 2017. The graph gives the fraction of total variance explained by principal components 1-5 [PC 1 (dark blue), PC 2 (light blue), PC3 (yellow), PC4-5 (red)]. The length of the rolling window is 7 days (336 observations).

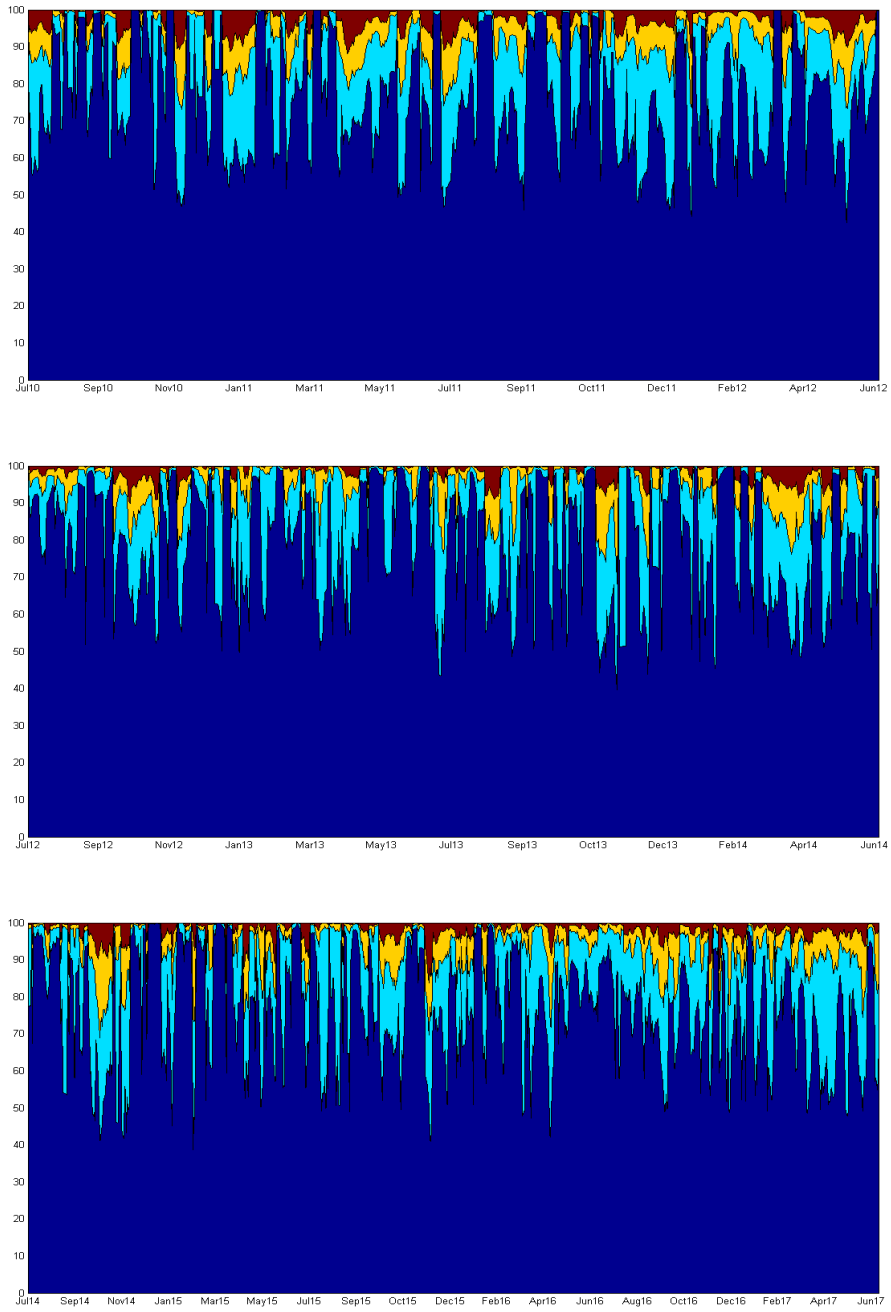

Figure 5.5: Zoom-in of the cumulative risk fraction of the 1st-5th principal components. PCA is applied to the deseasonalised half-hourly spot prices of five individual markets from 1 July 2010 to 30 June 2017. The graph gives the fraction of total variance explained by principal components 1-5 [PC 1 (dark blue), PC 2 (light blue), PC3 (yellow), PC4-5 (red)]. The rolling window has a length of 7 days (336 observations). The entire sample period is divided into three sub-periods based around carbon taxation. The upper panel is from 1 July 2010 to 30 June 2012. The middle panel is from 1 July 2012 to 30 June 2014. The lower panel is from 1 July 2014 to 30 June 2017.

mally below 100 AUD/MWh but jumped above 1000 AUD/MWh in the first two days of February 2011. Similarly, in the summer 2014 - 2015, prices in QLD rose

sharply above 1000 AUD/MWh several times due to record demand and rebidding, also resulting in dramatic changes to this measure. The fraction of variance explained by the first principal component was above 90% for half a month, and even above 95% for most of the time. Another example occurred in May 2013 when the measure steadily went up due to increasing prices in SA. Except for the fact that prices fluctuated around 100 AUD/MWh, the daily spot price reached 409.01 AUD/MWh and 611.86 AUD/MWh on 17th May and 3rd June, respectively. The increase was caused by tight supply conditions as some traditional plants shut down temporarily.

Another possibility for observing the increase in this measure is that the five individual markets are exposed to common risks. Immediately before the execution and the repeal of the carbon pricing policy, an upward trend occurred in the measure, indicating the uncertainty that was widely recognised by the market. The dynamic cumulative risk fraction of the first principal component rose to 99.81% on 30 June, more than twice as much as that on 2 June, namely 43.78%. The impact of this policy on principal components is elaborated in Section 5.2.3.

Regardless of the cumulative risk fraction of the first principal component (PC1) or of the first two principal components (PC1-2) shown in Table 5.3, the risk concentration significantly rose in the first year of the carbon pricing policy. The average of PC1 rose from 75% to 82%, and the average of PC1-2 changed from 92% to 95%. This was partly due to the high demand and rebidding in SA and VIC as well as the congestion and tight supply conditions in QLD during the summer 2012 - 2013 (Australian Energy Regulator, 2013). In the financial year 2016 - 2017, the maximum PC1 decreased whereas the minimum PC1 climbed to a record high level. This indicates that, unlike the past situation where the risk in a single market drove this measure, the whole market is now facing more uncertainty.

Table 5.3: Summary statistics of cumulative risk fraction of the first and first two principal components. The measure is based on the deseasonalised half-hourly spot prices for the past seven years. Cumulative risk fraction refers to the fraction of total variance explained by the first (PC1) and first two (PC1-2) principal components. The sample period refers to the financial year in Australia. For example, 2010 - 2011 is from 1 July 2010 to 30 June 2011.

	PC1				PC1-2			
	Mean	Max.	Min.	SD.	Mean	Max.	Min.	SD.
Full Sample	77.43	99.99	38.77	16.01	92.99	100.00	68.11	6.64
2010 - 2011	77.36	99.99	46.61	16.17	91.90	100.00	73.09	7.60
2011 - 2012	75.21	99.93	42.57	15.61	92.10	99.98	73.34	6.01
2012 - 2013	81.79	99.85	43.36	14.82	95.01	99.97	76.28	5.40
2013 - 2014	77.10	99.67	39.59	17.66	93.04	99.93	68.11	7.37
2014 - 2015	79.75	99.94	38.77	17.84	93.45	99.98	68.87	7.58
2015 - 2016	77.55	99.53	40.89	14.92	93.66	99.83	69.71	6.01
2016 - 2017	73.28	97.88	47.77	13.18	91.72	99.46	74.43	5.52

5.2.2 Granger Causality Network

Apart from the cumulative risk fraction, another interconnectedness measure adopted in this present study is based on bidirectional Granger causality networks. The network is composed of nodes and links. Each node represents an individual state and each arrowed link represents the Granger causality relationship between each pair of regions. If the time series of state B is Granger-caused by that of state A at a significant level, then a link is directed from node A to node B in the connectivity network. The ratio of the number of significant links over the number of all possible links is regarded as an overall measure of the linear inter-connection. To be specific, the Granger causality network is built every day according to prices over the past seven days as shown in Figure 5.6. In addition, the corresponding in-degree and out-degree of individual states are drawn in Figure 5.7.

Three noticeable spikes occurred in the dynamic causality index during the sample period. The first one was in the 2010 - 2011 summer when the high demand for electricity caused the shortage in the whole market. At that time, VIC

and TAS had the most susceptible prices among the NEM jurisdictions, which could be spotted from the high in-degree values, while those in NSW, QLD and SA had influence on other regions. As NSW, QLD and SA all experienced extremely high spot prices during that time, this is evidence of the negative consequences from price contagion. The daily spot price in NSW moved above 1200 AUD/MWh on 1 and 2 February whereas it is normally below 50 AUD/MWh. The daily spot price in QLD jumped above 1000 AUD/MWh as well on 2 February and in SA, it changed abruptly even to 2347.11 AUD/MWh on 31st January from 68.93 AUD/MWh on the previous day.

Another spike occurred just before carbon pricing commenced. SA and VIC had very volatile electricity prices and affected the other states, especially TAS. In SA, the daily spot price declined below zero from 28th June, 2012, hit the bottom of -103.16 AUD/MWh on 30th June and jumped to 283.88 AUD/MWh two days later. The third time that the dynamic causality index reached 0.7 or above was around June 2013 when SA faced very tight supply conditions due to temporary plant closures. The high prices in SA were not only due to the power shortage, but major generators also undertook opportunistic bidding and raised the spot price (Australian Energy Regulator, 2013). This induced fluctuations in the prices of other sub-markets, including VIC and TAS. When a substantial reduction occurred in generation capacity due to the closure of Alinta's Northern power station in SA in June 2016, the dynamic causality index (DCI) also increased as this event affected the entire market.

From a network perspective, the different jurisdictions in the NEM are not closely connected in the sense that there are only 3.34 Granger causality relationships on average among the 20 possibilities. As shown in Table 5.4, the yearly average of this measure has reached the highest value through time for the financial year 2016 - 2017, while the maximum during that year was the lowest. The reasons are complex and multiple, including a tight supply-demand balance due to shutdown of several major plants and record demand in summer, as well as local spikes due to transmission constraints.

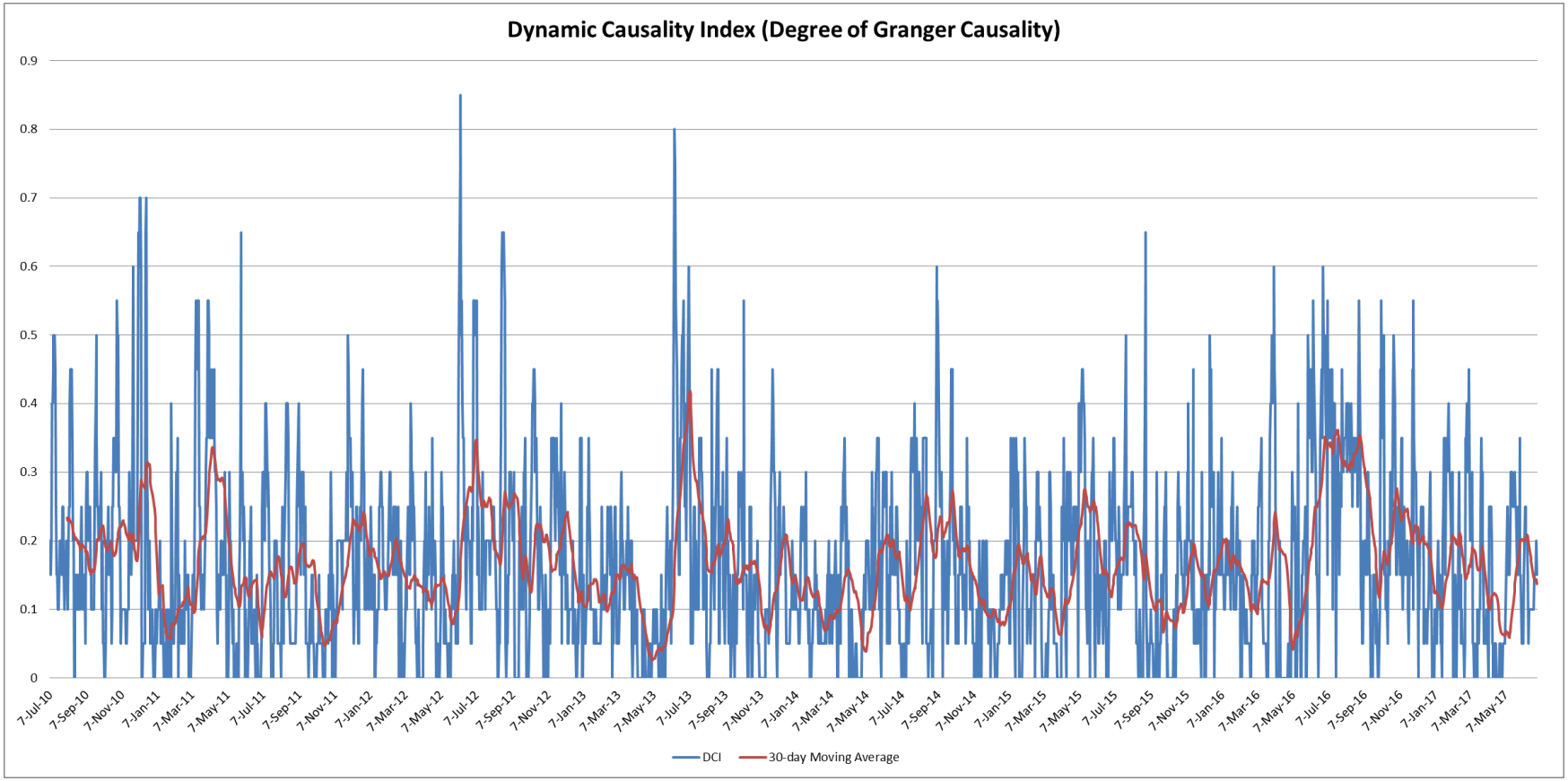

Figure 5.6: Dynamic causality index (degree of Granger causality) and its 30-day moving average line. The dynamic causality index (DCI) is the number of links as a percentage of all possible links. The link represents the linear Granger causality relationship at the 1% level of significance. It is calculated on a daily basis from the deseasonalised half-hourly spot prices of five individual markets from 1 July 2010 to 30 June 2017. The rolling window length is 7 days (336 observations).

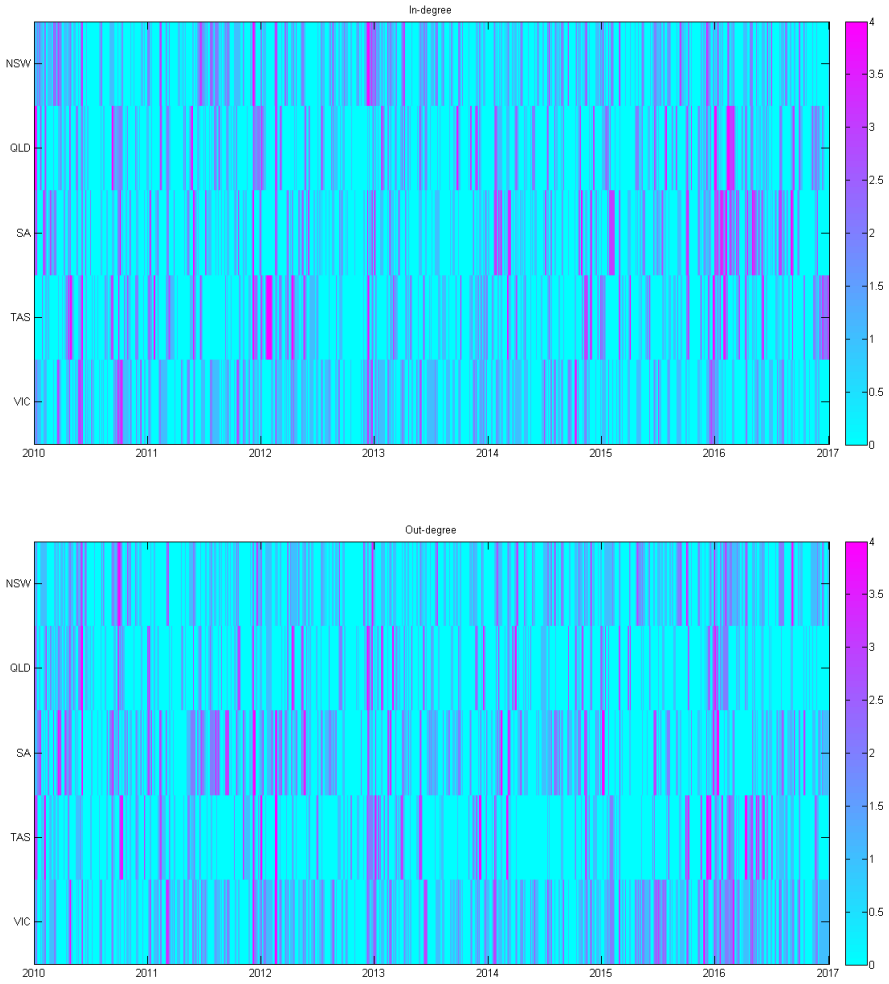

Figure 5.7: In-degree and out-degree values of the five regional markets in the NEM. Red (blue) indicates larger (smaller) values in measures of in-degree and out-degree, as shown on the right side column. In-degree is the number of links that end at a particular node and out-degree is the number of links that start at a particular node in a network. The link here represents the linear Granger causality relationship at the 1% level of significance. The bars on the y-axis represent, from top to bottom, NSW, QLD, SA, TAS and VIC, respectively. The rolling window length is 7 days (336 observations).

Table 5.5 illustrates the role generally played by each region in the Granger causality network constructed from the deseasonalised spot prices. Over the sample period, NSW was most vulnerable to price changes of the other states and SA was the most influential state. However, SA was also relatively easily affected by the other states. Given that both NSW and SA are net electricity importers most of the time, this reflects that they are quite dependent on the power supply from other states, and that their own power sources are not sufficient to support their consumption. The difference between NSW and SA is that one

Table 5.4: Summary statistics of the dynamic causality index. The dynamic causality index (DCI) is the number of links as a percentage of all possible links. The link represents the linear Granger causality relationship at the 1% level of significance. It is calculated on a daily basis from the deseasonalised half-hourly spot prices of five individual markets from 1 July 2010 to 30 June 2017. The rolling window length is 7 days (336 observations).

	Mean	Max.	Min.	SD.	#Obs.
Full Sample	0.167	0.850	0	0.134	2551
2010 - 2011	0.184	0.700	0	0.153	359
2011 - 2012	0.156	0.850	0	0.125	366
2012 - 2013	0.173	0.800	0	0.152	365
2013 - 2014	0.147	0.600	0	0.111	365
2014 - 2015	0.158	0.600	0	0.122	365
2015 - 2016	0.161	0.650	0	0.137	366
2016 - 2017	0.193	0.550	0	0.132	365

of the domestic power sources on which SA relies is wind which is intermittent in nature, leading to a volatile pattern in the interregional trade. On the other hand, NSW relies on fossil fuels. And VIC is the second most influential state as it is a net exporter of electricity and, geographically, it is at a very central position .

Table 5.5: Yearly average of in-degree and out-degree over the full sample period. In-degree is the number of links that end at a particular node and out-degree is the number of links that start at a particular node in a network. The link here represents the linear Granger causality at the 1% level of significance. The rolling window length is 7 days (336 observations).

	NSW	QLD	SA	TAS	VIC
In-degree	0.691	0.657	0.671	0.668	0.660
Out-degree	0.647	0.519	0.810	0.586	0.784

According to the trend of in-degree and out-degree values shown in Figure 5.8, SA has become more and more reliant on outer power sources. This finding can also be supported by the increasing import of electricity. This loss of independence has resulted in a rising level of in-degrees and a falling level of out-degrees, implying that prices in SA incline to be affected and less influential. Conversely,

VIC has an ascending out-degree and a descending in-degree, which means that VIC is able to exert greater influence on other states than before. This is partly due to the role it plays in the NEM as a net exporter, and also to its highly-connected geographical position. VIC has transmission lines connecting to three adjacent states which is the most among all jurisdictions.

Table 5.6 provides details of the directions of the Granger causality relationships. In the full sample, the link with the highest probability of existing is between VIC and SA, the probability being 28% from SA to VIC and 23% from VIC to SA. The Granger causality relationships from NSW to QLD and from VIC to TAS are also robust, with the probabilities being 22% and 21% respectively. This demonstrates the importance of physical interconnections as transmission lines underlie these significant relationships. For the same reason, NSW is the most influential region for QLD, just as VIC is for SA; VIC is for TAS; and SA is for VIC. However for NSW, the most critical region is neither QLD nor VIC, but SA, although SA and NSW have no physical connection. One possible explanation is that NSW imports a large quantity of power from VIC, but the allocation of VIC's export also depends on other connected states, such as SA and TAS. However, the issue of power system security is particularly severe in SA; thus, SA is always in the consideration, which impacts on the power availability to NSW.

In addition, three abnormally high values are observed in the average adjacency matrix from 1 July 2016 to 30 June 2017, namely, from VIC to SA; from NSW to QLD; and from VIC to TAS. With regard to the first relationship, SA experienced power supply shortage several times during the financial year 2016 - 2017 due to the coal plant closures, low wind speed and the Heywood outage, which resulted in its reliance on VIC. Thus, electricity prices in VIC had a significant impact on those in SA. In regard to QLD, the reason it follows changes in NSW prices is that NSW is the only state with which it has transmission lines. Especially when it was facing its own record demand, QLD experienced the opportunistic rebidding and spikes occurring over the summer 2016 - 2017. In the same vein, the reason for the third situation above is that VIC is the only

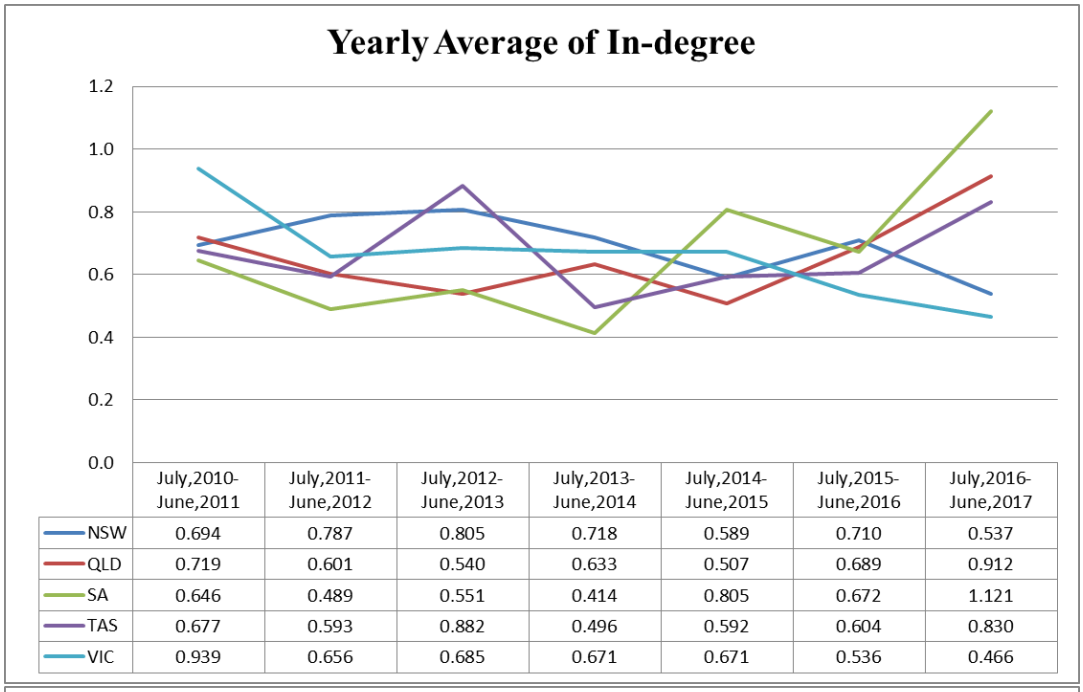

	July,2010-June,2011	July,2011-June,2012	July,2012-June,2013	July,2013-June,2014	July,2014-June,2015	July,2015-June,2016	July,2016-June,2017
NSW	0.694	0.787	0.805	0.718	0.589	0.710	0.537
QLD	0.719	0.601	0.540	0.633	0.507	0.689	0.912
SA	0.646	0.489	0.551	0.414	0.805	0.672	1.121
TAS	0.677	0.593	0.882	0.496	0.592	0.604	0.830
VIC	0.939	0.656	0.685	0.671	0.671	0.536	0.466

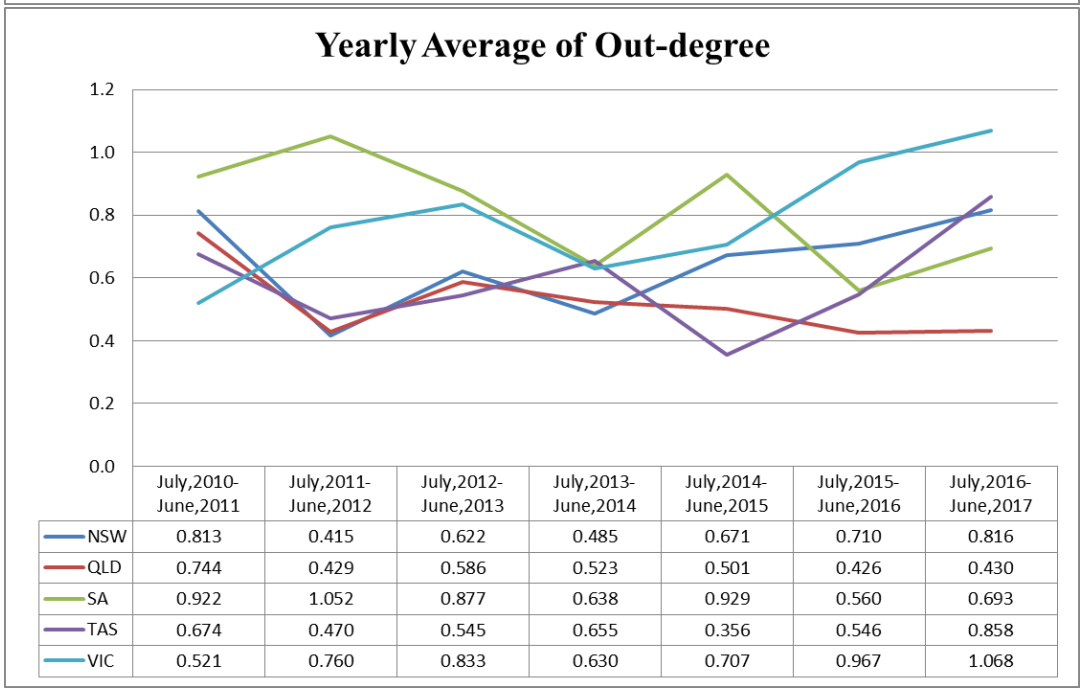

	July,2010-June,2011	July,2011-June,2012	July,2012-June,2013	July,2013-June,2014	July,2014-June,2015	July,2015-June,2016	July,2016-June,2017
NSW	0.813	0.415	0.622	0.485	0.671	0.710	0.816
QLD	0.744	0.429	0.586	0.523	0.501	0.426	0.430
SA	0.922	1.052	0.877	0.638	0.929	0.560	0.693
TAS	0.674	0.470	0.545	0.655	0.356	0.546	0.858
VIC	0.521	0.760	0.833	0.630	0.707	0.967	1.068

Figure 5.8: Yearly average of in-degree and out-degree. In-degree and out-degree are produced from Granger causality networks, where all links are directed from the cause to the effect. The networks are based on the deseasonalised half-hourly spot prices of five individual markets from 1 July 2010 to 30 June 2017. In-degree is the number of links that end at a particular node and out-degree is the number of links that start at a particular node. The link here represents the linear Granger causality at the 1% level of significance. The rolling window length is 7 days (336 observations).

jurisdiction in the NEM that has a physical connection with TAS.

Table 5.6: Average adjacency matrix from Granger causality networks. Each entry $a_{i,j}$ in ith row and jth column of the 5×5 matrix represents the percentage that prices of ith region Granger-causes those of jth region. Only results over 2016-2017 and the full sample are listed. Others are in Table A.1.

	NSW	QLD	SA	TAS	VIC		NSW	QLD	SA	TAS	VIC
	2016 - 2017						Full Sample				
NSW	0	0.362	0.274	0.148	0.033	NSW	0	0.224	0.163	0.142	0.118
QLD	0.093	0	0.170	0.121	0.047	QLD	0.155	0	0.117	0.139	0.109
SA	0.137	0.132	0	0.216	0.208	SA	0.208	0.145	0	0.177	0.280
TAS	0.170	0.205	0.304	0	0.178	TAS	0.141	0.129	0.163	0	0.153
VIC	0.137	0.214	0.373	0.345	0	VIC	0.188	0.159	0.227	0.211	0

5.2.3 Impact of Carbon Pricing

The carbon pricing put into practice from 1 July 2012 to 30 June 2014 was the central plank of Australia's climate change response (Australian Energy Regulator, 2013). Carbon pricing applied to all generators with carbon emissions; thus, it had a wider impact than any other policy that aimed at encouraging the usage of renewables and clean energy. Table 5.7 compares the coefficients in the first principal component when PCA is conducted before, during and after the implementation of the carbon taxing policy. A larger weight is allocated to the region that experienced extreme price observations, which supports the finding in subsection 5.2.1 that spikes drive abrupt changes to the cumulative risk fraction. As SA and NSW experienced record demand and extremely high prices in the summer 2010 - 2011, the coefficients in front of their price time series are 0.99 and 0.11, respectively. Again in the summers of 2012 - 2013 and 2013 - 2014, SA and VIC witnessed high demand for electricity and generator rebidding made the situation even worse. It explained the coefficients of SA and VIC, 0.90 and 0.43, respectively, between 1 July 2012 and 30 June 2014. From November 2014 to March 2015, the dominant generators in QLD used rebidding strategies to raise spot prices in trading intervals which caused spikes in the tight market condi-

tions (Australian Energy Regulator, 2015). Combined with import constraints and record demand, this situation occurred again in QLD in February 2017. This is the reason why QLD was the state that took the highest coefficient from SA after the repeal of carbon taxing. However, generally speaking, the risk is still concentrated in SA most of the time due to various reasons which include but are not limited to tight supply conditions, the weather-dependent nature of wind power and the rebidding of dominant generators.

Table 5.7: Coefficients of the first principal component. Coefficients of the first principal component are calculated from PCA conducted over three sample periods: July 2010 - June 2012, July 2012 - June 2014 and July 2014 - June 2017.

	Entire period	Before tax	During tax	After tax
NSW	0.18	0.11	0.02	0.19
QLD	0.44	0.07	0.02	0.94
SA	0.86	0.99	0.90	0.28
TAS	0.05	0.02	0.01	0.04
VIC	0.17	0.09	0.43	0.08

Table 5.8: Descriptive statistics of the dynamic cumulative risk fraction of the first principal component. The cumulative risk fraction is the percentage of total variance explained by the first (few) principal component(s). Tax refers to the adoption of carbon pricing policy from 1 July 2012 to 30 June 2014.

	MEAN	SD	SKEWNESS	KURTOSIS	#Obs.
Entire sample	77.43	16.01	-0.22	1.87	2551
Before tax	76.28	15.91	0.02	1.83	725
During tax	79.36	16.50	-0.39	1.83	724
After tax	76.79	15.66	-0.26	1.99	1090

Paired t-test for the null hypothesis that mean difference = 0:
Between "before tax" and "during tax": t-value = -3.68, p-value = 0.00025;
Between "during tax" and "after tax": t-value = 5.39, p-value = 0.00000.

Except for the static PCA employed to demonstrate the change in risk sources through time, the summary statistics of risk measures are listed in Table 5.8 and Table 5.9. The cumulative risk fraction of the first principal component increased

Table 5.9: Descriptive statistics of the dynamic causality index (degree of Granger causality). The dynamic causality index (DCI) is the percentage of the number of Granger causality relationships over the number of all possible links. Granger causality relationships are determined at 1% significance level. Tax refers to the adoption of carbon pricing policy from 1 July 2012 to 30 June 2014.

	MEAN	SD	SKEWNESS	KURTOSIS	#Obs.
Entire sample	0.167	0.134	1.078	4.455	2551
Before tax	0.170	0.140	1.318	5.265	725
During tax	0.157	0.131	1.357	5.754	724
After tax	0.171	0.131	0.687	3.023	1090

Paired t-test for the null hypothesis that mean difference = 0:
Between "before tax" and "during tax": t-value = 1.73, p-value = 0.0838;
Between "during tax" and "after tax": t-value = -2.91, p-value = 0.0037.

from approximately 76% to 79% after the introduction of carbon pricing and came down to about 77% afterwards. These changes are significant in terms of the paired-sample t-test. As this policy had a greater influence on the jurisdiction that relies more on fossil fuels, this change was indeed captured by the measure that gauges the degree of risk concentration. However, the dynamic causality index decreased from 0.17 to 0.16 and went up again to 0.17 over the sample period. These differences are also significant according to the paired-sample t-test. It reflects that dynamic causality index measures the level of interconnectedness in a different dimension from that measured by cumulative risk fraction.

Chapter 6

Regression Analysis

The regression models in this chapter are aimed at examining the potential of interconnectedness measures to predict variables of concern for the spot market. Two estimation methods are employed in this study, namely, ordinary least squares and quantile regression. The first method is for selecting the appropriate model, while the second one is used to address the coefficient patterns for the range of quantiles from 0.1 to 0.9.

6.1 Least Squares Regression

In consideration of five regional markets, 35 linear regression models in total are ready to be built. For each market, seven daily statistics are used, as elaborated in Table 4.2. The procedure of stepwise model building is conducted in the order of the magnitude of the correlation coefficients as showed in Table A.2, Table A.3 and Table A.4. As shown in Table 4.1, these alternative explanatory variables include the basic description of the past price behaviour, such as the first (mean), second (variance) and third (skewness) moment; price spikes; and different measures of volatility. In addition, the overall measures of interconnectedness are considered, with these comprising the in-degree and out-degree of each market; the cumulative risk fraction of the first principal component and that of the first two principal components; and the dynamic causality index (DCI).

In a stepwise procedure, additional significant explanatory variables are added

to the model, until for the final model all included variables have significant coefficients and the overall goodness of fit cannot be increased significantly by adding other variables. The applied model selection criterion is the adjusted R^2 which penalises the loss of degrees of freedom (*df*) that occurs when an extra variable is added and a model is expanded:

$$\bar{R}^2 = 1 - \frac{n-1}{n-K}(1-R^2) \tag{6.1}$$

where n is the number of samples; K is the number of explanatory variables; and

$$R^2 = \frac{[\sum_i (y_i - \bar{y})(\hat{y}_i - \hat{\bar{y}})]^2}{[\sum_i (y_i - \bar{y})^2][\sum_i (\hat{y}_i - \hat{\bar{y}})^2]} \tag{6.2}$$

where y_i is the value of the dependent variable; $\bar{y}$ is the mean of the sample series; and $\hat{y}$ represents the predicted value for y_i.

The explanatory variables considered are all calculated based on the preprocessed half-hourly spot prices over seven days to make them consistent. According to the information collected over one week, our intention was to forecast a variety of daily statistics on the following day.

Table 6.1 illustrates the estimation results of individual models, including those in NSW, QLD and SA. All coefficients in the table are obtained as Newey-West estimators in consideration of heteroskedasticity. The numbers in brackets are the corresponding t-statistics.

In NSW, the weekly average value, the weekly standard deviation and the number of spikes in the last seven days have relatively great predictive power for some of the daily statistics. For QLD, the weekly maximum value and the average daily range over the last seven days are helpful for forecasting several daily statistics. In SA, the number of spikes and the average daily standard deviation over the last seven days are good predictors for the current daily statistics.

In QLD, the out-degree, which is the number of links pointed from QLD in the constructed Granger causality network, could be used in particular to provide some information on maximum value, skewness and the possibility of spikes on

the next day. Therefore, if QLD is comparatively influential during the previous week, the maximum value of spot prices on the following day is more likely to be lower and the probability that spikes will occur also becomes lower. The possible explanation is that the influential state is in most cases the electricity exporter, which means it has enough power supply; thus, it is less likely to have extreme observations. For the same reason, the models forecast higher maximum and range values as well as more spikes to occur if the in-degree of SA, which is the number of states whose prices Granger-caused prices in SA over the last week, has increased. Similar to the explanation for QLD, greater vulnerability to the prices of other states means more reliance on outer power supply. The loss of independence means that SA is faced with more uncertainty in the spot market. Moreover, this leaves SA subject to the rebidding of dominant generators that have the ability to exercise market power, resulting in potential price increases. That is the reason why the estimation results show that the in-degree has sizable predictive power for the daily maximum and range values as well as for the number of spikes in SA.

Table 6.2 illustrates the estimation results of individual models, including those in TAS and VIC. All coefficients in the table are obtained as Newey-West estimators in consideration of heteroskedasticity. The numbers in brackets are the corresponding t-statistics. For the models in TAS, the average daily standard deviation over the last seven days has the greatest power among other alternative variables for forecasting the daily statistics. In VIC, the average daily standard deviation and the weekly skewness over the last seven days are the most powerful predictors.

Contrary to the situation in SA, the increase in the in-degree of TAS over the previous week leads to smaller values for maximum; skewness; and less spike occurrence. The higher in-degree indicates greater reliance on the outer power supplier. This reflects the point that importing power from VIC effectively alleviates the tight supply-demand balance in TAS. Unlike SA, in TAS, there is only one generator which is owned by the government. Thus, it is less likely for that

Table 6.1: Coefficients in the predictive models. Panel A (B, C) includes seven predictive models concerning NSW (QLD, SA). Dependent variables are average, maximum, minimum, range, standard deviation and skewness of the half-hourly spot prices, and the number of price spikes in one day. Explanatory variables are weekly statistics and five connectedness measures over the past seven days. All coefficients in the table are obtained as Newey-West estimators, taking heteroskedasticity into consideration. The numbers in brackets are the corresponding t-statistics. ***, ** and * represent 1%, 5% and 10% significance level, respectively.

Panel A: NSW															
	Mean	Max	Min	Range	Range2	Std	Std2	Skew	#Spike	Indegree	Outdegree	Pca1	Pca2	Dci	Adjusted R^2
Mean	0.462*** (2.82)											-0.00002* (-1.49)			8.60%
Max		4.042*** (3.59)							-0.024** (-2.24)						11.53%
Min			0.262*** (3.77)			0.253*** (3.98)	-0.797*** (-5.19)		0.004*** (4.17)		-0.001* (-1.54)				44.85%
Range	-2.465*** (-2.66)			-0.237*** (-3.77)		5.664*** (4.51)			-0.032*** (-2.81)						14.63%
Std	-0.453*** (-2.70)						1.207*** (4.08)		-0.006*** (-2.44)						17.86%
Skew	- 21.312*** (-3.42)					- 24.832*** (-4.39)	52.408*** (5.64)	0.106*** (4.55)							7.19%
#Spike				-0.284* (-1.59)		6.619** (2.25)									13.11%
Panel B: QLD															
Mean	0.343*** (4.84)			0.003* (1.71)											5.68%
Max					0.566*** (6.60)			0.003** (2.04)			-0.011** (-1.98)				17.95%
Min					-0.034*** (-2.59)										0.21%
Range	-3.191*** (-4.14)	0.112*** (3.66)		-0.144*** (-4.77)	0.612*** (4.37)	1.735*** (5.79)									25.55%
Std		0.024*** (3.44)				-0.389** (-2.41)	0.926*** (3.28)								16.81%
Skew		-0.586** (-2.22)			3.050*** (4.81)			0.079*** (6.00)			-0.132** (-2.58)				9.64%
#Spike	-12.285** (-2.19)	0.382*** (3.21)		-0.075** (-2.01)					0.089*** (3.84)		-0.030* (-1.92)				14.12%
Panel C: SA															
Mean									0.001*** (3.48)						2.74%
Max				-0.047*** (-3.18)			1.557*** (3.17)	0.003*** (4.23)	0.006** (2.05)	0.015* (1.92)					5.95%
Range							0.921** (2.10)		0.008** (2.48)	0.016* (1.85)					3.97%
Std	-0.548*** (-3.60)					-0.165* (-1.61)	0.465** (2.38)	0.0003* (1.77)	0.003*** (4.36)						5.54%
Skew						-7.721*** (-3.81)	17.043*** (4.66)	0.046*** (7.26)							4.35%
#Spike	- 10.136*** (-2.93)				-0.659*** (-2.17)				0.116*** (4.16)	0.075*** (1.63)					11.82%

Table 6.2: Coefficients in the predictive models. Panel D (E) includes seven predictive models concerning TAS (VIC). Dependent variables are average, maximum, minimum, range, standard deviation and skewness of the half-hourly spot prices, and the number of price spikes in one day. Explanatory variables are weekly statistics and five connectedness measures over the past seven days. All coefficients in the table are obtained as Newey-West estimators, taking heteroskedasticity into consideration. The numbers in brackets are the corresponding t-statistics. ***, ** and * represent 1%, 5% and 10% significance level, respectively.

Panel D: TAS															
	Mean	Max	Min	Range	Range2	Std	Std2	Skew	#Spike	Indegree	Outdegree	Pca1	Pca2	Dci	Adjusted R^2
Mean	-0.392*** (5.35)				-0.056*** (-2.89)		0.282** (2.54)								9.00%
Max							1.352*** (3.61)		0.001* (1.67)	-0.007*** (-2.73)					3.09%
Min							-0.549*** (-3.28)								2.00%
Range							2.100*** (6.62)								4.43%
Std					-0.192*** (-6.02)		1.387*** (8.83)	0.0005** (2.41)							12.39%
Skew		-0.839*** (-3.04)				- 14.093*** (-3.46)	43.937*** (5.69)	0.082*** (5.27)	-0.044*** (-4.89)	-0.124*** (-3.67)					4.75%
#Spike	-15.697* (-1.91)			-0.186** (-2.57)				0.007* (1.60)	0.133*** (5.37)	-0.025** (-2.11)					55.46%
Panel E: VIC															
Mean	0.306*** (4.52)							0.001*** (4.70)							5.02%
Max					-0.588*** (-2.68)		4.310*** (3.52)						0.0007** (2.03)		2.95%
Min	0.537*** (2.71)					0.712*** (5.6)	-2.048*** (-7.13)		0.003*** (3.09)						4.84%
Range		-0.109*** (-2.96)					3.437*** (6.07)	0.004*** (3.97)							4.72%
Std	-0.435*** (-4.65)				-0.265*** (-4.59)		1.799*** (5.87)	0.0004*** (2.93)							6.69%
Skew				-0.505*** (-2.95)			24.479*** (4.66)	0.051*** (6.19)	-0.131** (-2.41)				0.013*** (2.69)		3.93%
#Spike								0.004** (2.33)	0.025* (1.66)				0.0013** (2.39)		1.16%

generator to take advantage of the power shortage and sustain the high price. In addition, the cumulative risk fraction of the first two principal components has predictive power for the daily maximum and skewness values as well as for the number of spikes in VIC. A high cumulative risk fraction is always due to the extent of risk concentration. In most cases, VIC will play the role of exporter and support states that are experiencing power shortage. That is possibly why VIC is more likely to witness extreme observations in this particular situation.

6.2 Quantile Regression

Based on the models specified by the least squares estimation, quantile regression is employed to examine the various quantiles of the distribution of individual dependent variables. The derived coefficients indexed by the quantile q provide richer information on their relationships than are available from the linear model. Given that the model is nonparametric, it requires a much less detailed specification of the distribution of the dependent variable conditional on the explanatory variables (Greene, 2012). All figures in this section display the estimates of the explanatory variable elasticity of the dependent variable for the range of quantiles from 0.1 to 0.9. Confidence limits shown in the figures are based on the asymptotic normality of the estimator. They are computed as the estimated elasticity plus and minus 1.96 times the estimated standard error. All coefficients with explicit patterns are drawn in Figure 6.1 till Figure 6.21.

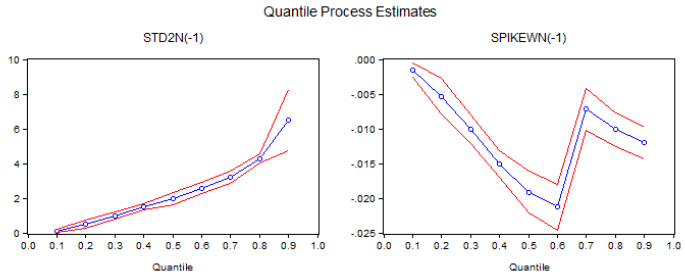

Figure 6.1: Quantile process estimates in the predictive model of the daily maximum in NSW. The coefficients are those for the average daily standard deviation and the number of spikes over seven days.

The left panel of Figure 6.1 displays the estimates of the average daily standard

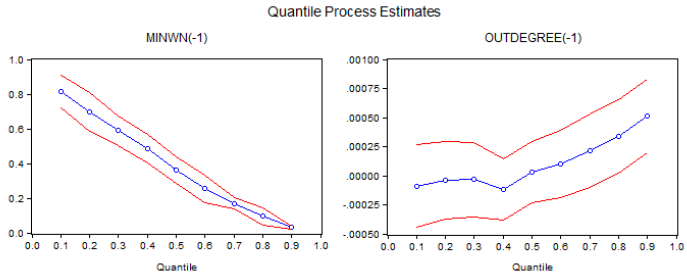

Figure 6.2: Quantile process estimates in the predictive model of the daily minimum in NSW. The coefficients are those for the weekly minimum value and the number of links directed from NSW in the constructed Granger causality network over seven days.

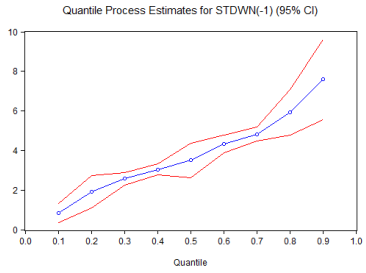

Figure 6.3: Quantile process estimates in the predictive model of the daily range in NSW. The coefficient is that for the weekly standard deviation over seven days.

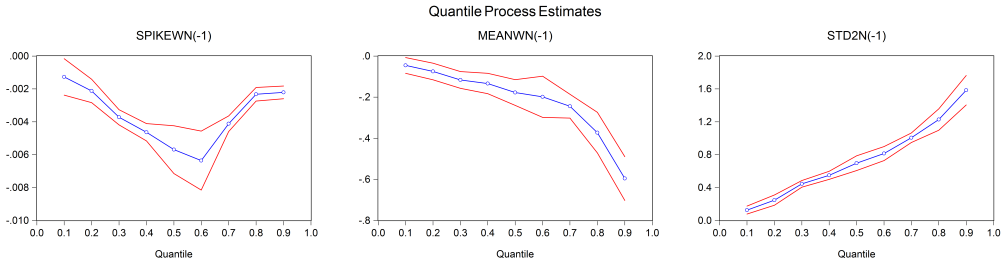

Figure 6.4: Quantile process estimates in the predictive model of the daily standard deviation in NSW. The coefficients are those for the weekly average, the average daily standard deviation and the number of price spikes over seven days.

deviation elasticity of the maximum value on the next day. It is shown that, as the maximum value goes up, the average daily standard deviation over the last seven days plays a more and more important role. This ascending influence on the dependent variable also appears in the predictive models of the daily minimum, range, standard deviation and skewness values in NSW; the daily average, maximum and skewness values in QLD; the daily maximum, standard deviation and skewness values in SA; the daily maximum and skewness values

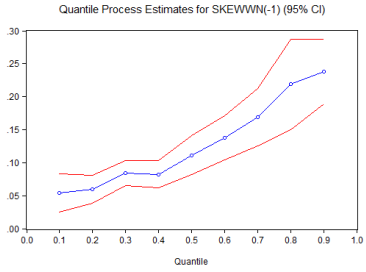

Figure 6.5: Quantile process estimates in the predictive model of the daily skewness in NSW. The coefficient is that for the weekly skewness over seven days.

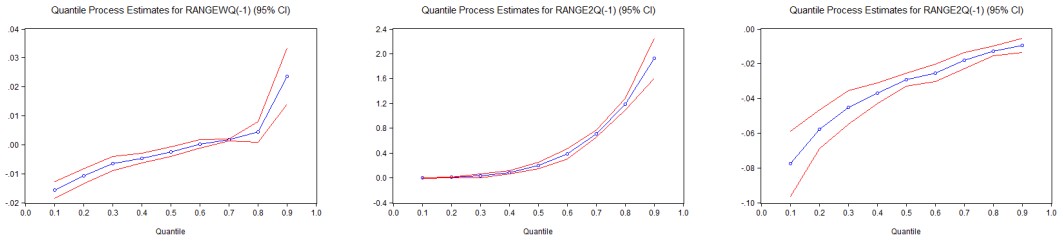

Figure 6.6: Quantile process estimates in the predictive model of the daily average, maximum and minimum in QLD, respectively. The coefficient in the model of the average value is that for the weekly range. The coefficient in the models of the maximum and minimum values is that for the average daily range over seven days.

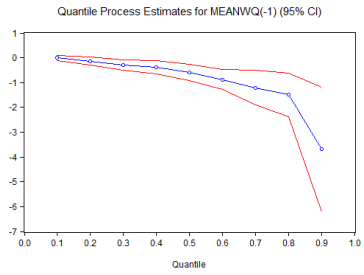

Figure 6.7: Quantile process estimates in the predictive model of the daily range in QLD. The coefficient is that for the weekly average value over seven days.

in TAS; and the daily average, range, standard deviation and skewness values in VIC. Conversely, the descending impact emerges in the predictive models of the daily minimum value in NSW, the daily minimum value in QLD, the daily average and minimum values in TAS, and the daily minimum value in VIC.

However, a huge difference is evident between the coefficients at 0.6 and 0.7 quantiles for the number of spikes in the last seven days, which suggests an inverted U-shaped impact of this variable on the daily maximum value in NSW.

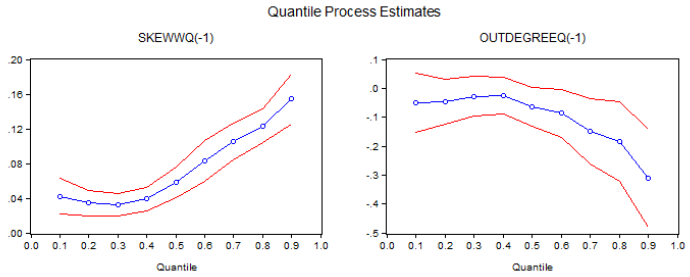

Figure 6.8: Quantile process estimates in the predictive model of the daily skewness in QLD. The coefficients are those for the weekly skewness and the number of links directed from QLD in the constructed Granger-causality network over seven days.

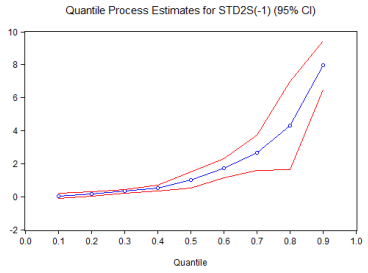

Figure 6.9: Quantile process estimates in the predictive model of the daily maximum in SA. The coefficient is that for the average daily standard deviation over seven days.

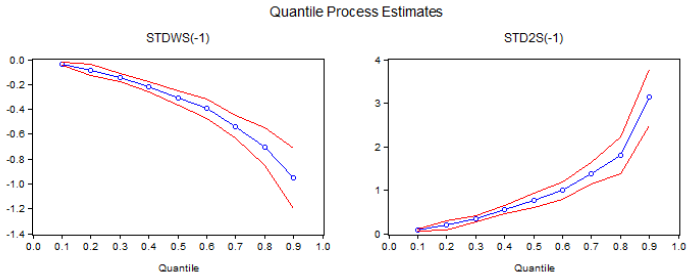

Figure 6.10: Quantile process estimates in the predictive model of the daily standard deviation in SA. The coefficients are those for the weekly standard deviation and the average daily standard deviation over seven days.

This is similar to the predictive model of the daily standard deviation in NSW. The coefficients of the number of spikes over the last week are presented as an inverted U-shaped curve, indicating that its greatest influence is shown when the dependent variable is at its 0.6 quantile.

In the predictive model of the daily range in QLD, the elasticity of the weekly average value suddenly increases at 0.9 quantile. A similar abrupt change to the elasticity of the explanatory variable also happens to the model of the daily

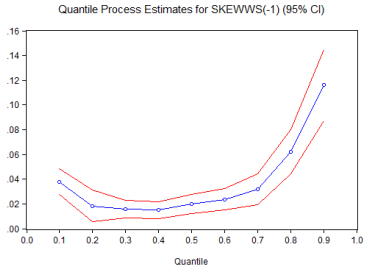

Figure 6.11: Quantile process estimates in the predictive model of the daily skewness in SA. The coefficient is that for the skewness over seven days.

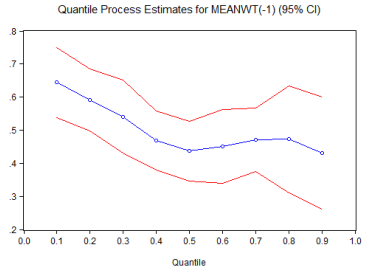

Figure 6.12: Quantile process estimates in the predictive model of the daily average in TAS. The coefficient is that for the weekly average value over seven days.

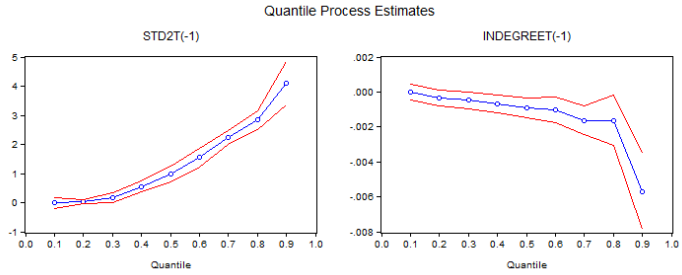

Figure 6.13: Quantile process estimates in the predictive model of the daily maximum in TAS. The coefficients are those for the daily average standard deviation and the number of links directed to TAS in the constructed Granger causality network over seven days.

maximum value and that of the daily skewness in VIC. The cumulative risk fraction of the first two principal components starts to exert a huge impact at 0.8 and 0.9 quantiles.

Overall, all the figures show the patterns of different coefficients in the prediction of different daily variables for the range of quantiles from 0.1 to 0.9. Some have a certain trend and change gradually, while others have a dramatic change at some specific quantiles or have an inverted U-shaped curve.

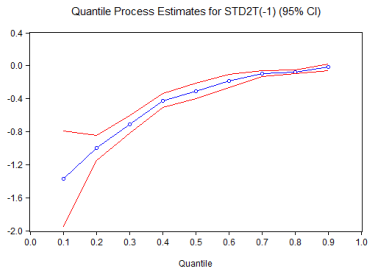

Figure 6.14: Quantile process estimates in the predictive model of the daily minimum in TAS. The coefficient is that for the average daily standard deviation over seven days.

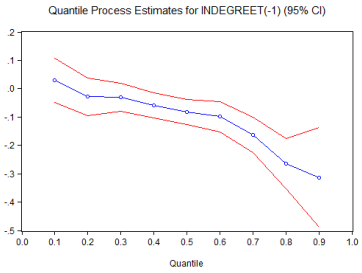

Figure 6.15: Quantile process estimates in the predictive model of the daily skewness in TAS. The coefficient is that for the number of links directed to TAS in the constructed Granger causality network over seven days.

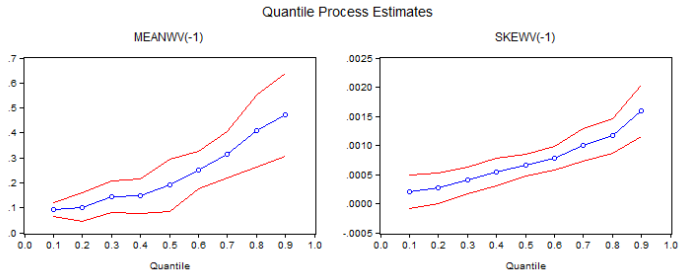

Figure 6.16: Quantile process estimates in the predictive model of the daily average in VIC. The coefficients are those for the weekly average and the weekly skewness over seven days.

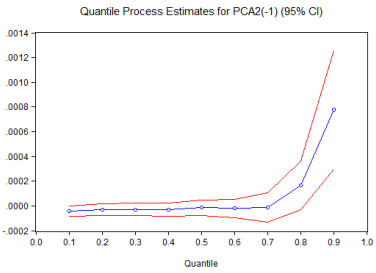

Figure 6.17: Quantile process estimates in the predictive model of the daily maximum in VIC. The coefficient is that for the cumulative risk fraction of the first two principal components over seven days.

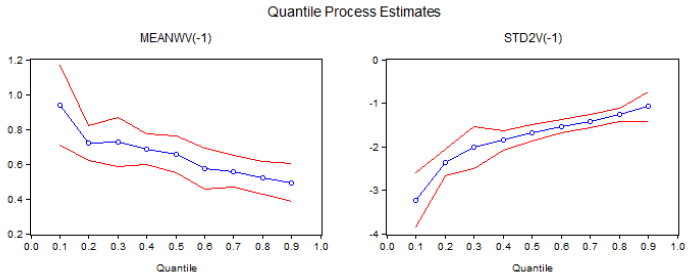

Figure 6.18: Quantile process estimates in the predictive model of the daily minimum in VIC. The coefficients are those for the average daily standard deviation over seven days and the weekly average.

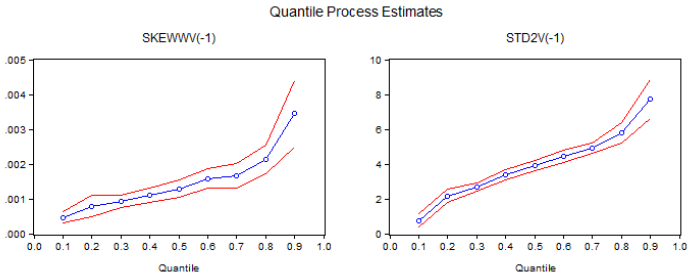

Figure 6.19: Quantile process estimates in the predictive model of the daily range in VIC. The coefficients are those for the weekly skewness and the average daily standard deviation over seven days.

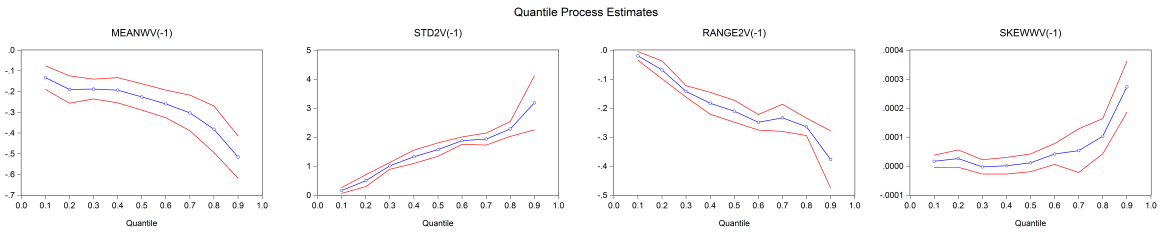

Figure 6.20: Quantile process estimates in the predictive model of the daily standard deviation in VIC. The coefficients are those for the weekly average value and the skewness as well as the average daily standard deviation and the average daily range over seven days.

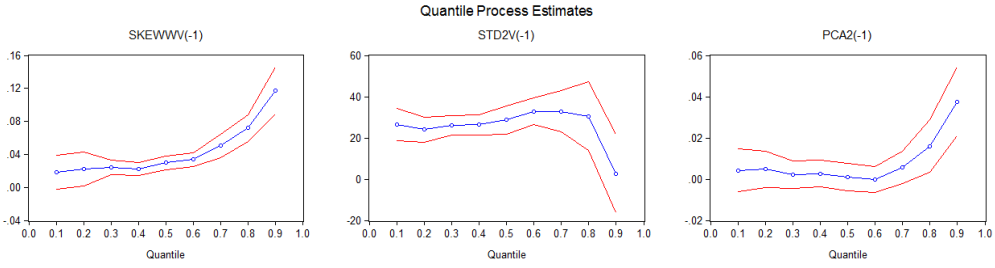

Figure 6.21: Quantile process estimates in the predictive model of the daily skewness in VIC. The coefficients are those for the weekly skewness, the average daily standard deviation and the cumulative risk fraction of the first two principal components over seven days.

Chapter 7

Conclusions

This study examines interconnectedness and systemic risks in the Australian National Electricity Market (NEM). Using deseasonalised half-hourly spot prices in five regional markets from 1 July 2010 to 30 June 2017, we intend to gain insights into the interaction between the spot prices in different states. Drawing the dynamic patterns of the derived interconnectedness measures, we examine the drivers behind trends and changes in these measures, and assess the magnitude of systemic risk and the mechanism of the carbon pricing impact on this interdependence. Furthermore, additional regression analysis is also conducted to investigate the predictive power of the derived measures for future spot prices in each of the considered markets.

Following the framework originally developed in Billio et al. (2012), two streams of interconnectedness measures are considered. Specifically, principal component analysis (PCA) is conducted to provide a broad view of connections by the fraction of the total variance explained by the first few principal components. As each principal component is orthogonal, the information contained in several series is summarised in order of descending explanatory power. Further, Granger causality network analysis is employed to gauge the interdependence level between regional spot prices by constructing an intricate abstract web based on Granger causality relationships.

During the sample period, the cumulative risk fraction of the first principal component increased to approximately 82% in the first year of carbon taxation

and gradually dropped to about 73% in the financial year 2016 - 2017. The average value of this measure across the entire sample was about 77%. As this is largely affected by extreme observations, this result indicates that during 2016 - 2017, individual markets faced local risks, especially in terms of price spikes. However, another interdependence measure, the dynamic causality index (DCI), has an upward trend from 0.15 in 2013 - 2014 to 0.19 in 2016 - 2017. It reflects a slightly increasing scale of integration across the considered markets. The divergence of the cumulative risk fraction and the dynamic causality index (DCI) also appeared in the comparative analysis on the impact of the carbon taxation policy. The cumulative risk fraction increased approximately from 76% to 79% after the introduction of carbon taxation and reduced to less than 77% afterwards. In contrast, the DCI decreased from 0.17 before the carbon pricing to 0.16 and went up again to 0.17 after the repeal of this policy. This finding confirms that these two measures captured different information in the market.

In addition, we showed the time-varying patterns of the interconnectedness measures and linked them to significant market events, including price spikes; unexpected high demand for electricity; a sudden increase in price volatility; opportunistic rebidding of dominant generators; temporary or permanent closures of major power stations, as well as upgrades and limitations in transmission capacity. Therefore, these measures could be used as an effective tool to monitor the changing market conditions in the NEM.

From the directional Granger causality relationships, the average in-degree and out-degree suggest that NSW is most vulnerable to price changes of other states and that SA is also easily affected by other states. Given that both NSW and SA are net electricity importers most of the time, this finding reflects that whether a state is a risk sink depends on its power source structure and the general supply independence. On the other hand, VIC is the second most influential region during the sample period because VIC is a net exporter of electricity and locates at a very central position geographically.

Furthermore, the patterns of in-degree and out-degree inform the role played

by each region in the NEM. In particular, SA has ascending in-degrees, from 0.41 to 1.12, and descending out-degrees, from 1.05 to 0.56, which results from the loss of power supply independence. It indicates that SA becomes more and more reliant on outer power sources and less influential. On the contrary, VIC has a rising level of out-degree, from 0.52 to 1.07, and a falling in-degree, from 0.94 to 0.47, thus showing the greater influence VIC is able to exert on the other states. This is partly because VIC is typically a net exporter of electricity to the states around and is also physically connected to other states. VIC is the only region that has transmission lines with three other states in the network, namely NSW, SA and TAS.

The significance of interconnectors is supported by the average adjacency matrix of Granger causality networks as well. In the full sample, the link that has the highest probability to exist is between VIC and SA, that is, 28% from SA to VIC and 22.7% from VIC to SA. The Granger causality relationships from NSW to QLD and that from VIC to TAS are also robust, with probabilities of 22.4% and 21.1%, respectively. These pairs all have physical interconnections, the so-called interconnectors, linking them. For the same reason, NSW is the most influential region for QLD, just as VIC is for SA; VIC is for TAS; and SA is for VIC. However, for NSW, the most influential region is neither QLD nor VIC, but SA with which NSW has no physical connection with. One of the possible explanations is that, in most cases, NSW imports power from VIC, but the allocation of VIC's export also depends on other connected states, such as SA and TAS. The issue of power system security in SA is particularly severe; thus, SA is always in the consideration, with this impacting on the power availability for NSW.

In addition to the descriptive analysis, the predictive models built in this present study suggest some explanatory power of the interconnectedness measures in forecasting the daily statistics. For example, the out-degree of QLD, which is the number of links pointed from QLD in the constructed Granger causality network, is significantly helpful for providing information for the maximum value,

the skewness and the possibility of spikes on the following day. The models also forecast higher maximum and range values as well as more spikes to occur if the in-degree of SA, which is the number of states whose prices Granger-caused those in SA over the last week, has increased. Moreover, the increase in the in-degree of TAS over the last week leads to smaller maximum, and skewness values and less spike occurrence on the following day. Except for the interdependence measures derived from the Granger causality network analysis, the cumulative risk fraction of the first two principal components also has predictive power for the daily maximum and skewness values as well as for the number of spikes in VIC.

To the best of our knowledge, this is the pioneer study to capture the network structure of Granger causality relationships between the regional half-hourly spot prices in the NEM. It is also one of the first studies to apply network theory to the electricity market.

However, despite these efforts, this study still has some limitations, with three such limitations proposed as follows. First, in the process of looking for the appropriate predictive model for daily statistics, we might fail to consider other relevant variables and adopt the wrong functional form. It poses a problem of inaccuracy in the estimation results and the conclusions drawn.

Second, any abstract relationship revealed in the multivariate analysis of prices must have real economic activities behind. Just as our study shows, the interconnectedness measures are related with the interregional trade. But due to the lack of intricate data on interregional transactions, this present study only provides very rough evidence of it. With access to more information on the trade flow, the detailed mechanism of price contagion could be investigated.

Lastly, since electricity spot prices in an exporting region have an impact on those in the importing region, the velocity of the price convergence depends on transmission constraints and supply adequacy of the exporter. On the one hand, if the transmission capacity of the interconnector is limited, the convergence might be relatively slow. Thus whether this limitation becomes a bottleneck for the

integration procedure is an interesting topic to be studied. On the other hand, if cheap power supply in the exporting region is not adequate, it might not be enough to reduce electricity prices in the importing state. So another related topic of interest is what kind of power source structure should be adopted to make each market be flexible under the circumstances of abrupt high demand and unexpected changes in supply.

References

Aderounmu, A. A., Wolff, R., 2014a. Assessing tail dependence in electricity markets. Available at SSRN 2373591.

Aderounmu, A. A., Wolff, R., 2014b. Modeling dependence of price spikes in Australian electricity markets. Energy Risk 11 (2), 60–65.

Allen, F., Carletti, E., 2013. What is systemic risk? Journal of Money, Credit and Banking 45 (s1), 121–127.

Amini, H., Cont, R., Minca, A., 2013. Resilience to contagion in financial networks. Mathematical finance.

Apergis, N., Fontini, F., Inchauspe, J., 2016. Integration of regional electricity markets in Australia: A price convergence assessment. Energy Economics 52, 176–182.

Arinaminpathy, N., Kapadia, S., May, R. M., 2012. Size and complexity in model financial systems. Proceedings of the National Academy of Sciences 109 (45), 18338–18343.

Australian Energy Regulator, 2013. State of the energy market [online]. Released December 20, 2013 ,from https://www.aer.gov.au/publications/state-of-the-energy-market-reports/state-of-the-energy-market-2013.

Australian Energy Regulator, 2015. State of the energy market [online]. Released December 18, 2015 ,from https://www.aer.gov.au/publications/state-of-the-energy-market-reports.

Australian Energy Regulator, 2017. State of the energy market [online]. Released May 30, 2017 ,from https://www.aer.gov.au/publications/state-of-the-energy-market-reports/state-of-the-energy-market-may-2017.

Australian Government Productivity Commission, 2013. Electricity network regulatory frameworks, productivity commission inquiry report.

Barabási, A.-L., Albert, R., 1999. Emergence of scaling in random networks. Science 286 (October), 509–512.

Bech, M. L., Atalay, E., 2010. The topology of the federal funds market. Physica A: Statistical Mechanics and its Applications 389 (22), 5223–5246.

Benth, F. E., Benth, J. S., Koekebakker, S., 2008. Stochastic modelling of electricity and related markets. Vol. 11. World Scientific.

Benth, F. E., Kiesel, R., Nazarova, A., 2012. A critical empirical study of three electricity spot price models. Energy Economics 34 (5), 1589 – 1616.

Bierbrauer, M., Menn, C., Rachev, S., Trück, S., 2007. Spot and derivative pricing in the EEX power market. Journal of Banking & Finance 31, 3462–3485.

Bierbrauer, M., Trück, S., Weron, R., 2004. Modeling electricity prices with regime switching models. Computational Science-ICCS 2004, 859–867.

Billio, M., Getmansky, M., Lo, A. W., Pelizzon, L., 2012. Econometric measures of connectedness and systemic risk in the finance and insurance sectors. Journal of Financial Economics 104 (3), 535–559.

Bisias, D., Flood, M., Lo, A. W., Valavanis, S., 2012. A survey of systemic risk analytics. Annual Review of Financial Economics 4 (1), 255–296.

Bluhm, M., Faia, E., Krahnen, J. P., 2014. Endogenous banks' networks, cascades and systemic risk. Tech. rep., Sustainable Architecture for Finance in Europe(SAFE), sAFE Working Paper No. 12.

Boisseleau, F., 2004. The role of power exchanges for the creation of a single european electricity market: market design and market regulation.

Bollino, C., Polinori, P., 2008. Contagion in electricity markets: does it exist? Working Paper (University of Perugia).

Boss, M., Elsinger, H., Summer, M., Thurner 4, S., 2004. Network topology of the interbank market. Quantitative Finance 4 (6), 677–684.

Bunn, D. W., Gianfreda, A., 2010. Integration and shock transmissions across european electricity forward markets. Energy Economics 32 (2), 278–291.

Caccioli, F., Shrestha, M., Moore, C., Farmer, J., 2014. Stability analysis of financial contagion due to overlapping portfolios. Journal of Banking & Finance.

Cartea, A., Figueroa, M., 2005. Pricing in electricity markets: A mean reverting jump diffusion model with seasonality. Applied Mathematical Finance 12(4), 313–335.

Castagneto-Gissey, G., Chavez, M., Fallani, F. D. V., 2014. Dynamic granger-causal networks of electricity spot prices: A novel approach to market integration. Energy Economics 44, 422–432.

Christensen, T. M., Hurn, A. S., Lindsay, K. A., 2012. Forecasting spikes in electricity prices. International Journal of Forecasting 28 (2), 400–411.

Ciarreta, A., Zarraga, A., 2012. Analysis of volatility transmissions in integrated and interconnected markets: The case of the Iberian and French markets. Documentos de Trabajo BILTOKI (4), 1.

Ciarreta, A., Zarraga, A., 2015. Analysis of mean and volatility price transmissions in the MIBEL and EPEX electricity spot markets. Energy Journal 36 (4).

Clements, A., Fuller, J., Hurn, S., 2013. Semi-parametric forecasting of spikes in electricity prices. Economic Record 89 (287), 508–521.

Clements, A., Herrera, R., Hurn, A., 2015. Modelling interregional links in electricity price spikes. Energy Economics 51, 383–393.

Cont, R., Moussa, A., Santos, E., 2011. Network structure and systemic risk in banking systems. In: Handbook on Systemic Risk. Cambridge University Press, pp. 327–368.

Craig, B., Von Peter, G., 2014. Interbank tiering and money center banks. Journal of Financial Intermediation 23 (3), 322–347.

Daubechies, I., 1992. Ten lectures on wavelets. SIAM.

De Menezes, L. M., Houllier, M. A., 2015. Germany's nuclear power plant closures and the integration of electricity markets in europe. Energy Policy 85, 357–368.

De Menezes, L. M., Houllier, M. A., 2016. Reassessing the integration of European electricity markets: A fractional cointegration analysis. Energy Economics 53, 132–150.

De Vany, A. S., Walls, W. D., 1999. Cointegration analysis of spot electricity prices: insights on transmission efficiency in the western us. Energy Economics 21 (5), 435–448.

Degryse, H., Nguyen, G., et al., 2007. Interbank exposures: An empirical examination of contagion risk in the belgian banking system. International Journal of Central Banking 3 (2), 123–171.

Dempster, G., Isaacs, J., Smith, N., 2008. Price discovery in restructured electricity markets. Resource and Energy Economics 30(2), 250–259.

Eydeland, A., Wolyniec, K., 2003. Energy and power risk management: New developments in modeling, pricing, and hedging. Vol. 206. John Wiley & Sons.

Fanone, E., Gamba, A., Prokopczuk, M., 2013. The case of negative day-ahead electricity prices. Energy Economics 35, 22 – 34, quantitative Analysis of Energy Markets.

Fricke, D., Lux, T., 2015. On the distribution of links in the interbank network: Evidence from the e-mid overnight money market. Empirical Economics 49 (4), 1463–1495.

Füss, R., Mahringer, S., Prokopczuk, M., Sep. 2015. Electricity Spot and Derivatives Pricing when Markets are Interconnected. Working Papers on Finance 1323, University of St. Gallen, School of Finance.

Gai, P., Haldane, A., Kapadia, S., 2011. Complexity, concentration and contagion. Journal of Monetary Economics 58 (5), 453–470.

Gai, P., Kapadia, S., 2010. Contagion in financial networks. In: Proceedings of the Royal Society of London A: Mathematical, Physical and Engineering Sciences. The Royal Society, p. rspa20090410.

Garnaut, R., 2011. Update paper 8: Transforming the electricity sector. Garnaut Climate Change Review, Update 2011.

Geman, H., Roncoroni, A., 2006. Understanding the fine structure of electricity prices. Journal of Business 79(3), 1225–1262.

Gianfreda, A., Grossi, L., 2012. Forecasting italian electricity zonal prices with exogenous variables. Energy Economics 34 (6), 2228 – 2239.

Green, H., Kordzakhia, N., Thoplan, R., 2014. Multi-factor statistical modelling of demand and spot price of electricity. Quality Technology & Quantitative Management 11 (2), 151–165.

Greene, W. H., 2012. Econometric analysis.

Hafner, C. M., Herwartz, H., 2006. Volatility impulse responses for multivariate garch models: An exchange rate illustration. Journal of International Money and Finance 25 (5), 719–740.

Haldrup, N., Nielsen, M., 2006. A regime switching long memory model for electricity prices. Journal of Econometrics 135 (1-2), 349–376.

Higgs, H., 2009. Modelling price and volatility inter-relationships in the australian wholesale spot electricity markets. Energy Economics 31(5), 748–756.

Higgs, H., Worthington, A., 2008. Stochastic price modelling of high volatility, mean-reverting, spike-prone commodities: The australian wholesale spot electricity market. Energy Economics 30, 3172–3185.

Houllier, M. A., de Menezes, L. M., 2012. A fractional cointegration analysis of european electricity spot prices. In: European Energy Market (EEM), 2012 9th International Conference on the. IEEE, pp. 1–6.

Hüser, A.-C., 2015. Too interconnected to fail: A survey of the interbank networks literature. The Journal of Network Theory in Finance 1 (3), 1–50.

Ignatieva, K., Trück, S., 2016. Modeling spot price dependence in australian electricity markets with applications to risk management. Computers and Operations Research 66, 415–433.

Imakubo, K., Soejima, Y., et al., 2010. The microstructure of japans interbank money market: Simulating contagion of intraday flow of funds using boj-net payment data. Monetary and Economic studies 28, 151–180.

Iori, G., Jafarey, S., Padilla, F. G., 2006. Systemic risk on the interbank market. Journal of Economic Behavior and Organization 61 (4), 525–542.

Janczura, J., Trück, S., Weron, R., Wolff, R. C., 2013. Identifying spikes and seasonal components in electricity spot price data: A guide to robust modeling. Energy Economics 38, 96–110.

Janczura, J., Weron, R., 2010. An empirical comparison of alternate regime-switching models for electricity spot prices. Energy Economics 32(5), 1059–1073.

Kalantzis, F., Milonas, N. T., 2010. Market integration and price dispersion in the european electricity market. In: Energy Market (EEM), 2010 7th International Conference on the European. IEEE, pp. 1–6.

Le Pen, Y., Sévi, B., 2010. Volatility transmission and volatility impulse response

functions in European electricity forward markets. Energy Economics 32(4), 758–770.

Lenzu, S., Tedeschi, G., 2012. Systemic risk on different interbank network topologies. Physica A: Statistical Mechanics and its Applications 391 (18), 4331–4341.

Lucia, J. J., Schwartz, E., 2002. Electricity prices and power derivatives: Evidence from the Nordic power exchange. Review of Derivatives Research 5, 5–50.

Manner, H., Türk, D., Eichler, M., 2016. Modeling and forecasting multivariate electricity price spikes. Energy Economics 60, 255–265.

Mistrulli, P. E., 2011. Assessing financial contagion in the interbank market: Maximum entropy versus observed interbank lending patterns. Journal of Banking & Finance 35 (5), 1114–1127.

Nepal, R., Foster, J., et al., 2016. Testing for market integration in the Australian National Electricity Market. The Energy Journal 37 (4), 215–238.

Nowotarski, J., Tomczyk, J., Weron, R., 2013. Robust estimation and forecasting of the long-term seasonal component of electricity spot prices. Energy Economics 39, 13–27.

Park, H., Mjelde, J., Bessler, D., 2006. Price dynamics among U.S. markets. Energy Economics 28(1), 81–101.

Phillips, P. C., Sul, D., 2007. Transition modeling and econometric convergence tests. Econometrica 75 (6), 1771–1855.

Pilipovic, D., 1997. Energy Risk: Valuing and Managing Energy Derivatives. McGraw-Hill.

Pilipovic, D., 2007. Energy risk: Valuing and managing energy derivatives. McGraw Hill Professional.

Sahu, S. K., Dey, D. K., Branco, M. D., 2003. A new class of multivariate skew distributions with applications to bayesian regression models. Canadian Journal of Statistics 31 (2), 129–150.

Schlueter, S., 2010. A long-term/short-term model for daily electricity prices with dynamic volatility. Energy Economics 32 (5), 1074–1081.

Smith, M. S., 2015. Copula modelling of dependence in multivariate time series. International Journal of Forecasting 31 (3), 815–833.

Smith, M. S., Gan, Q., Kohn, R. J., 04 2012. Modelling dependence using skew t copulas: Bayesian inference and applications. Journal of Applied Econometrics 27 (3), 500–522.

Stevenson, M. J., Moreira do Amaral, L. F., Peat, M., 2006. Risk management and the role of spot price predictions in the australian retail electricity market. Studies in Nonlinear Dynamics & Econometrics 10 (3).

Tse, Y. K., Tsui, A. K. C., 2002. A multivariate generalized autoregressive conditional heteroscedasticity model with time-varying correlations. Journal of Business & Economic Statistics 20 (3), 351–362.

Weron, R., 2006. Modeling and Forecasting Loads and Prices in Deregulated Electricity Markets. Wiley, Chichester.

Weron, R., 2014. Electricity price forecasting: A review of the state-of-the-art with a look into the future. International Journal of Forecasting 30 (4), 1030 – 1081.

Worthington, A., Kay-Spratley, A., Higgs, H., 2005. Transmission of prices and price volatility in Australian electricity spot markets: A multivariate garch analysis. Energy Economics 27(2), 337–350.

Zachmann, G., 2008. Electricity wholesale market prices in Europe: Convergence? Energy Economics 30(4), 1659–1671.

Appendix A

Appendix

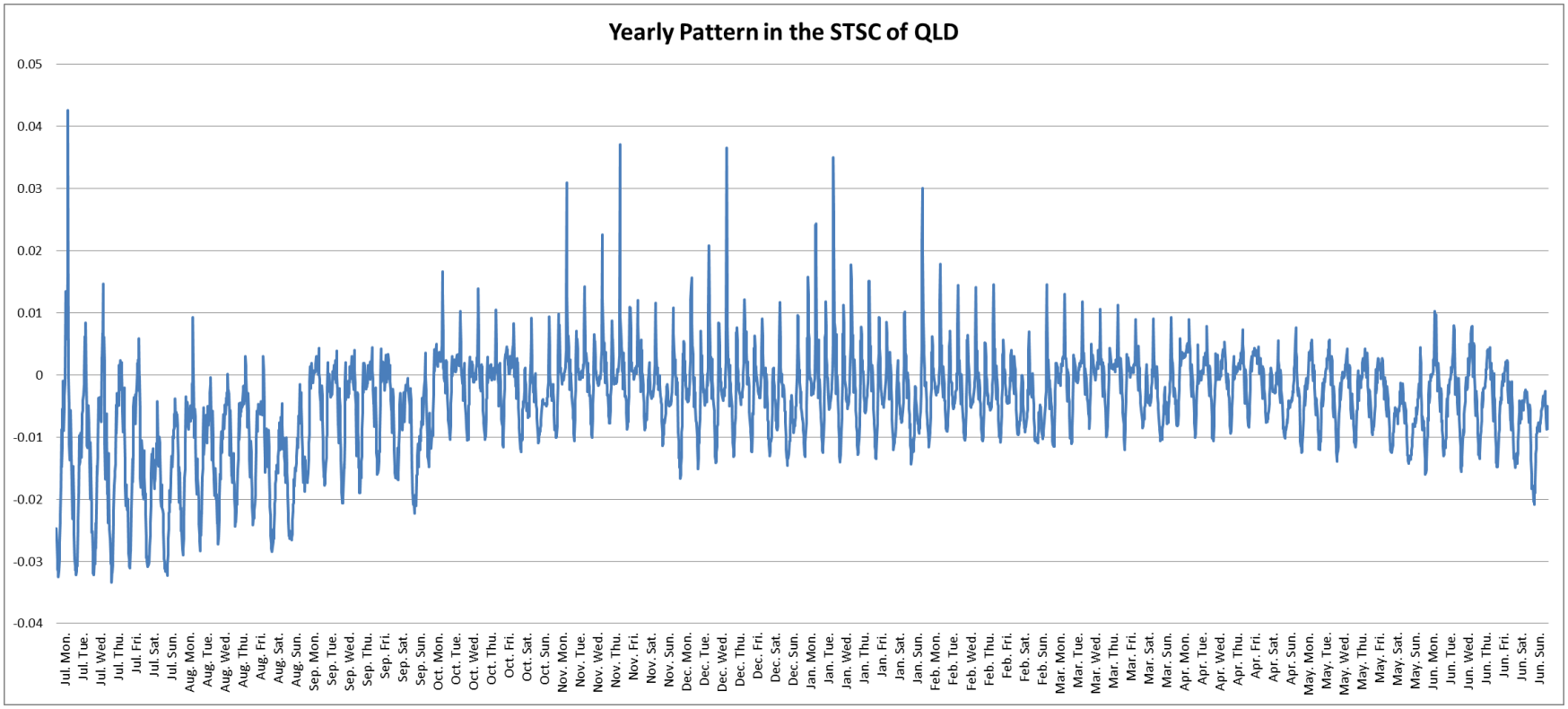

Figure A.1: Yearly pattern in the STSC estimated from the half-hourly spot prices in QLD. The STSC is estimated after removal of the estimated LTSC. The median of all values at the same time stamp is treated as the STSC of that time.

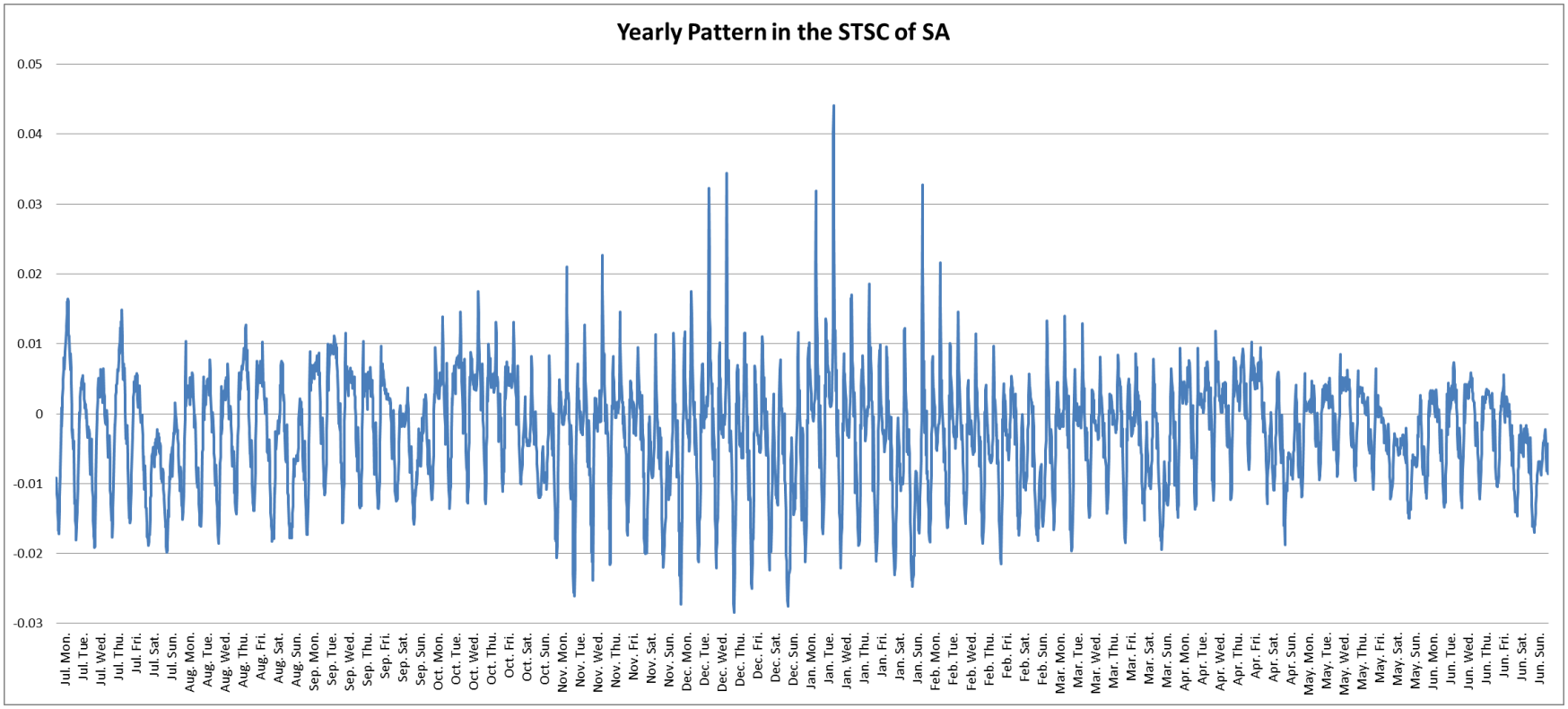

Figure A.2: Yearly pattern in the STSC estimated from the half-hourly spot prices in SA. The STSC is estimated after removal of the estimated LTSC. The median of all values at the same time stamp is treated as the STSC of that time.

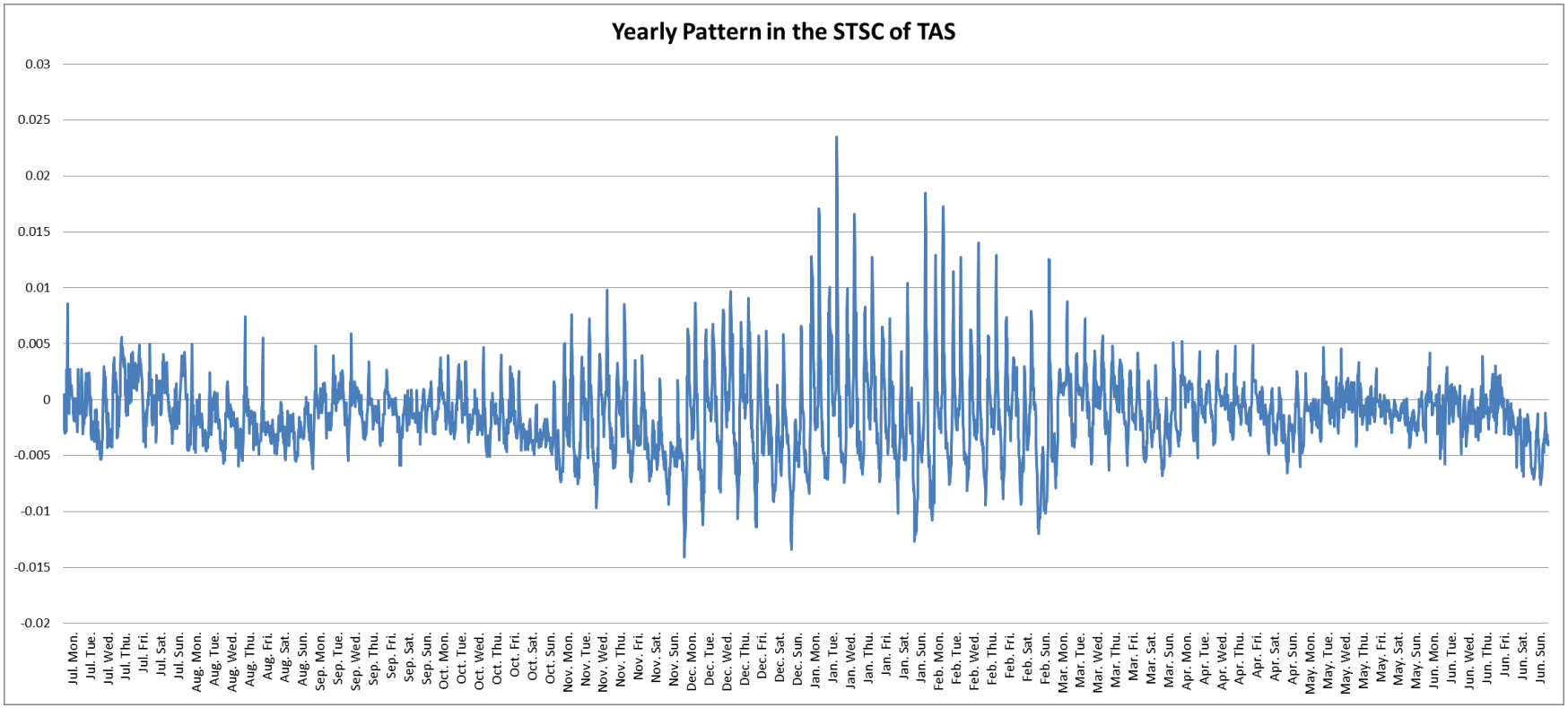

Figure A.3: Yearly pattern in the STSC estimated from the half-hourly spot prices in TAS. The STSC is estimated after removal of the estimated LTSC. The median of all values at the same time stamp is treated as the STSC of that time.

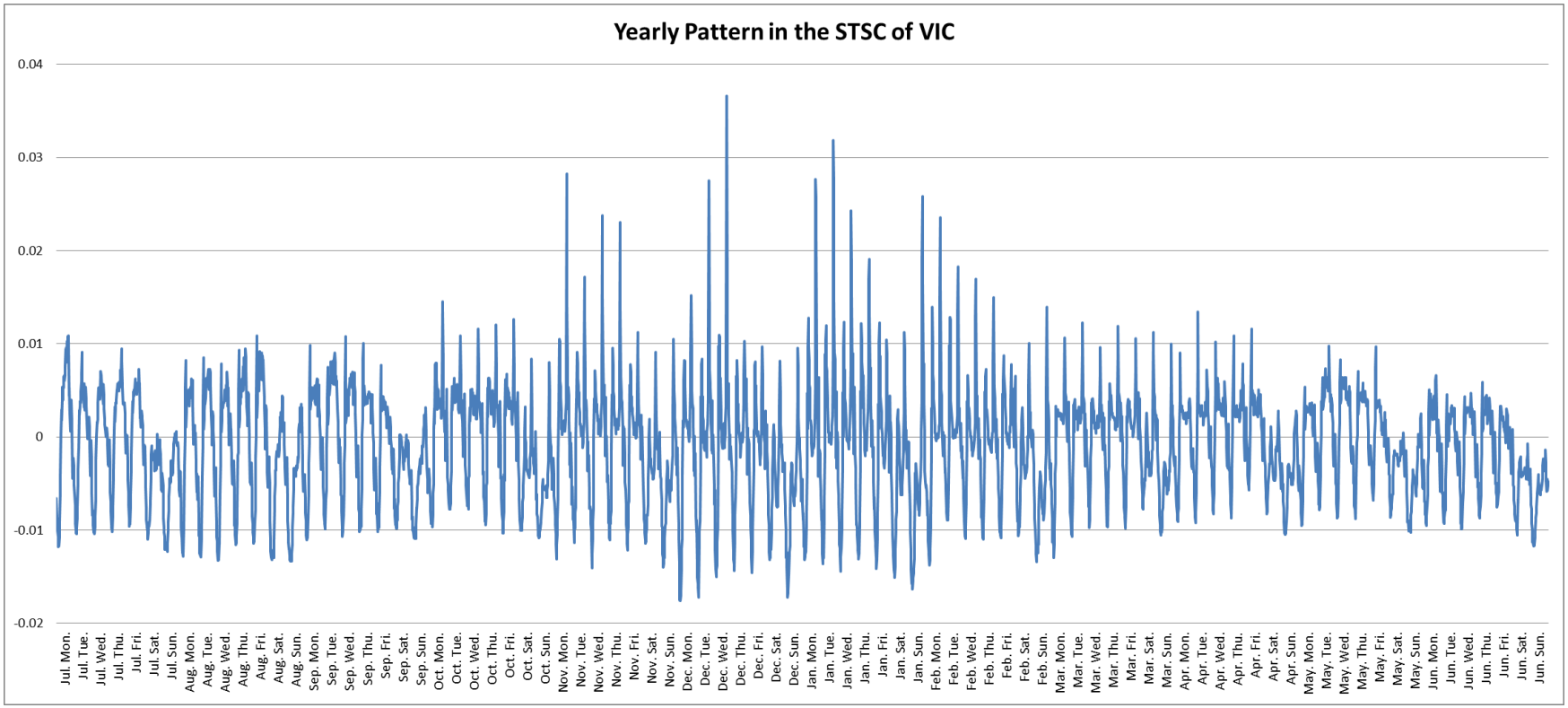

Figure A.4: Yearly pattern in the STSC estimated from the half-hourly spot prices in VIC. The STSC is estimated after removal of the estimated LTSC. The median of all values at the same time stamp is treated as the STSC of that time.

Table A.1: Average adjacency matrix from Granger causality networks. Each entry $a_{i,j}$ in ith row and jth column of the 5×5 matrix represents the percentage that prices of ith region Granger-causes those of jth region during seven financial years: 2010 - 2011, 2011 - 2012, 2012 - 2013, 2013 - 2014, 2014 - 2015, 2015 - 2016, 2016 - 2017. The full sample is from 1 July 2010 to 30 June 2017. The relationship is at 1% confidence level.

	NSW	QLD	SA	TAS	VIC		NSW	QLD	SA	TAS	VIC
		2010 - 2011						2011 - 2012			
NSW	0	0.292	0.159	0.159	0.203	NSW	0	0.153	0.068	0.117	0.077
QLD	0.212	0	0.150	0.123	0.259	QLD	0.139	0	0.112	0.117	0.060
SA	0.231	0.173	0	0.231	0.287	SA	0.306	0.227	0	0.172	0.347
TAS	0.153	0.145	0.187	0	0.189	TAS	0.098	0.104	0.096	0	0.172
VIC	0.097	0.109	0.150	0.164	0	VIC	0.243	0.117	0.213	0.186	0
		2012 - 2013						2013 - 2014			
NSW	0	0.164	0.115	0.225	0.118	NSW	0	0.216	0.077	0.090	0.101
QLD	0.195	0	0.115	0.197	0.079	QLD	0.192	0	0.079	0.129	0.123
SA	0.238	0.123	0	0.197	0.318	SA	0.142	0.107	0	0.137	0.252
TAS	0.134	0.096	0.145	0	0.170	TAS	0.184	0.145	0.132	0	0.195
VIC	0.238	0.156	0.175	0.263	0	VIC	0.200	0.164	0.126	0.140	0
		2014 - 2015						2015 - 2016			
NSW	0	0.186	0.238	0.126	0.121	NSW	0	0.197	0.213	0.126	0.175
QLD	0.115	0	0.140	0.137	0.110	QLD	0.139	0	0.055	0.148	0.085
SA	0.247	0.140	0	0.178	0.364	SA	0.153	0.115	0	0.107	0.186
TAS	0.088	0.066	0.126	0	0.077	TAS	0.158	0.142	0.156	0	0.090
VIC	0.140	0.115	0.301	0.151	0	VIC	0.260	0.235	0.249	0.224	0
		2016 - 2017						Full Sample			
NSW	0	0.362	0.274	0.148	0.033	NSW	0	0.224	0.163	0.142	0.118
QLD	0.093	0	0.170	0.121	0.047	QLD	0.155	0	0.117	0.139	0.109
SA	0.137	0.132	0	0.216	0.208	SA	0.208	0.145	0	0.177	0.280
TAS	0.170	0.205	0.304	0	0.178	TAS	0.141	0.129	0.163	0	0.153
VIC	0.137	0.214	0.373	0.345	0	VIC	0.188	0.159	0.227	0.211	0

Table A.2: Correlation coefficients between the explanatory variables and the dependent variables. All variables in Panel A (B) are concerned with NSW (QLD). Those in the first column refer to average, maximum, minimum, range, standard deviation and skewness of the half-hourly spot prices, and the number of price spikes in one day. The variables in the first row are weekly statistics and five connectedness measures over the past seven days. See Table 4.1 for the details. All coefficients in the table are Pearson's correlation coefficients.

Panel A: NSW														
	Mean	Max	Min	Range	Range2	Std	Std2	Skew	#Spike	Indegree	Outdegree	Pca1	Pca2	Dci
Mean	0.294	0.228	-0.014	0.226	0.278	0.282	0.281	0.080	0.215	0.061	-0.021	-0.033	0.005	0.022
Max	0.212	0.246	-0.122	0.250	0.313	0.306	0.315	0.121	0.214	0.014	-0.004	-0.016	0.019	0.018
Min	0.001	-0.172	0.572	-0.199	-0.332	-0.283	-0.344	-0.021	-0.100	0.022	-0.084	0.008	-0.008	-0.114
Range	0.209	0.256	-0.163	0.261	0.334	0.323	0.337	0.121	0.219	0.012	0.002	-0.016	0.020	0.027
Std	0.232	0.282	-0.179	0.288	0.371	0.359	0.374	0.120	0.237	0.029	0.005	-0.017	0.020	0.039
Skew	0.075	0.121	-0.017	0.120	0.164	0.148	0.160	0.202	0.085	-0.048	0.000	0.034	0.061	-0.025
#Spike	0.281	0.268	-0.051	0.268	0.338	0.347	0.346	0.081	0.297	0.041	-0.023	-0.018	0.014	0.007
Panel B: QLD														
	Mean	Max	Min	Range	Range2	Std	Std2	Skew	#Spike	Indegree	Outdegree	Pca1	Pca2	Dci
Mean	0.232	0.200	0.007	0.159	0.209	0.204	0.211	0.054	0.191	-0.029	-0.028	0.035	0.041	-0.019
Max	0.229	0.379	0.014	0.301	0.419	0.372	0.407	0.148	0.315	-0.023	-0.075	0.044	0.082	-0.027
Min	-0.019	-0.042	0.002	-0.036	-0.050	-0.044	-0.048	0.005	-0.047	-0.038	-0.024	-0.009	-0.013	-0.059
Range	0.212	0.354	0.012	0.282	0.393	0.349	0.382	0.129	0.300	-0.004	-0.056	0.043	0.079	0.002
Std	0.225	0.364	0.013	0.289	0.401	0.365	0.396	0.123	0.314	-0.011	-0.051	0.053	0.082	-0.001
Skew	0.119	0.247	0.022	0.189	0.245	0.211	0.234	0.224	0.161	-0.021	-0.092	0.029	0.086	-0.050
#Spike	0.234	0.292	0.005	0.235	0.326	0.307	0.325	0.082	0.354	-0.026	-0.054	0.041	0.050	-0.030

Table A.3: Correlation coefficients between the explanatory variables and the dependent variables. All variables in Panel C (D) are concerned with SA (TAS). Those in the first column refer to average, maximum, minimum, range, standard deviation and skewness of the half-hourly spot prices, and the number of price spikes in one day. The variables in the first row are weekly statistics and five connectedness measures over the past seven days. See Table 4.1 for the details. All coefficients in the table are Pearson's correlation coefficients.

Panel C: SA														
	Mean	Max	Min	Range	Range2	Std	Std2	Skew	#Spike	Indegree	Outdegree	Pca1	Pca2	Dci
Mean	0.155	0.072	0.006	0.050	0.069	0.089	0.097	0.013	0.167	0.067	0.050	-0.012	0.013	0.042
Max	0.108	0.174	0.024	0.112	0.176	0.159	0.194	0.109	0.216	0.106	0.002	0.023	0.060	0.047
Min	0.012	0.005	0.046	-0.029	-0.035	-0.039	-0.039	0.030	-0.016	0.003	0.005	0.005	0.021	0.000
Range	0.080	0.137	-0.008	0.107	0.163	0.151	0.180	0.070	0.183	0.084	-0.002	0.016	0.036	0.038
Std	0.092	0.139	-0.011	0.111	0.173	0.164	0.196	0.062	0.204	0.083	-0.001	0.019	0.039	0.035
Skew	0.047	0.154	0.078	0.059	0.105	0.072	0.101	0.184	0.091	0.080	-0.025	0.026	0.063	0.026
#Spike	0.199	0.144	0.014	0.096	0.165	0.169	0.205	0.046	0.327	0.098	0.060	0.014	0.041	0.057
Panel D: TAS														
	Mean	Max	Min	Range	Range2	Std	Std2	Skew	#Spike	Indegree	Outdegree	Pca1	Pca2	Dci
Mean	0.266	0.011	0.009	0.006	0.042	0.079	0.113	-0.012	0.208	-0.055	-0.024	-0.011	0.003	-0.033
Max	0.054	0.112	-0.012	0.103	0.150	0.144	0.172	0.087	0.131	-0.039	0.001	-0.027	-0.003	-0.026
Min	-0.024	-0.080	0.060	-0.096	-0.130	-0.114	-0.143	-0.024	-0.107	-0.066	-0.015	-0.012	-0.025	-0.029
Range	0.059	0.132	-0.034	0.131	0.187	0.175	0.211	0.089	0.160	-0.010	0.007	-0.019	0.007	-0.012
Std	0.094	0.146	-0.035	0.144	0.239	0.242	0.313	0.081	0.301	-0.009	0.007	-0.020	0.024	-0.018
Skew	0.014	0.104	0.002	0.091	0.135	0.103	0.122	0.152	0.045	-0.064	-0.023	-0.011	0.013	-0.054
#Spike	0.158	0.057	-0.009	0.054	0.216	0.268	0.422	0.015	0.730	-0.061	-0.043	-0.003	0.061	-0.094

Table A.4: Correlation coefficients between the explanatory variables and the dependent variables. All variables are concerned with VIC. Those in the first column refer to average, maximum, minimum, range, standard deviation and skewness of the half-hourly spot prices, and the number of price spikes in one day. The variables in the first row are weekly statistics and five connectedness measures over the past seven days. See Table 4.1 for the details. All coefficients in the table are Pearson's correlation coefficients.

Panel E: VIC														
	Mean	Max	Min	Range	Range2	Std	Std2	Skew	#Spike	Indegree	Outdegree	Pca1	Pca2	Dci
Mean	0.189	0.113	0.004	0.103	0.107	0.132	0.124	0.081	0.092	0.012	0.050	0.001	0.011	0.043
Max	0.101	0.113	-0.010	0.107	0.144	0.146	0.160	0.095	0.108	0.000	0.039	0.015	0.040	0.036
Min	-0.013	-0.021	0.048	-0.035	-0.108	-0.073	-0.125	0.012	-0.014	-0.022	-0.017	0.012	0.013	-0.040
Range	0.099	0.112	-0.024	0.111	0.168	0.159	0.188	0.085	0.105	0.007	0.041	0.010	0.034	0.046
Std	0.100	0.117	-0.034	0.119	0.188	0.177	0.215	0.082	0.097	0.006	0.055	0.004	0.033	0.056
Skew	0.054	0.084	0.015	0.073	0.113	0.094	0.113	0.148	0.041	-0.023	0.055	0.042	0.073	0.027
#Spike	0.058	0.099	0.013	0.087	0.065	0.093	0.068	0.078	0.099	0.023	-0.002	0.014	0.029	0.013